AD-A220 749

BERKELEY SCHOLARS, INC.

BRA-88-W024R
February 1988

Research on Short-wavelength
Free Electron Lasers

FINAL REPORT
Contract Number
N-00014-86-C-2055

for

Plasma Physics Division
US Naval Research Laboratory
Washington DC 20375

from

Berkeley Scholars
PO Box 983
Berkeley CA 94701

BRA-88-W024R
February 1988

Research on Short-wavelength
Free Electron Lasers

FINAL REPORT

Contract Number

N-00014-86-C-2055

for

Plasma Physics Division
US Naval Research Laboratory
Washington DC 20375

from

Berkeley Scholars
PO Box 983
Berkeley CA 94701

TABLE OF CONTENTS

I. INTRODUCTION

This is the final report for Contract N00014-86-C-2055. It covers research performed by Berkeley Scholars, Inc. from 6 December 1985 to 5 December 1987. The research involved the theoretical and numerical analysis of the physics of free electron lasers using relativistic particle beams.

The major emphasis of the research was to obtain design criteria for the development of a two-stage FEL oscillator operating in the trapped particle mode, and for a UV-FEL operating in an oscillator configuration with an intense CO_2 laser beam as a pumping source instead of the usual wiggler field. In order to carry out this program it is necessary to provide an appropriate model for the radiation physics of both types of FEL's, to examine the relevant nonlinear wave-particle dynamics, and to model the characteristics, development and evolution of the associated electron beam.

Task 1, to develop a general model for the radiation physics occurring in a FEL with specific application to a two-stage FEL oscillator operating in the trapped-particle mode, and to a UV-FEL operating in an an oscillator configuration that uses an intense CO_2 laser beam as a pumping source, is a necessary prerequisite for Task 2 and Task 3. These tasks are model applications, and the research addressing these tasks has given rise to new results. This final report documents the research, and the six appendices contain the details of the work. Articles prepared from the appendices have been submitted to professional journals or technical conferences. These articles have been prepared in collaboration with scientists from the Plasma Theory Branch at the Naval Research Laboratory.

The effects of radiation damping on beam quality in the inverse free electron laser accelerator are discussed in Appendix I, also published in the journal Particle Accelerators. A beam envelope equation is derived and solved for an arbitrarily tapered wiggler field. The expression for the evolution of the normalized transverse beam emittance is derived and found to decrease exponentially with distance due to radiation damping until it is limited by quantum excitation. Our results show that substantial improvements in beam quality can be realized for acceleration distances comparable to the radiation damping e-folding length.

The subsequent appendices give an account of the subsequent part of our research, viz., analyses directly addressing the electron beam quality issues that form task three of the statement of work. Appendix II, also published in Physical Review Letters, concerns the nonlinear particle-wave processes that can give rise to radiation focusing and guiding in a free electron laser. If the centroid of the electron beam is transversely displaced the radiation can be guided by the electron beam. A spatial modulation on the electron beam envelope can also modify the radiation field. These and other phenomena are studied using a novel source dependent modal representation of the fully three dimensional radiation field, the Source Dependent Expansion (SDE) method. Among the merits of this approach is that few modes are needed for an accurate description of the radiation.

Appendix III, also published in the Physical Review **A**, is a further study of the focusing and guidance of the radiation by the electron beam using the SDE method. Fast and accurate numerical solutions of the fully three dimensional FEL problem can be obtained over distances of many Raleigh lengths. The effects of finite emittance and wiggling of the electron beam can also be studied. Appendix IV, presented at the 1986 International FEL conference in Scotland, treats similar material. Appendix V, presented at the 1986 Conference of Particle Accelerators, expands on this work by examining the perfectly guided radiation beams in the Compton exponential gain regime of an FEL.

Appendix VI, also published in the Physical Review **A**, uses the SDE method for a related problem, viz., the optical gain, phase shift, and spatial profile of the coupled electron and radiation beams in an FEL. This research was carried out in collaboration with B. Hafizi from SAIC and with NRL personnel. The gain, phase shift, wavefront curvature and radius of the radiation envelope in a free electron laser amplifier are obtained in the small signal regime. The electron beam is assumed to have a Gaussian density distribution in the transverse direction. Numerical calculations indicate that the radius and curvature of the radiation beam entering a wiggler asymptote to unique, spatially constant values after a finite transition region. However, in the asymptotic regime the wavefronts diverge. Analytical expressions for the gain, phase shift, curvature and spot size are derived. It is shown analytically that small perturbations of the optical waist and curvature about the matched value are spatially damped out, indicating the stability of the matched envelope. When the electron beam is modulated in space, the optical spot size oscillates with an almost identical wavelength but delayed in phase. In the case of small amplitude, long-wavelength betatron oscillation of the electron beam envelope, generation of optical sidebands in wave number space is examined. The effect of the dispersion characteristics of the primary wave is found to be negligible for typical experimental parameters.

II. TECHNICAL DISCUSSION

Electron beam quality as measured by the transverse emittance is usually determined by the gun and propagation configurations in accelerators (see Ting and Sprangle, 1987 for this discussion). Under idealized conditions, the transverse normalized beam emittance remains a constant of motion as the beam propagates through the accelerator. Therefore, to improve the quality of the beam, it is necessary to decrease the beam emittance at the injection point. However, since the normalized beam emittance is essentially the transverse area in phase space for the collection of beam particles, one can in principle reduce the emittance if a dissipative mechanism is introduced. A natural candidate for such a dissipation mechanism is the induced synchrotron radiation damping due to the transverse motion of the particles in an external periodic transverse magnetic field. It is this mechanism that will be focused on in Appendix I when the external magnetic field is chosen to be a helical wiggler field. Since this radiation damping effect is small at low energies, it is in the context of the recently proposed high energy IFEL accelerators (references 1-11 in Appendix I) that will be emphasized and concentrated on in Appendix I.

First, the electron orbits in an IFEL accelerator must be obtained. A fully relativistic formulation of the equations of motion which include radiation damping force is considered. The damping coefficients are obtained from the transverse dynamics of the particles while the axial dynamics describe the acceleration of the particles. In the second section, a relativistic envelope equation for the average radius of the electron beam is derived, assuming continuous emission of the synchrotron radiation. It is apparent from this envelope equation that the normalized transverse emittance decays exponentially at a rate given by the radiation damping coefficient. The envelope equation is solved using a WKB method and the spatial evolution of the beam radius is obtained. Quantum excitation sets a minimum value on the normalized transverse emittance in an IFEL accelerator and it is derived in the fourth section of Appendix I. Strong focusing is found to be necessary to reduce such minimum to an acceptable value. An example is given in the last section of Appendix I for a set of proposed IFEL accelerator parameters (reference 2 in Appendix I). It is found that radiation damping does reduce the emittance of the accelerated electron beam while resulting in an insignificant loss in particle energy.

In analyzing radiation focusing and steering in the FEL by using a source dependent expansion technique, it is found that in the one-dimensional analysis of the FEL the radiation field, wiggler field and electron beam resonantly couple so as to modify the longitudinal wave number of the radiation field (references 1-3 in Appendix III; also see Sprangle, Ting and Tang, 1987a for this discussion). This can lead to focusing of the radiation beam, a phenomena which has been shown to play a central role in the practical utilization of the FEL (reference 9 in Appendix III) since in many proposed experiments the short wavelength radiation beam will not be confined or guided by a waveguide structure. Furthermore, the interaction length (wiggler length) is usually long compared to the Rayleigh length associated with the radiation beam. Therefore, focusing of the radiation beam via the resonant interaction with the electron beam is necessary in order to overcome the natural tendency of the radiation beam to diffract. If diffraction of the radiation field were not fully or partially offset by the focusing effect, the FEL would suffer from reduced gain and efficiency.

Two primary objectives are associated with the use of a source dependent expansion technique in the analyses presented in Appendix III (Sprangle, Ting and Tang, 1987a) and Appendix IV (Sprangle, Ting and Tang, 1987b), namely to present a general method of formulating and solving problems involving radiation focusing and guiding for mechanisms in which the refractive index is known and to apply this approach to the focusing and steering of radiation in FELs with arbitrary gain. The method is a general, self-consistent, fully nonlinear, modal representation with application to the phenomena of radiation focusing and guiding in FELs. The source function (driving current) is incorporated self-consistently into the functional dependence of the radiation waist, the radiation wave front curvature and the radiation complex amplitude. The fundamental mode remains dominant throughout the evolution of the radiation field due to the source dependent nature of this mo< expansion. This source dependent expansion (SDE) scheme appears to have a num er of advantages over the conventional vacuum representation (reference 7 in Appendix IV). Among the advantages are that relatively few modes are needed, compared to the vacuum expansion approach, to accurately describe the radiation beam. Because far fewer modes are needed, fast numerical solutions of the fully three-dimensional wave equation can be obtained over long propagation distances. It therefore appears feasible, using the SDE approach, to incorporate simultaneously into the model for the driving current density, the effects of electron beam emittance, energy spread, wiggler gradients, sideband frequencies, etc. Furthermore, since the lowest order terms in this expansion are a good approximation to the radiation field even for propagation distances long compared to a Rayleigh length, valuable insight concerning focusing and guiding can be obtained.

III. BIBLIOGRAPHY

Hafizi, B., P. Sprangle and A. Ting, "Optical Gain, Phase Shift, and Profile in Free-Electron Lasers", *Phys. Rev. A* **36**, 1739-1746 (1987).

Sprangle, P., A. Ting and C. M. Tang, "Radiation Focusing and Guiding with Application to the Free-Electron Laser", *Phys. Rev. Letters* **59**, 202-205 (1987a).

Sprangle, P., A. Ting and C. M. Tang, "Analysis of Radiation Focusing and Steering in the Free-Electron Laser by use of a Source-Dependent Expansion Technique", *Phys. Rev. A* **36**, 2773-2781 (1987b).

Sprangle, P., A. Ting and C. M. Tang, "Radiation Focusing and Guiding in the Free Electron Laser", *Nucl. Instr. and Meth. in Phys. Res.* **A259**, 136-142 (1987).

Sprangle, P., A. Ting, B. Hafizi and C. M. Tang, "Radiation Focusing, Guiding and Steering in Free Electron Lasers", submitted to proceedings of Particle Accelerator Conference, Washington, DC (1987).

Ting, A. C. and P. A. Sprangle, "Effects of Radiation Damping on Beam Quality in the Inverse Free-Electron Laser Accelerator", *Particle Accelerators* **22**, 149-160 (1987).

IV. APPENDICES

Appendix I:

Effects of radiation damping on beam quality in the
inverse Free Electron Laser Accelerator

I. Single Particle Dynamics

We shall consider the motion of an electron under the influence of a helical wiggler field and a circularly polarized electromagnetic wave with the inclusion of the radiation reaction force. The fully relativistic equation of motion is [14]

$$\frac{d\underline{p}}{dt} = -|e|(\underline{E} + \frac{\underline{v} \times \underline{B}}{c}) + \underline{F}^R , \tag{1}$$

where

$$\underline{F}^R = \tau_R \{\frac{\underline{p}}{m_o^2 c^2} [(\frac{\gamma^2 - 1}{\gamma})(\frac{d|\underline{p}|}{dt})^2 - \gamma(\frac{d\underline{p}}{dt})^2] + \frac{d}{dt}(\gamma\frac{d\underline{p}}{dt})\} ,$$

is the radiation damping force, $\tau_R = 2|e|^2/3m_o c^3$, and $\gamma^2 = 1 + |\underline{p}|^2/m_o^2 c^2$. The radiation field is given by its vector potential $\underline{A}_L = A_L(\cos\phi\hat{e}_x - \sin\phi\hat{e}_y)$, where $\phi = kz-\omega t$. We shall assume z-dependence for both the magnitude and period of the wiggler field. The vector potential $\underline{A}_W$ for the helical wiggler field is given by $\underline{A}_W = A_W[\cos\theta\hat{e}_x + \sin\theta\hat{e}_y]$ where $A_W = A_W(z)$ and $\theta = \int_0^z k_W(z')dz'$. The requirement that the wiggler field satisfies both $\nabla \cdot \underline{B}_W = 0$ and $\nabla \times \underline{B}_W = 0$ introduces transverse variation as well as a nonzero z-component of the magnetic field.[15]

Since we shall be primarily interested in laser driven accelerators, the normalized wiggler field strength $a_W = |e|A_W/m_o c^2$ is assumed to be much greater than the corresponding quantity $a_L = |e|A_L/m_o c^2$ for the radiation, i.e., $a_W \gg a_L$. It can then be shown that the major contribution to the radiation damping is from the wiggler field.

We shall first look at the radiation damping term in Eq. (1). By neglecting the transverse dependence of the wiggler field for a beam that is confined sufficiently close to the axis, we have the immediate consequence that the canonical momenta in the x and y directions are constants of motion

and may be chosen to be zero. The mechanical momenta are then given by

$p_x = \frac{|e|}{c} \underline{A}_T \cdot \hat{e}_x$, $p_y = \frac{|e|}{c} \underline{A}_T \cdot \hat{e}_y$, where $\underline{A}_T = \underline{A}_W + \underline{A}_L$. Also, in the zeroth

order approximation, the total relativistic energy is conserved which leads

to $\dot{\gamma} = 0$ and $\dot{p}_z = 0$. Therefore, the only significant term remaining in the

radiation reaction force is

$$\underline{F}^R = \tau_R \gamma [\frac{d^2 \underline{p}}{dt^2} - \frac{\underline{p}}{m_0^2 c^2} (\frac{d\underline{p}}{dt})^2].$$

Neglecting terms of order $a_L/a_W \ll 1$, the components of the radiation reaction

force are $F_x^R = - \nu_\perp c p_x$, $F_y^R = - \nu_\perp c p_y$, $F_z^R = - \nu_\parallel c p_z$, where

$$\nu_\perp = \tau_R \gamma k_W^2 c (a_W^2 + 1), \tag{2a}$$

$$\nu_\parallel = \tau_R \gamma k_W^2 c a_W^2 , \tag{2b}$$

are respectively the spatial decay coefficients due to radiation damping in

the transverse and axial directions. Note that $\nu_\perp \approx \nu_\parallel$ for $a_W^2 \gg 1$ which is

the case in the IFEL accelerator.

The most significant feature of the transverse motions of the electrons

is the betatron oscillation caused by either the inhomogeneity of the wiggler

field in the transverse plane or other focusing mechanisms. It can be shown

that, for small oscillations about the axis of the wiggler field, the

transverse equations of motion are,

$$\frac{d^2 x}{dz^2} + K_B^2 x = -(\frac{\gamma'}{\gamma} + \nu_\perp) \frac{dx}{dz} , \tag{3a}$$

$$\frac{d^2 y}{dz^2} + K_B^2 y = -(\frac{\gamma'}{\gamma} + \nu_\perp) \frac{dy}{dz} , \tag{3b}$$

where $d/dt = v_z \partial/\partial z$, $v_z = c$, $' = \partial/\partial z$ have been used, and K_B is the wave

number of the longitudinal betatron oscillation. For betatron oscillations that are originated from the $\underline{v} \times \underline{B}$ force due to the nonzero magnetic field in the z-direction of the realizable wiggler field,[15] $K_B = a_w k_w / (\sqrt{2}\gamma)$.

The axial motion of the electron is governed by

$$\frac{dp_z}{dz} = \gamma m \frac{dv_z}{dz} + mv_z \frac{d\gamma}{dz} = -\frac{|e|}{c^2} (\underline{v} \times \underline{B})_z - \nu_{\parallel} p_z , \qquad (4)$$

where

$$\frac{d\gamma}{dz} = \frac{-|e|\underline{v} \cdot \underline{E}}{m_o c^3} - \frac{(\nu_{\perp}|p_{\perp}|^2 + \nu_{\parallel} p_{\parallel}^2)}{m_o^2 c^3 \gamma} .$$

It is straightforward to show that the axial electron acceleration is

$$\frac{dv_z}{dz} = -\frac{c}{2\gamma^2} \frac{\partial a_w^2}{\partial z} + \frac{2a_w a_L k_w c}{\gamma^2} \sin \psi - \frac{2k_w}{k} \nu_{\parallel} v_z + \frac{3\nu_{\perp}|a_L a_w}{\gamma^2} \cos \psi , \qquad (5)$$

where $\psi = \theta + \phi = \int_o^z [k + k_w(z') - \omega/v_z(z')]dz' + \psi_o$ is the phase between the electrons and the ponderomotive wave generated by the beating between the radiation and wiggler fields, and ψ_o is the initial phase at the entrance of the interaction region. Equation (5) can be transformed into the following pendulum equation

$$\frac{d^2\psi}{dz^2} = \frac{dk_w}{dz} - \frac{k}{2\gamma^2} \frac{\partial a_w^2}{\partial z} + \frac{2 a_w a_L k k_w}{\gamma^2} \sin \psi - \frac{2\nu_{\perp}|k_w}{c} + \frac{3\nu_{\perp}|a_L a_w k}{c\gamma^2} \cos \psi . \qquad (6)$$

The rate of change of relativistic energy may be obtained from Eq. (4) and is

$$\frac{d\gamma}{dz} = \frac{a_L a_w k}{\gamma} \sin \psi - \nu_{\parallel}\gamma + \frac{\nu_{\perp}|a_L a_w}{\gamma}(\frac{k}{k_w} - 2) \cos \psi - \frac{\nu_{\perp}|}{\gamma}(a_w^2 + a_L^2) . \qquad (7)$$

5

Equations (3), (6) and (7) will be the basic equations we shall use in studying the effects on beam quality due to radiation damping. The terms containing $\cos \psi$ in Eqs. (5), (6) and (7) as well as the last term in Eq. (7) may be neglected when the conditions $a_w^2 \gg a_L^2$, $a_w^2 \gg 1$, $k \gg k_w$, and $\gamma^2 \gg 1$ are satisfied. These conditions are easily achieved in high energy IFEL accelerators.

II. Derivation of Envelope Equation with Radiation Damping

The single particle equations of motion that we have developed in the last section will enable us to study the macroscopic behavior of the beam. This is accomplished by considering the evolution of various averaged quantities associated with the single particle variables.[12,13] We begin by multiplying Eq. (3a) by x' and x, and Eq. (3b) by y' and y, where $'$ denotes $\partial/\partial z$. Combining the resulting equations yields the following set of equations

$$\frac{1}{2} \frac{d}{dz} \beta_\perp^2 + \frac{K_B^2}{2} \frac{d}{dz} r^2 = -\mu\beta_\perp^2 , \tag{8a}$$

$$\frac{1}{2} \frac{d^2}{dz^2} r^2 - \beta_\perp^2 + K_B^2 r^2 = -\frac{\mu}{2} \frac{d}{dz} r^2 , \tag{8b}$$

$$\frac{d\ell}{dz} = -\mu\ell , \tag{8c}$$

where $r^2 = x^2 + y^2$, $\beta_\perp^2 = x'^2 + y'^2$, $\mu = \gamma'/\gamma + \nu_\perp$, and $\ell = (x'y - y'x)$ is the normalized angular momentum. We eliminated $\beta_\perp^2$ by substituting Eq. (8b) into Eq. (8a). By taking transverse ensemble averages over beam particles in Eq. (8), and denoting the ensemble average of r^2 by $a^2 = \langle r^2 \rangle$, we obtain an equation which governs the evolution of the root-mean-square radius of the electron beam,

$$\mu^2 \frac{d}{dz} a^2 + \mu \frac{d^2}{dz^2} a^2 + 2\mu K_B^2 a^2 + \frac{d}{dz}(\frac{\mu}{2} \frac{d}{dz} a^2) + \frac{1}{2} \frac{d^3 a^2}{dz^3} + \frac{d}{dz}(K_B^2 a^2)$$
$$+ K_B^2 \frac{d}{dz} a^2 = 0 . \tag{9}$$

It is easy to show that the integration factor for Eq. (9) is $g^2 a^2$ where $g^2 = \gamma^2 \exp(2\int_0^z \nu_\perp dz')$. Equation (9) can now be put into the form $d/dz[\, g^2(a^3 a'' + \mu a^3 a' + a^4 K_B^2)] = 0$, and can be integrated to give

$g^2[a^3 a'' + \mu a^3 a' + a^4 K_B^2] = H^2$, where H^2 is a constant of motion associated with the beam. It can be shown that, using the following representation for the particles' normalized transverse velocities,[12]

$$\underline{\beta}_\perp = \frac{a'}{a} r \, \hat{e}_r + \frac{Lr}{a^2} \, \hat{e}_\theta + \delta\underline{\beta}_\perp \, ,$$

where $\delta\underline{\beta}_\perp$ is the normalized transverse velocity spread, and $L = \langle \ell \rangle$ from Eq. (8c), the constant H^2 is given by

$$H^2 = \gamma^2(0) L^2(0) + \gamma^2 a^2 \langle |\delta\underline{\beta}_\perp|^2 \rangle \exp(2\int_0^z \nu_\perp dz') \, ,$$

where $\gamma(0) = \gamma(z=0)$ and $L(0) = L(z=0)$. We may therefore define the squared normalized beam emittance[12,16] as $\epsilon_n^2(z) = \gamma^2 a^2 \langle |\delta\underline{\beta}_\perp|^2 \rangle$ and arrive at the following envelope equation

$$\frac{d^2 a}{dz^2} + \left(\frac{1}{\gamma} \frac{d\gamma}{dz} + \nu_\perp \right) \frac{da}{dz} + K_B^2 a - \frac{[\epsilon_n^2(z) + \gamma^2 L^2(z)]}{\gamma^2 a^3} = 0 \, . \qquad (10)$$

The spatial dependence of the normalized emittance and average angular momentum are given respectively by

$$\epsilon_n(z) = \epsilon_n(0) \exp(-\int_0^z \nu_\perp dz') \, , \qquad\qquad (11a)$$

$$L(z) = (\gamma(0)/\gamma) L(0) \exp(-\int_0^z \nu_\perp dz') \, , \qquad\qquad (11b)$$

where $\epsilon_n(0) = \epsilon_n(z=0)$. Equation (10) together with Eq. (11a,b) constitute the beam envelope equation with radiation damping terms included.

One can see that when $\nu_\perp = 0$, Eq. (11a) shows that ϵ_n remains constant and Eq. (10) reduces to the usual relativistic beam envelope equation where

ϵ_n is the familiar normalized beam emittance.[12,16] Therefore, in the presence of radiation damping, the root-mean-square beam radius is still described by an envelope equation but the normalized beam emittance is no longer constant but decays exponentially according to Eq. (11a). However, the decay of the normalized beam emittance will eventually be limited by quantum excitation due to the discrete nature of the synchrotron radiation. It is shown in a later section that when an equilibrium is reached between these two competing processes, the minimum normalized emittance achievable through radiation damping in the IFEL accelerator is given by $(\epsilon_n)_{min} = 3\hbar a_w^3 k_w/(\sqrt{2} m_o c K_B)$.

In the presence of radiation damping, the average angular momentum also decays exponentially as given by Eq. (11b). However, one may choose $L(0) = 0$ for beam generation schemes that do not impart an average angular momentum to the electron beam, i.e., zero magnetic field at the cathode. We shall assume that this is the case in our study of beam quality. We shall also not distinguish between $\nu_\perp$ and $\nu_\parallel$, and will denote both by ν.

III. Evolution of Beam Radius

The equation for the root-mean-square radius a in Eq. (10) is nonlinear. It is found, however, that the mean square radius a^2 satisfies Eq. (9), which is a linear differential equation. For beam focusing provided by the wiggler, Eq. (9) may be solved exactly for untapered wiggler fields when $\gamma' = 0$. If $\gamma' \neq 0$ or when the tapering is known, it can be solved using a WKB method if we assume the coefficients are slowly varying. Equation (9) can be simplified in certain limits of accelerator designs to facilitate analytical study. It can be shown that, $\gamma'/\gamma \ll K_B$ and $\nu \leq K_B$, which allow us to arrive at the following approximate equation

$$S''' + 3\mu S'' + 4K_B^2 S' + [4\mu K_B^2 + 2(K_B^2)']S = 0 , \tag{12}$$

where $S = a^2$.

In order to obtain net acceleration of the electrons trapped in the ponderomotive potential, the wiggler field must be spatially tapered. In such a case, the envelope equation, Eq. (12), is a linear differential equation with spatially dependent coefficients. We solved it by using the WKB-method which assumes these coeffients to be slowly-varying functions of longitudinal distance. By assuming both K_B'/K_B and $\mu \ll K_B$, the general solution to Eq. (12) is found to be

$$S = e^{-M} \frac{K_B(0)}{K_B(z)} [A + B \cos 2\Sigma + C \sin 2\Sigma] ,$$

where $M = \int_0^z \mu(z')dz'$, and $\Sigma = \int_0^z K_B(z')dz'$. The coefficients A, B, C can be found by using the initial conditions for a matched beam, $a(z=0) = a_0$, $a'(z=0) = 0$, $a''(z=0) = 0$. The matched beam radius a_0 is related to the

10

initial transverse emittance $a_o^4 = \epsilon_n^2(0)/(K_B^2(0)\gamma^2(0))$. Using the initial conditions, we arrive at the following expression for the root-mean-square beam radius,

$$a = a_o\, e^{-M/2} \left[\frac{K_B(0)}{K_B(z)}\right]^{1/2}\left[\, 1 + \frac{\mu(0) + K_B'(0)/K_B(0)}{2K_B(0)}\, \sin 2\Sigma\right]^{1/2} . \qquad (13)$$

Equation (13) shows that the beam radius does not remain constant even when the beam is matched at injection. In addition to the exponential decay from the radiation damping, the beam envelope developes an induced betatron oscillation. However, the normalized emittance is just an exponential decay given by Eq. (11a).

We may gain some insight into the general effect of radiation damping on the transverse emittance by studying Eq. (12) in the case of untapered wiggler field. We shall first consider the case where $\gamma' = 0$. This could be the situation when the acceleration mechanism is saturated by the radiation damping and the beam energy is constant. The evolution of the beam radius is then given by the appropriate limit of Eq. (13). Since there is no tapering of the wiggler, the solution is exact and given by

$$a = a_o e^{-\nu z/2}\left[\, 1 + \frac{\nu}{2K_B}\, \sin 2K_B z\,\right]^{1/2} .$$

The beam radius again exponentially decays with an induced betatron oscillation. Since γ is constant, the damping rate ν is constant, and the normalized emittance ϵ_n is given by $\epsilon_n(z) = \epsilon_n(0)\, \exp(-\nu z)$.

Next, we consider the situation when an accelerated beam is cooled by passing it through an untapered external wiggler field. Since the beam decelerates due to the synchrotron radiation damping, we have $\gamma'/\gamma = -\nu$.

11

This gives $\mu = 0$ and since $K_B = a_w k_w/(\sqrt{2}\gamma)$, the betatron wave number K_B is a function of z. The spatial dependence of γ can be evaluated using $\gamma'/\gamma = -\nu$, and Eq. (13) reduces to $a = a_o(1 + \nu_o^2 z^2)$, where $\nu_o = \tau_R a_w^2 k_w^2 \gamma_o c$. Although the beam radius remains constant up to order of $O(z^2)$, the normalized beam emittance decreases algebraically, $\varepsilon_n = \varepsilon_n(0)/(1+\nu_o z)$.

The relevance of the above analysis depends on the magnitude of the damping rate ν_o. For the following set of accelerator parameters,[2] $E_L = 1.5 \times 10^9$ V/cm., $B_w = 50$ kG., $\lambda_w = 1$ m, it is estimated that the e-fold length, $1/\nu_o$, could be as short as ≤ 600 m for $\gamma_o = 10^5$. Therefore, our results show that one can improve, by induced synchrotron radiation, the quality of an electron beam by passing it through an external wiggler field.

IV. Quantum Excitation

An estimate for the minimum transverse normalized beam emittance due to quantum excitation in an IFEL accelerator can be obtained from the following qualitative treatment. Similar arguments can be made for electron beams in storage rings.[17,18] The normalized transverse velocity and radial displacement of an electron in a wiggler field are given by $\beta_w = a_w/\gamma$, and $r_w = a_w\lambda_w/(2\pi\gamma)$. For a fluctuation δE in the energy of the electron, the corresponding fluctuations in r_w and β_w are $\delta r_w = \eta\delta E/E$, and $\delta\beta_w = \xi\delta E/E$, where $\eta = a_w\lambda_w/(2\pi\gamma)$ and $\xi = a_w/\gamma$. The increase in normalized emittance due to such fluctuations is[17,19] $\Delta\epsilon_n = \gamma[K_B\langle\delta r_w^2\rangle + \langle\delta\beta_w^2\rangle/K_B]$, which for a weakly focusing channel, $K_B \ll k_w$, can be approximated by $\Delta\epsilon_n = \gamma\langle\delta\beta_w^2\rangle/K_B = (\gamma\xi^2/K_B)\langle\delta E^2\rangle/E^2$. Due to the discrete nature of the synchrotron radiation, $\langle\delta E^2\rangle$ is given by $N(\hbar\omega_c)^2$ where $N = Pz/(c\hbar\omega_c)$ is the number of photons emitted in a distance z, P is the synchrotron radiation power, and $\hbar\omega_c$ is the energy associated with a quantum of synchrotron radiation. We can therefore obtain the rate of change of ϵ_n due to quantum excitation,

$$\left(\frac{d\epsilon_n}{dz}\right)_{Q.E.} = \frac{\gamma\xi^2}{K_B}\frac{P\hbar\omega_c}{cE^2} .$$

However, with radiation damping, the total change in ϵ_n is given by

$$\left(\frac{d\epsilon_n}{dz}\right) = -\nu\epsilon_n + \left(\frac{d\epsilon_n}{dz}\right)_{Q.E.} .$$

The normalized emittance, ϵ_n, reaches a minimum, $d\epsilon_n/dz = 0$, when the two effects are balanced. This gives $\epsilon_n = \gamma\xi^2\hbar\omega_c/(K_B E)$ for the minimum normalized emittance, where we have used $\nu c = P/E$. For synchrotron radiation, $\hbar\omega_c = 3\hbar c\gamma^3/(2\rho)$ where $\rho = \gamma/(a_w k_w)$ is the radius of curvature of the electron orbit in the wiggler. The minimum transverse normalized beam emittance is then approximately given by

$$(\epsilon_n)_{min} = 3\hbar a_w^3 k_w / (2m_o c K_B) \ . \tag{14}$$

In the case of weak focusing due to wiggler transverse gradients, $K_B = a_w k_w / (\sqrt{2}\gamma)$, and the minimum normalized emittance is

$$(\epsilon_n)_{min} = 3\hbar\gamma a_w^2 / (\sqrt{2}m_o c) \ . \tag{15}$$

Using the accelerator parameters at the end of section III, Eq. (15) gives the value of the minimum normalized emittance to be ~1.8 cm-rad. Such a large value of the minimum emittance indicates the inadequacy of the weak focusing from the wiggler transverse gradients. Strong focusing from, for example, a rotating quadrupole field produced by a pair of (or four) helical current windings[20,21] may be required. The betatron wavenumber for such a focusing mechanism[22] is given by $K_B^2 = |e|(\partial B/\partial r)/\gamma m_o c^2$, where $\partial B/\partial r$ is the magnetic field gradient of the quadrupole field on axis. For $\partial B/\partial r$~250 G/cm, a_w=600, λ_w=10m, and γ=4x10^{5}, Eq.(14) gives a minimum normalized emittance of ϵ_n~0.13 cm-rad. Another possible strong focusing force could be the electrostatic radial electric field of an ion column. Such a column could be created by the ionization of the residual gas by a low energy, high current electron beam pulse preceeding the main accelerating beam pulse.[23-25] The betatron wavenumber for such a focusing mechanism can be easily shown to be $K_B^2 = \omega_{pi}^2 (m_i/m_o)/(2\gamma c^2)$, where ω_{pi} is the ion plasma frequency and (m_i/m_o) is the mass ratio between the ions and the electrons. For n_i=10[12]/cm^{3}, a_w=600, λ_w=10m, and γ=4x10^{5}, Eq. (14) gives a minimum normalized emittance of ϵ_n~0.04 cm-rad. An additional benefit of having ion focusing in the IFEL accelerator is that the radial plasma electron density profile in an ion column can also be a focusing medium for the laser beam.

V. Numerical Example

We shall consider only resonant particles whose phase ψ satisfies the conditions $d\psi/dz = 0$ and $d^2\psi/dz^2 = 0$. The first condition gives

$$\gamma_R = \frac{|e|\sqrt{k}}{\sqrt{2}m_0 c^2} B_w k_w^{-3/2}, \tag{16a}$$

$$\gamma_R' = R_1 k_w^{1/2} - R_2 B_w^4 k_w^{-3}, \tag{16b}$$

$$\nu = \frac{\sqrt{2}}{3} \frac{|e|^5}{m_0^4 c^8} B_w^3 k_w^{-3/2} \sqrt{k}, \tag{16c}$$

where $R_1 = \sqrt{2}|e|E_L \sin\psi_R/(m_0 c^2 \sqrt{k})$, $R_2 = |e|^6 k/(3m_0^5 c^{10})$, ψ_R is the resonance phase, E_L the laser electric field strength, and k the laser wave number. The second condition together with the pendulum equation, Eq. (6), provide the spatial dependences of k_w and B_w,

$$3 k_w' - \frac{2k_w}{B_w} B_w' + \frac{4E_L}{k} \sin\psi_R \frac{k_w^3}{B_w} - \frac{2\sqrt{2}mc^2}{|e|\sqrt{k}} R_2 \frac{B_w^3}{\sqrt{k_w}} = 0. \tag{17}$$

Equation (17) shows that the required tapering of the wiggler field may be obtained by prescribing ψ_R and a relationship between k_w and B_w in Eq. (17). As an example, we assume the tapering of the wiggler field to be that of a maximum rate IFEL accelerator.[2] For such a case the wiggler strength and the wiggler period are related by the following power law,

$$B_w = (R_1/6R_2)^{1/4} k_w^{7/8}.$$

Equation (17) may then be solved to give

$$B_w = B_w(0)[1 + R_4 z]^{-7/9}, \tag{18a}$$

$$k_w = k_w(0)[1 + R_4 z]^{-8/9},\qquad\qquad\text{(18b)}$$

where

$$R_4 = \frac{9\sqrt{2}mc^2}{|e|\sqrt{k}} R_2(R_1/6R_2)^{3/7} B_w(0)^{9/7}.$$

Evaluating Eqs. (11) and (16a) with (16c) and (18a,b) gives the nromalized transverse emittance and the resonant energy of the beam as functions of the propagation distances.

For our example, we ill consider the following set of accelerator parameters[2]: $E_L = 1.5 \times 10^9$ V/cm, $B_w(0) = 50$ kG, $\lambda_w(0) = 100$ cm, and $\lambda = 10.6$ μm with a resonance phase of $\sin \psi_R = 0.6$. The initial conditions are for a matched beam with a radious of 1mm and a normalized emittance of $\varepsilon_0 = 0.205$ cm-rad, and the required beam injection energy is ∿52 GeV. The beam is allowed to propagate for 1 km without depleting the laser radiation. We repeated the calculation by assuming there is not radiation damping but with the same power law tapering of the wiggler field.

The results are represented in Figs. 1, 2, and 3. The open squares denote the presence of radiation damping, while open circles denote its absence. From Fig. 1, we can see that the final energy is not significantly reduced by the radiation damping. Figure 2 shows the exponential decay of the normalized emittance. At the end of the one-kilometer accelerator, the normalized emittance is reduced to 0.05 cm-rad, which is very close to the minimum normalized emittance of ∿0.04 cm-rad at that point if ion-column focusing is assumed in the accelerator. In Fig. 3, the appropriate tapering of K_w and B_w for the two cases is shown.

Conclusion

We have studied the evolution of transverse emittance and the beam radius due to the radiation damping effect in an IFEL accelerator. We derived the beam envelope equation, Eq. (10), which includes the effects of radiation damping, and have demonstrated that the normalized transverse emittance decreases exponentially with a damping rate given by the radiation damping coefficient ν until it reaches a minimum value due to quantum excitation. The beam envelope equation was solved analytically for a slowly-varying wiggler field. We have derived an expression for the minimum normalized emittance in the IFEL accelerator and showed that strong focusing is essential in reducing this minimum emittance due to quantum excitation. We have shown that radiation damping can play an important role in improving beam quality without a significant sacrifice in beam energy.

References

1. P. Sprangle and Cha-Mei Tang, IEEE Trans. Nucl. Sci. NS-28, 3346 (1981).

2. E. D. Courant, C. Pellegrini and W. Zakowicz, Phys. Rev. A 32, 2813 (1985).

3. C. Pellegrini, in Proceedings of the ECFA-RAL Meeting, Oxford, 1982 (unpublished).

4. C. Pellegrini, in Laser Accelerator of Particles, Proceedings of the Workshop on the Laser Acceleration of Particles, ed. by P. J. Channel, (AIP, New York, 1982), p. 138.

5. C. Pellegrini, P. Sprangle and W. Zakowicz, in Proceedings of the 12th International Conference on High Energy Accelerators, (Fermi National Accelerator Laboratory, Batavia, Ill., 1983), p. 473.

6. C. Pellegrini and R. Campisi, in Physics of High Energy Particle Accelerators, Proceedings of Lectures given at the National Summer School on High Energy Particle Accelerators, ed. by M. Month, (AIP, New York, 1983), p. 1058.

7. Robert B. Palmer, J. Appl. Phys. 43, 3014 (1972).

8. A. A. Kolomenskii and A. N. Lebedev, Soviet Physics JETP 23, 733 (1966).

9. H. Motz, Contemp. Phys. 20, 547 (1979).

10. W. B. Colson and S. K. Ride, Appl. Phys. 20, 61 (1979).

11. N. M. Kroll, P. L. Morton and M. N. Rosenbluth, IEEE QE-17, 1436 (1981).

12. E. P. Lee and R. K. Cooper, Particle Accelerators 7, 83 (1976).

13. P. Sprangle and Cha-Mei Tang, Laser Acceleration of Particles, AIP conf. Proc. 130, 156 (1985).

14. L. D. Landau and E. M. Lifshitz, The Classical Theory of Fields, Pergamon Press (1975).

15. Cha-Mei Tang, Proc. Intl. Conf. Lasers, 164 (1982).

16. J. D. Lawson, The Physics of Charged-Particle Beams, Oxford (1978).

17. M. Sands, in Physics with Intersecting Storage Rings, ed. by B. Touschek, Acad. Press, NY (1971).

18. M. Sands, Report SLAC/AP-47 (1985).

19. J. Sandweiss, private communication.

20. C. A. Kapetanakos, P. Sprangle, S. J. Marsh, C. Agritellis, D. Dialetis,

A. Prakash, Part. Accel., <u>18</u>, 73 (1985).

21. C. W. Roberson, A. Mondelli, D. Chernin, Phys. Rev. Lett., <u>50</u>, 507 (1983).

22. T. F. Wang, R. K. Cooper, in <u>Free Electron Lasers</u>, Proc. of the 7th Int'l Conf. on FEL's, Tahoe City, Sept.8-13, 1985, ed. by E. T. Scharlemann and D. Prosnitz (North-Holland-Amsterdam), p.138.

23. R. J. Briggs, J. C. clark, T. J. Fessenden, R. E. Hester, E. J. Lauer, in <u>2nd Intl topical Conf. on High-Power Electron and Ion Beam Research and Technology</u>, 1977, Vol II of II, p.319.

24. R. J. Briggs, Lawrence Livermore Nat'l Lab. Report, UCID-19187 (1981).

25. K. W. Struve, E. J. lauer, F. W. Chambers, in <u>Proc. Fifth Int'l Conf on High-Power Part. Beams</u>, San Francisco, CA (1983), ed. by R. Briggs and A. J. Toepfler, p.408.

Figure Captions

Fig. 1   Evolution of beam energy in an IFEL accelerator with and without

radiation damping.

Fig. 2   Exponential decay of normalized beam emittance, ϵ_n^2 .

Fig. 3   Spatial tapering of wiggler period and field with and without
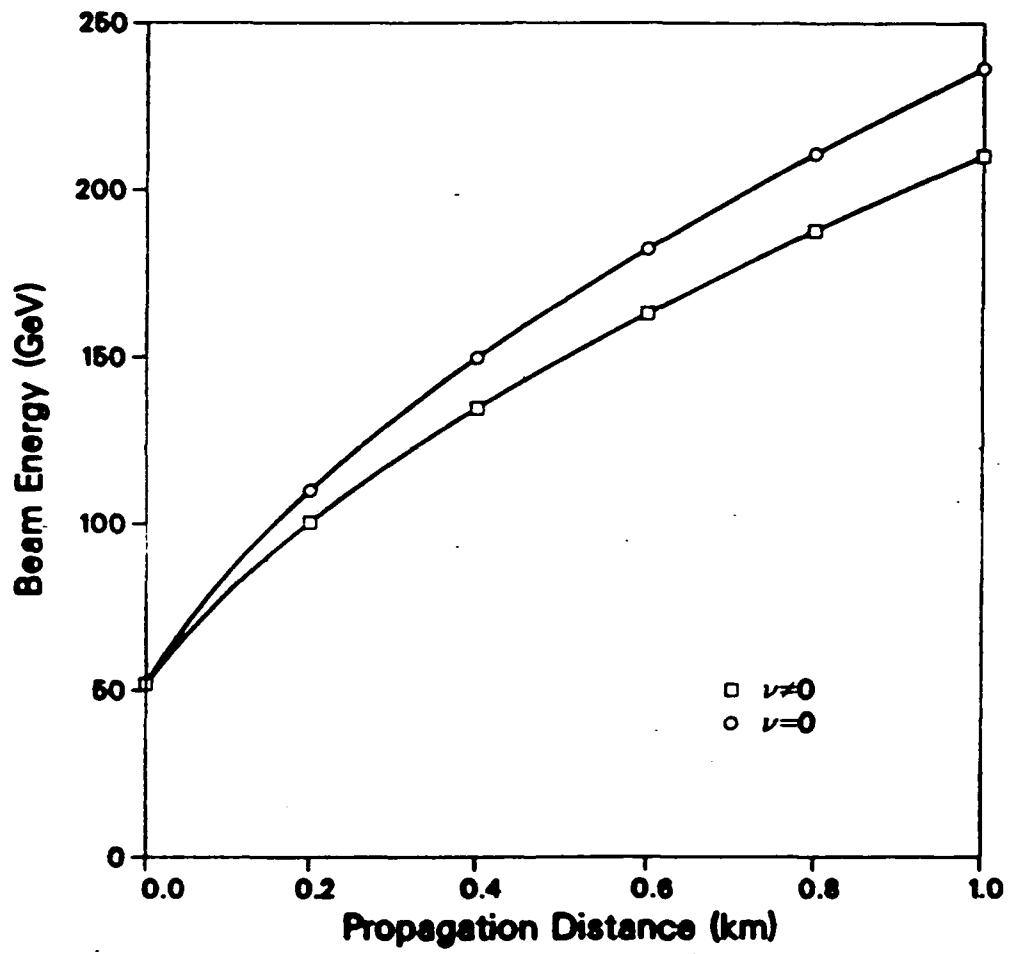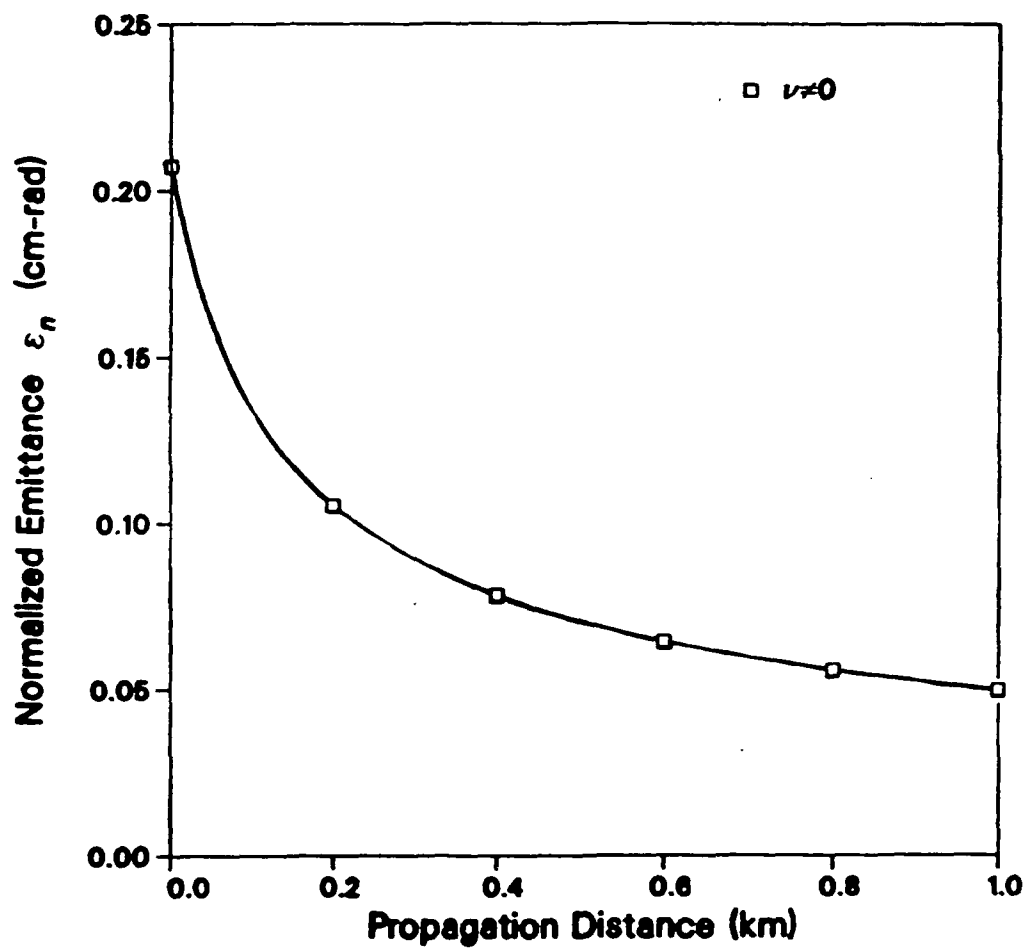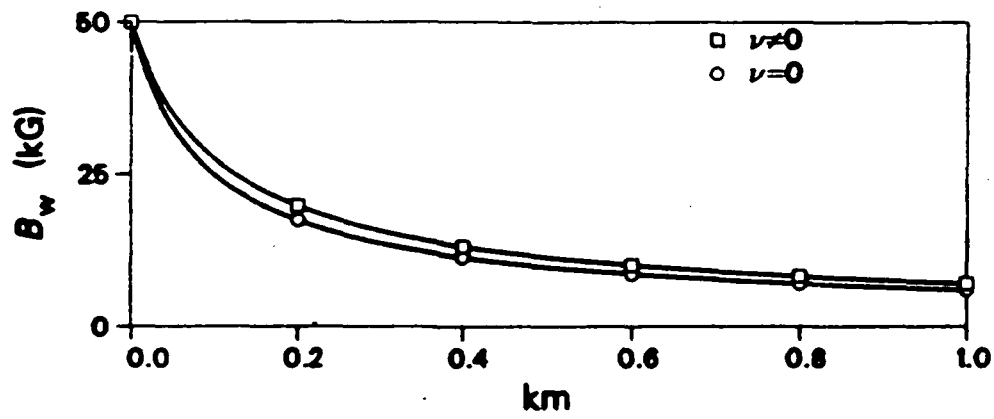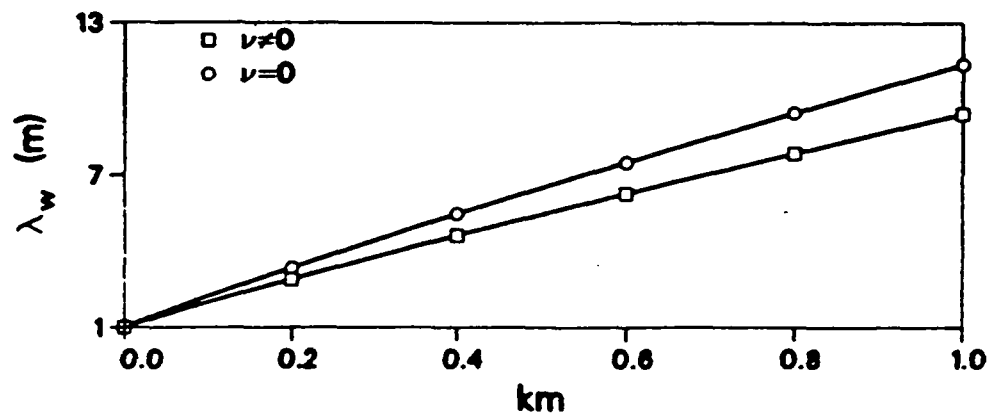
radiation damping.

Fig. 1

Fig. 2

Fig. 3

Appendix II:

Radiation focusing and guiding with applications
to the Free Electron Laser

In the one-dimensional analysis of the free electron laser (FEL) the radiation field, wiggler field and electron beam resonantly couple so as to modify the longitudinal wave number of the radiation field.[1-3] This resonant interaction can lead to focusing of the radiation beam. This phenomena was first analyzed for the low gain FEL with transverse effects[4] where it was shown that the diffractive spreading of the radiation beam could be overcome by a focusing effect arising from the modified index of refraction. This radiation focusing phenomena has been shown to play a central role in the practical utilization of the FEL,[5] since, in many proposed experiments the radiation beam will not be confined or guided by a waveguide structure. Recently optical guiding in FELs has been studied in the small signal, exponential growth regime,[6-9] for the asymptotic behavior of the radiation beam.

In this letter, we present a general, self-consistent, fully nonlinear, modal representation formalism which we apply to the phenomena of radiation focusing and guiding in FELs. The novel aspect of our modal expansion is that the characteristics of the modes are governed by the driving current density, as opposed to a heuristic numerical approach,[10] and hence it is called the "source dependent expansion" (SDE). Instead of using the usual modal expansion consisting of vacuum Laguerre-Gaussian functions[11] we incorporate the source function (driving current) self-consistently into the functional dependence of, i) the radiation waist, ii) the radiation wave front curvature, as well as iii) the radiation complex amplitude. Because of the source dependent nature of our modal expansion, the fundamental mode remains dominant throughtout the evolution of the radiation field. This approach, which can be applied to a wide range of problems, lends itself to fast and accurate numerical solutions as well as to a better analytical description of the FEL focusing and guiding problem.

1

Using the SDE approach in numerical simulations of the FEL, one can efficiently incorporate simultaneously the effects of electron beam emittance, energy spread, wiggler gradients, sideband frequencies, etc.

An envelope equation for the radiation is derived which describes the transient as well as asymptotic behavior of the radiation beam. The effects on the radiation beam of a transversely displaced electron beam as well as a longitudinally modulated electron beam have also been considered.

In our model the vector potential of the radiation field is $\underset{\sim R}{A}(r,\theta,z,t) = (1/2)A(r,\theta,z)\exp(i(\omega z/c-\omega t))e_x + c.c.$, where $A(r,\theta,z)$ is the complex amplitude, ω is the frequency and c.c. denotes the complex conjugate. The radiation field satisfies the reduced wave equation,

$$\left[\frac{1}{r}\frac{\partial}{\partial r}\left(r\frac{\partial}{\partial r}\right) + \frac{1}{r^2}\frac{\partial^2}{\partial \theta^2} + 2i\frac{\omega}{c}\frac{\partial}{\partial z}\right]a(r,\theta,z) = S(r,\theta,z), \qquad (1)$$

where $a(r,\theta,z) = |e|A/m_0c^2 = |a|\exp(i\phi)$ is the normalized complex radiation field amplitude and we have assumed that $a^{-1}\partial a/\partial z \ll \omega/c$. The source function, S, has the general form

$$S(r,\theta,z) = (\omega/c)^2(1-n^2(r,\theta,z,a))a(r,\theta,z), \qquad (2)$$

where $n(r,\theta,z,a)$ is the complex index of refraction.

We choose the following representation for $a(r,\theta,z)$ in terms of associated Laguerre polynomials,

$$a(r,\theta,z) = \sum_m \sum_p C_{m,p}(\theta,z)D_m^p(r), \qquad (3)$$

where m and p = 0,1,2,$\cdots$,

$$C_{m,p}(\theta,z) = a_{m,p}(z)\cos p\theta + b_{m,p}(z)\sin p\theta, \qquad (4a)$$

$$D_m^p(r) = \left(\frac{\sqrt{2}r}{r_s(z)}\right)^p L_m^p\left(\frac{2r^2}{r_s^2(z)}\right)e^{-(1 - i\alpha(z))r^2/r_s^2(z)}. \qquad (4b)$$

In Eqs. (4a,b), $a_{m,p}(z)$ and $b_{m,p}(z)$ are complex, $r_s(z)$ is the radiation spot size, $\alpha(z)$ is related to the curvature of the wavefront and L_m^p is the associated Laguerre polynomial. The z dependence of these parameters will be determined by the source function in Eq. (1).

Substituting (3) into (1) and using the orthogonality properties of L_m^p, cos pθ, and sin pθ, we obtain,

$$\left(\frac{\partial}{\partial z} + A_{m,p}(z)\right)\begin{pmatrix} a_{m,p} \\ b_{m,p} \end{pmatrix} - imB(z)\begin{pmatrix} a_{m-1,p}(z) \\ b_{m-1,p}(z) \end{pmatrix} - i(m+p+1)B^*(z)\begin{pmatrix} a_{m+1,p}(z) \\ b_{m+1,p}(z) \end{pmatrix}$$

$$= -i\begin{pmatrix} F_{m,p}(z) \\ G_{m,p}(z) \end{pmatrix}, \tag{5a,b}$$

where

$$A_{m,p}(z) = r_s'/r_s + i(2m+p+1)\left((1 + \alpha^2)c/\omega r_s^2 - \alpha r_s'/r_s + \alpha'/2\right), \tag{6a}$$

$$B(z) = -\left(\alpha r_s'/r_s + (1 - \alpha^2)c/\omega r_s^2 - \alpha'/2\right) - i\left(r_s'/r_s - 2\alpha c/\omega r_s^2\right), \tag{6b}$$

the prime denotes $\partial/\partial z$, $*$ denotes the complex conjugate and

$$\begin{pmatrix} F_{m,p}(z) \\ G_{m,p}(z) \end{pmatrix} = \frac{c}{2\pi\omega}\frac{m!}{(m+p)!}\int_0^{2\pi}d\theta\int_0^{\infty}d\xi\, S(\xi,\theta,z)\left(D_m^p(\xi)\right)^*\begin{pmatrix} (1+\delta_{p,0})^{-1}\cos p\theta \\ \sin p\theta \end{pmatrix},$$

$$\tag{6c,d}$$

where $\xi = 2r^2/r_s^2$. The equations for $a_{m,p}$ and $b_{m,p}$ in (5) are underdetermined, since the function B(z) can be shown to be arbitrary. If we choose B(z) = 0, for example, we would in effect be expanding the radiation field in the conventional vacuum Laguerre-Gaussian modes.[11] For a source free medium, B = 0 would be the most appropriate choice. In the presence of a source term a more appropriate choice for B(z) can be found. This is accomplished by considering the case where the radiation beam at

3

z = 0 has a Gaussian radial profile symmetric about the z-axis. Let us further assume that for $z > 0$ the radiation beam profile remains approximately Gaussian with a nearly circular cross section. In this case, we expect the magnitude of the coefficients, $a_{m,p}(z)$ and $b_{m,p}(z)$ to become progressively smaller as m and p take on larger values. A good approximation to the radiation beam is then given by the lowest order mode, $a_{0,0}(z)$. From (5a), we find that only the m = 0,1 and p = 0 equations are relevant and they are $(\partial/\partial z + A_{0,0})a_{0,0} = - iF_{0,0}$ and $P_{1,0} = Ba_{0,0}$. The second equation provides us with a specific expression for B(z) in terms of one of the moments, $F_{1,0}$, of the source term. The choice of $B(z) = F_{1,0}(z)/a_{0,0}(z)$ is source dependent and when substituted into (6b) yields first order coupled differential equations for the parameters, r_s and α, of the Laguerre-Gaussian expansion in (3) and (4a,b). The set of equations in (5a,b) may now be solved self-consistently for the modal coefficients $a_{m,p}$ and $b_{m,p}$.

We first consider the dynamics of an axially symmetric radiation field in the FEL. The appropriate index of refraction[4,5,7,12] for a Gaussian beam density profile is

$$n(r,z,a) = 1 + \frac{1}{2} \frac{\omega_b^2(r,z)}{\omega^2} \left\langle \frac{e^{-i\psi}}{\gamma} \right\rangle \frac{a_v}{|a(r,z)|} , \qquad (7)$$

where $\omega_b^2(r,z) = \omega_{b0}^2(r_{b0}/r_b(z))^2 \exp(-r^2/r_b^2(z))$, $r_b(z)$ is the electron beam radius, $r_{b0} = r_b(0)$, ω_{b0} is the initial beam plasma frequency on axis, $a_v = |e|B_v/k_v m_0 c^2$ is the normalized wiggler amplitude, γ is the electron's Lorentz factor, ψ is the electron's phase in the ponderomotive wave potential and $\langle \ \rangle$ denotes the ensemble average over all electrons. With the assumption that in the source function the complex radiation amplitude

can be approximated by the lowest order mode, we find that (2) can be written as

$$S(\xi,z) = -4\nu(a_w/r_b^2) \; \frac{a_{0,0}}{|a_{0,0}|} \; \left\langle \frac{e^{-i\psi}}{\gamma} \right\rangle \; e^{-\left(r_s^2/r_b^2 - i\alpha\right)\xi/2} \quad , \qquad (8)$$

where $\nu = (\omega_{b0} \, r_{b0}/2c)^2 = I_b/17 \times 10^3$ is Budker's constant and I_b is the electron beam current in amperes.

An envelope equation for the radiation beam can be obtained using (8) and (6b),

$$r_s'' + K^2(z,r_b,r_s,|a_{0,0}|)r_s = 0, \qquad (9)$$

where

$$K^2 = (2c/\omega)^2 \left[-1 + C^2 \langle \sin\psi \rangle^2 + 2C\langle \cos\psi \rangle + (\omega/2c)r_s^2 \, C' \langle \sin\psi \rangle \right] r_s^{-4}, \qquad (10)$$

and $C(z) = (2\nu/\gamma)H(z)a_w/|a_{0,0}(z)|$, measures the coupling between the radiation and electron beam, $H(z) = (1-F)/(1+F)^2$ and $F(z) = r_b^2/r_s^2$ is the filling factor. The first term on the right hand side of (10) is the usual diffraction term, the second and third terms are always focusing while the last term is usually a defocusing contribution. In the high gain trapped particle regime, $\langle \sin\psi \rangle$ and $\langle \cos\psi \rangle$ are approximately constant, while $|a_{0,0}(z)|$ increases with z. Hence, K strongly depends on z and a guided beam $(r_s' = 0)$ cannot be maintained. In the low gain trapped particle regime $|a_{0,0}(z)|$ increases slightly and, therefore, a guided beam can be approximately achieved. In either the Compton[13] or Raman exponential gain regime, conditions for a stable guided beam can be found.

The FEL parameters used in the following illustrations are similar to those used in Ref. 14 and are given in Table I where the resonant phase

5

approximation is used and $z_R = \pi r_s^2(0)/\lambda$ is the Rayleigh length. We present

first a comparison between; a) the exact numerical solution of the wave

equation in (1), (using 64x64 Fourier modes), b) the solution using a

vacuum Laguerre-Gaussian modal expansion (B = 0, using 10 modes) and c) the

solution from the Laguerre-Gaussian SDE approach (B = $F_{1,0}/a_{0,0}$, using 10

modes). For an axially symmetric configuration, we show in Fig. 1 the

evolution of the radiation beam amplitude on-axis obtained from methods

(a), (b) and (c). The SDE solution (c) is in excellent agreement with

solution (a) while solution (b), beyond a Rayleigh length, grossly deviates

from (a) and (c). The excellent results obtained with the SDE approach are

also reflected in the radiation amplitude profile. Figure 2 shows the

evolution of the radiation beam radius, r_E, in the linear, exponential gain

regime of the FEL for the parameters in Table I. Five transverse modes

were used in the numerical calculation.

We now consider the case where the electron beam centroid is displaced

transversely in the x direction. The index of refraction in this case is

given by (7) with $\omega_b^2(r,z)$ multiplied by $(1 + 2(r_s x_b/r_b^2)\cos\theta)$ where $x_b(z)$ is

the displacement of the electron beam's centroid and $|x_b| \ll r_b$. In the

FEL source term we consider only the lowest order symmetric and anti-

symmetric mode with respect to the x axis. The centroid of the radiation

beam is given approximately by

$$x_L(z) = \frac{r_s(z)}{\sqrt{2}} \left(\frac{a_{0,1}}{a_{0,0}}\right)_R , \qquad (11)$$

where x_L is defined so that $|a|$ is proportional to $\exp(-((x - x_L)^2 + y^2)/r_s^2)$

and $( )_R$ denotes the real part. Figure 3 shows the electron and radiation

beam centroids, $x_b = x_c (1-\text{sech}(k_c z))$ and x_L for $x_c = r_b/4 = .075\text{cm}$

and $\lambda_c = 2\pi/k_c = z_R/4 = 2.7\text{m}$. In these numerical illustrations, 10 radial

6

modes and 2 angular modes were used. After an initial transient, the radiation centroid is guided by and oscillates about the electron beam's centroid. We have also studied the situation where the electron beam centroid oscillates according to $x_b = x_c \sin k_c z$ with $x_c \ll r_b$ and $\lambda_c = 2\pi/k_c \lesssim z_R$. Because of the high gain in the radiation field the radiation centroid eventually follows the average position of the electron beam's centroid. When the electron beam centroid oscillation is due to the wiggler field, there is no change in the evolution of the radiation field.

Under certain conditions the electron beam envelope can be spatially modulated about the z-axis if the weak focusing force due to the wiggler gradient is not balanced by the defocusing forces arising from emittance and self field effects. It can be shown that the amplitude and waist of the radiation field undergo a modulation similar to the electron beam envelope modulation.

We have analyzed, using the SDE formalism, a number of effects associated with radiation focusing and guiding in the FEL. This approach can be readily generalized to include both spatial and temporal variations in the radiation field in order to study sideband generation and focusing effects simultaneously in the FEL.

Table I

Electron Beam

Current	I_b = 2kA, (ν = 0.118)
Energy	ε_b = 50 MeV, (γ = 100)
Radius	r_{b0} = 0.3 cm

Radiation Beam

Wavelength	λ = 10.6μm
Input Power	$P(z=0)$ = 230MW, ($|a(0,0)|$ = 1.84×10^{-4})
Spot Size	$r_s(0)$ = 0.6 cm, (z_R = 10.7 m)

Wiggler Field

Wavelength	λ_w = 8 cm
Wiggler Strength	B_w = 2.3 kG, (a_w = 1.716)
Resonant Phase	ψ_R = 0.358 rad

References

1. P. Sprangle and R. Smith, Phys. Rev. A, $\underline{21}$(1), 293 (1980).

2. P. Sprangle, C. M. Tang and W. Manheimer, Phys. Rev. A, $\underline{21}$(1), 302 (1980).

3. N. M. Kroll, P. L. Morton and M. N. Rosenbluth, IEEE J. Quantum Electron, QE-17, 1436 (1981).

4. P. Sprangle and C. M. Tang, Appl. Phys. Lett. $\underline{39}$(9), 677 (1981), also AIAA Journal, $\underline{19}$(9), 1164 (1981).

5. Free Electron Lasers, Proceedings of the 7th Intl. Conf. on FELs, Tahoe City, Sept. 8-13, 1985, edited by E. T. Scharlemann and D. Prosnitz (North-Holland-Amsterdam).

6. M. Xie, D. A. G. Deacon, ibid, p. 426.

7. E. T. Scharlemann, A. M. Sessler and J. S. Wurtele, Phys. Rev. Lett. $\underline{54}$ (17), 1925 (1985).

8. G. T. Moore, Opt. Comm., $\underline{52}$, 46 (1984), $\underline{54}$, 121 (1985).

9. G. T. Moore, Nucl. Inst. Meth. Phys. Res., $\underline{A239}$, 19 (1985).

10. G. I. Bourianoff, B. N. Moore, M. N. Rosenbluth, F. Waelbroeck, H. Waelbroeck, H. V. Wong, Bull. Am. Phys. Soc., $\underline{31}$, 1539 (1986).

11. C. M. Tang and P. Sprangle, IEEE J. of Quantum Electronics, QE-21, 970 (1985).

12. D. Prosnitz, A. Szoke and V. K. Neil, Phys. Rev. A $\underline{24}$, 1436 (1981).

13. B. Hafizi, P. Sprangle, A. Ting (to be published).

14. E. T. Scharlemann, J. Appl. Phys. $\underline{58}$(6), 2154 (1985).

Figure Captions

Fig. 1   Radiation amplitude on axis, $|a(0,z)|$ for a) exact numerical

solution (64x64 Fourier modes), b) vacuum modal expansion solution

(10 modes), and c) SDE solution (10 modes) at distance of

$z = 4z_R = 42.8$ m.

Fig. 2   Evolution of the radiation beam radius, 1/e widtn. r_L, for initial

spot sizes: a) 0.35 cm, b) 0.24 cm, and c) 0.15 cm.

Fig. 3   Electron and radiation beam centroids, x_b and x_L for a displaced

electron beam, $x_b = x_c(1-\text{sech}(k_c z))$ with $x_c = r_b/4$ and

$\lambda_c = 2\pi/k_c = z_R/4$.

Table Caption

Table I.   FEL simulation parameters
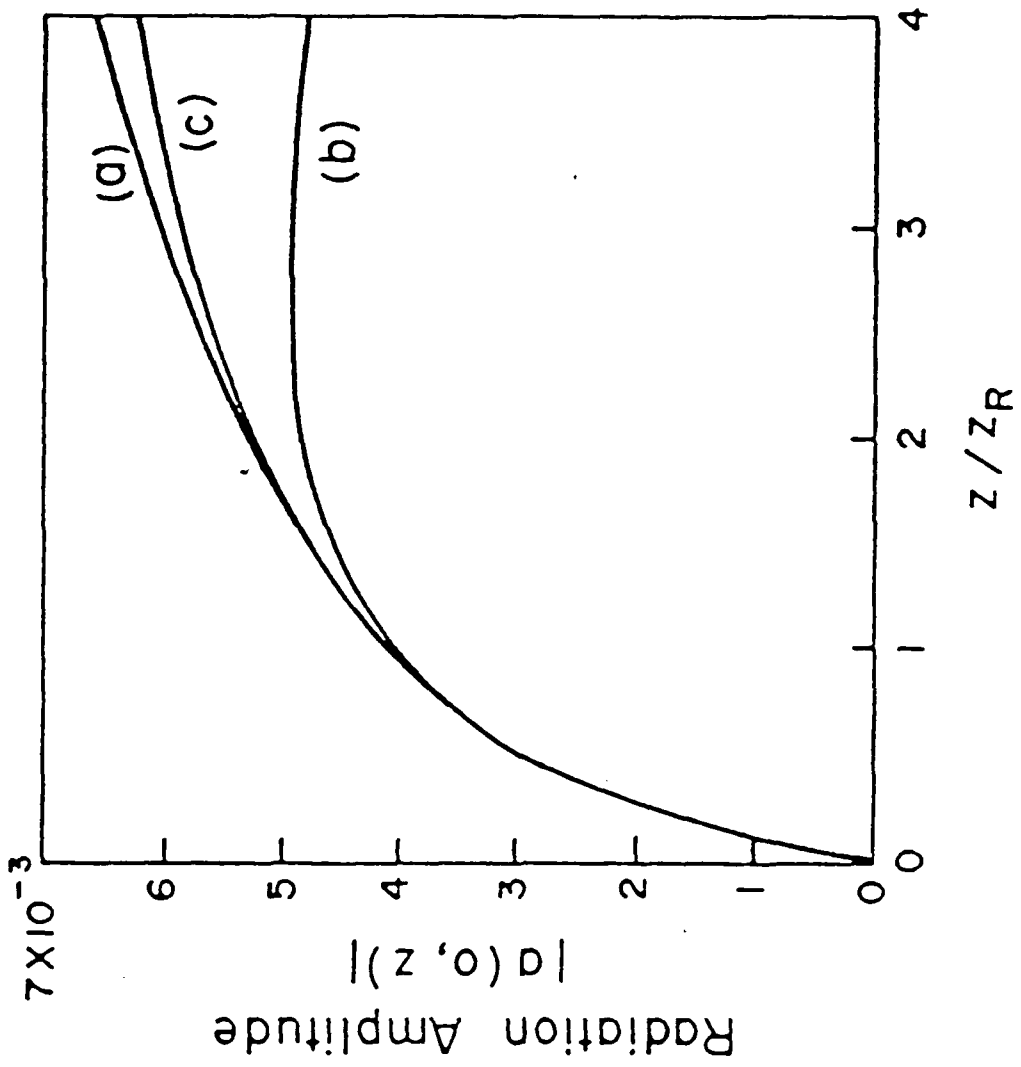
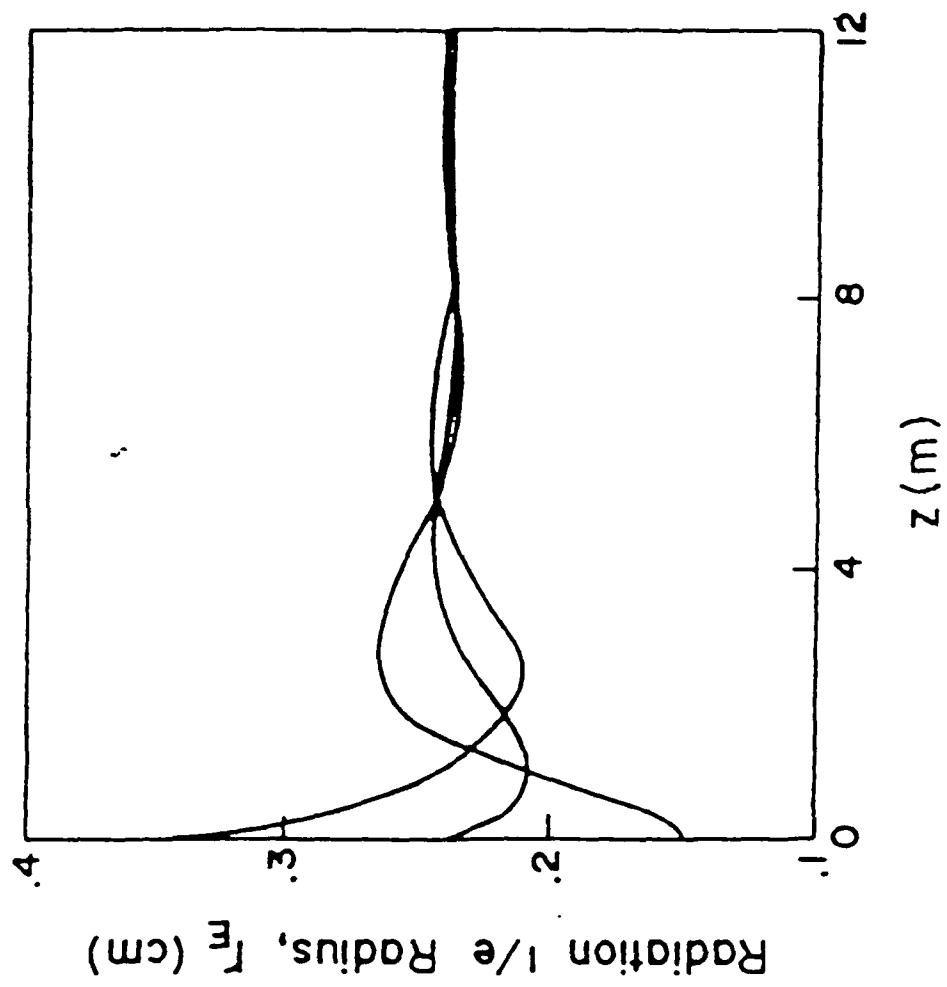Fig. 1

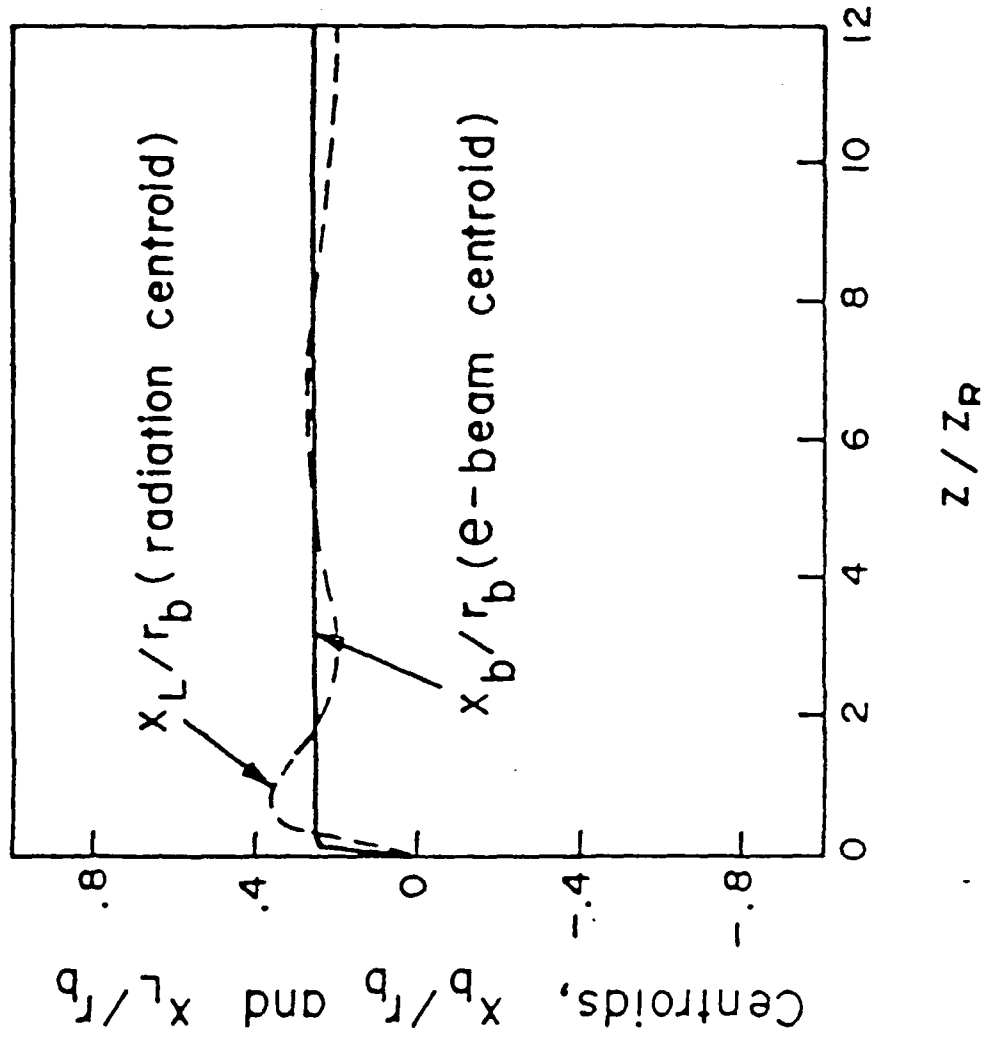**Radiation Amplitude** $|a(o,z)|$

z/z_R

Radiation 1/e Radius, r_E (cm)

z (m)

Fig. 2

Fig. 3

Appendix III:

Analysis of radiation focusing and steering in
the Free Electron Laser by use of a source dependent
expansion technique

II. Formulation of the Source Dependent Expansion (SDE)

The radiation focusing and guiding configuration for the FEL is shown in Fig. 1. In our model the vector potential of the linearly polarized radiation field is

$$\underset{\sim}{A}_R(r,\theta,z,t) = \frac{A(r,\theta,z)}{2} e^{i(\omega z/c-\omega t)} \hat{e}_x + c.c., \qquad (1)$$

where $A(r,\theta,z)$ is the complex radiation field amplitude, ω is the frequency and c.c. denotes the complex conjugate.

The wave equation is

$$\left(\frac{1}{r}\frac{\partial}{\partial r}\left(r\frac{\partial}{\partial r}\right) + \frac{1}{r^2}\frac{\partial^2}{\partial\theta^2} + \frac{\partial^2}{\partial z^2} - \frac{1}{c^2}\frac{\partial^2}{\partial t^2}\right)\underset{\sim}{A}_R = -\frac{4\pi}{c}J_x\hat{e}_x, \qquad (2)$$

where $J_x(r,\theta,z,t)$ is the driving current density associated with the medium. Substituting (1) into (2) leads to the following reduced wave equation,

$$\left(\frac{1}{r}\frac{\partial}{\partial r}\left(r\frac{\partial}{\partial r}\right) + \frac{1}{r^2}\frac{\partial^2}{\partial\theta^2} + 2i\frac{\omega}{c}\frac{\partial}{\partial z}\right)a(r,\theta,z) = S(r,\theta,z), \qquad (3)$$

where $a(r,\theta,z) = |e|A/m_oc^2 = |a|\exp(i\phi)$ is the normalized complex radiation field amplitude and we have assumed that $a(r,\theta,z)$ is a slowly varying function of z, i.e., $a^{-1}\partial a/\partial z \ll \omega/c$. The amplitude, $|a(r,\theta,z)|$, and phase $\phi(r,\theta,z)$ are real functions expressed in terms of the polar coordinates, r,θ and z. The source function, S, has the general form

$$S(r,\theta,z) = \frac{\omega^2}{c^2}(1-n^2(r,\theta,z,a))a(r,\theta,z), \qquad (4)$$

where $n(r,\theta,z,a)$ is the index of refraction associated with the medium and is in general complex and a function of r,θ,z as well as the radiation field, a.

We choose the following representation for $a(r, \theta, z)$ in terms of associated Laguerre polynomials,

$$a(r, \theta, z) = \sum_m \sum_p C_{m,p}(\theta, z) D_m^p(r), \qquad (5)$$

where $m = 0, 1, 2, \cdots$, $p = 0, 1, 2, \cdots$,

$$C_{m,p}(\theta, z) = a_{m,p}(z)\cos p\theta + b_{m,p}(z)\sin p\theta, \qquad (6a)$$

$$D_m^p(r) = \left(\frac{\sqrt{2}r}{r_s(z)}\right)^p L_m^p \left(\frac{2r^2}{r_s^2(z)}\right) e^{-(1 - i\alpha(z))r^2/r_s^2(z)}. \qquad (6b)$$

In Eqs. (6a,b), the complex coefficients $a_{m,p}(z)$ and $b_{m,p}(z)$ are functions of z, $r_s(z)$ is the radiation spot size, $\alpha(z)$ is related to the inverse of the radius of curvature of the radiation beam (curvature of wavefront) and L_m^p is the associated Laguerre polynomial. Solving for the unknown quantities $a_{m,p}$, $b_{m,p}$, r_s and α in terms of the source term S allows us to completely describe the radiation dynamics. It will be shown later that the representation in (5) is underspecified, there are more unknown quantities in (5) than available equations. The additional degrees of freedom in our representation allow us to specify particular functional relationships for the unknown quantities r_s and α in such a way that the number of terms (modes needed to accurately describe the radiation beam) is small.

To proceed with the derivation we substitute (5) into (3) and obtain

$$\sum_{m,p} \left[\partial C_{m,p}(\theta, z)/\partial z + C_{m,p}(\theta, z)\left\{\frac{\partial}{\partial z} - \frac{4ic}{\omega r_s^2} \left[\frac{\partial}{\partial \xi}\left(\xi \frac{\partial}{\partial \xi}\right) - \frac{p^2}{4\xi}\right]\right\}\right] D_m^p(\xi)$$

$$= -\frac{ic}{2\omega} S(\xi, \theta, z), \qquad (7)$$

5

where $\xi = 2r^2/r_s^2(z)$. It can be shown that the second term on the left side of (7) can be put into the form

$$\left\{\frac{\partial}{\partial z} - \frac{4ic}{\omega r_s^2}\left[\frac{\partial}{\partial \xi}\left(\xi \frac{\partial}{\partial \xi}\right) - \frac{p^2}{4\xi}\right]\right\}D_m^p(\xi)$$

$$= A_{m,p}(z)D_m^p(\xi) - i(m+1)B(z)D_{m+1}^p(\xi) - i(m+p)B^*(z)D_{m-1}^p(\xi), \qquad (8)$$

where

$$A_{m,p}(z) = r_s'/r_s + i(2m+p+1)\left[(1 + \alpha^2)c/\omega r_s^2 - \alpha r_s'/r_s + \alpha'/2\right], \qquad (9a)$$

$$B(z) = -\left(\alpha r_s'/r_s + (1 - \alpha^2)c/\omega r_s^2 - \alpha'/2\right) - i\left(r_s'/r_s - 2\alpha c/\omega r_s^2\right), \qquad (9b)$$

* denotes the complex conjugate and the prime denotes a derivative with respect to z, i.e., ′ = $\partial/\partial z$.

In obtaining (8) the following identities were used:

$$\xi U_m^p = (2m+p+1)U_m^p - (m+1)U_{m+1}^p - (m+p)U_{m-1}^p,$$

$$2\xi \partial U_m^p/\partial \xi = (2m+p-\xi)U_m^p - 2(m+p)U_{m-1}^p, \text{ and}$$

$$\xi \partial^2 U_m^p/\partial \xi^2 + \partial U_m^p/\partial \xi = (1/4)\left(\xi + p^2/\xi - 2(2m+p+1)\right)U_m^p,$$

where $U_m^p(\xi) = \xi^{p/2}L_m^p(\xi)\exp(-\xi/2)$. Substituting (8) into (7) and performing the operation

$$\int_0^{2\pi} (\cos p'\theta, \sin p'\theta)d\theta/2\pi,$$

on the resulting equation yields

6

$$\sum_{m=0}^{\infty} \left[D_m^p \left(\partial/\partial z + A_{m,p} \right) \begin{pmatrix} a_{m,p} \\ b_{m,p} \end{pmatrix} - i \left((m+1)B \ D_{m+1}^p + (m+p)B^* D_{m-1}^p \right) \begin{pmatrix} a_{m,p} \\ b_{m,p} \end{pmatrix} \right]$$

$$= \frac{-ic}{2\pi\omega} \int_0^{2\pi} d\theta \ S(\xi,\theta,z) \begin{pmatrix} (1+\delta_{p,o})^{-1}\cos p\theta \\ \sin p\theta \end{pmatrix}, \qquad (10a,b)$$

where $\delta_{p,o}$ is the Kronecker delta. Multiplying (10) by $(D_n^p)^*$ and integrating over ξ from 0 to ∞ yields

$$\left(\frac{\partial}{\partial z} + A_{m,p}(z) \right) \begin{pmatrix} a_{m,p} \\ b_{m,p} \end{pmatrix} - imB(z) \begin{pmatrix} a_{m-1,p}(z) \\ b_{m-1,p}(z) \end{pmatrix} - i(m+p+1)B^*(z) \begin{pmatrix} a_{m+1,p}(z) \\ b_{m+1,p}(z) \end{pmatrix}$$

$$= -i \begin{pmatrix} F_{m,p}(z) \\ G_{m,p}(z) \end{pmatrix}, \qquad (11a,b)$$

where

$$\begin{pmatrix} F_{m,p}(z) \\ G_{m,p}(z) \end{pmatrix} = \frac{c}{2\pi\omega} \frac{m!}{(m+p)!} \int_0^{2\pi} d\theta \int_0^{\infty} d\xi \ S(\xi,\theta,z) \left(D_m^p(\xi) \right)^* \begin{pmatrix} (1+\delta_{p,0})^{-1}\cos p\theta \\ \sin p\theta \end{pmatrix}.$$

$$(12a,b)$$

In obtaining (11) we used the orthogonality relation,

$$\int_0^{\infty} D_m^p(\xi) \left(D_n^p(\xi) \right)^* d\xi = \frac{(n+p)!}{n!} \ \delta_{m,n}.$$

The function $B(z)$ is arbitrary and is not specified. The equations for $a_{m,p}$ and $b_{m,p}$ in (11) are underdetermined, since the function $B(z)$ can be shown to be arbitrary. If we choose $B(z) = 0$, for example, we would in effect be expanding the radiation field in the conventional vacuum Laguerre-Gaussian modes.[11] We will show later that, in general, expansion

in terms of the vacuum modes, $B = 0$, would require far too many modes to accurately describe the radiation beam over distances of many Rayleigh lengths. A more appropriate choice for $B(z)$ will depend on the particular problem under consideration. Let us consider one of the most common situations where the radiation beam at $z = 0$ is known and has a Gaussian radial profile symmetric about the z-axis. In this case the complex radiation amplitude at $z = 0$, is given by $a(r,\theta,0) = a_{0,0} \exp$ $(-(1 - i\alpha(0))r^2/r_s^2(0))$ and is independent of θ. Let us further assume that for $z > 0$ the radiation beam profile remains approximately Gaussian with a nearly circular cross section. That is, the dominant part of the source $S(r,\theta,z)$ has an r and z dependence and the θ dependent part is weak. In this case we expect the magnitude of the coefficients, $a_{m,p}(z)$ and $b_{m,p}(z)$ to become progressively smaller as m and p take on larger values, i.e., $|a_{m,p}| \gg |a_{m+1,p}|$, $|a_{m,p+1}|$ and $|b_{m,p}| \gg |b_{m+1,p}|$, $|b_{m,p+1}|$. The lowest order approximation to the radiation beam is given by the $a_{0,0}(z)$ mode. Hence, if the $a_{0,0}$ mode gives a rough approximation to the radiation field we may solve for $a_{0,0}(z)$, $r_s(z)$ and $\alpha(z)$ using (11a). From (11a) we find that only the $m = 0,1$ and $p = 0$ equations are relevant and yield

$$(\partial/\partial z + A_{0,0})a_{0,0} = - iF_{0,0}, \tag{13a}$$

$$Ba_{0,0} = F_{1,0}. \tag{13b}$$

We now have a specific expression for $B(z)$, from (13b), in terms of one of the moments, $F_{1,0}$, of the source term. Substituting (9b) into $B(z) = F_{1,0}(z)/a_{0,0}(z)$ yields the following first order coupled differential equations for r_s and α

$$r_s' - 2c\alpha/\omega r_s = - r_s(F_{1,0}/a_{0,0})_I, \tag{14a}$$

8

$$\alpha' - 2(1 + \alpha^2)c/\omega r_s^2 = 2\left((F_{1,0}/a_{0,0})_R - \alpha(F_{1,0}/a_{0,0})_I\right), \quad (14b)$$

where $(\quad)_{R,I}$ denotes the real and imaginary part of the enclosed function. Since $r_s(z)$ and $\alpha(z)$ are now known from (14a,b) we may solve for $A_{m,p}(z)$ using (9a),

$$A_{m,p}(z) = 2c\alpha/\omega r_s^2 - (F_{1,0}/a_{0,0})_I$$
$$+ i(2m+p+1)\left(2c/\omega r_s^2 + (F_{1,0}/a_{0,0})_R\right). \quad (15)$$

Using $B(z) = F_{1,0}(z)/a_{0,0}(z)$ and the resulting equations for r_s and α in (14) allows us to solve for $a_{m,p}$ and $b_{m,p}$ in (11a,b).

It is useful at this point to consider the simple case of propagation of a radiation beam in vacuum (no source term). To illustrate this well-known limit we evaluate $a_{m,p}$, $b_{m,p}$, r_s and α in the source-free case, $F_{m,p} = G_{m,p} = B = 0$. Equations (14a,b) become $r_s'' = (2c/\omega)^2/r_s^3$ and $\alpha = (\omega/2c)r_s r_s'$ and have the solutions

$$r_s(z) = r_s(0)(1 + z^2/z_R^2)^{1/2}, \quad (16a)$$

$$\alpha(z) = z/z_R, \quad (16b)$$

where $r_s(0)$ is the minimum radiation spot size at $z = 0$, $z_R = (\omega/2c)r_s^2(0) = \pi r_s^2(0)/\lambda$ is the Rayleigh length and $\lambda = 2\pi c/\omega$ is the wavelength. From (10a) we find that $A_{m,p}(z) = 2(\alpha(z) + i(2m+p+1))c\omega r_s^2(z)$ which allows us to solve for $a_{m,p}$ and $b_{m,p}$ using (11)

$$\begin{pmatrix} a_{m,p}(z) \\ b_{m,p}(z) \end{pmatrix} = \begin{pmatrix} a_{m,p}(0) \\ b_{m,p}(0) \end{pmatrix} \left(r_s(0)/r_s(z)\right) e^{-i(2m+p+1)\tan^{-1}(z/z_R)}. \quad (17)$$

Equations (16a,b) and (17) together with the representation in (5), (6a,b) is in agreement with the conventional vacuum Gaussian-Laguerre form.

III. Radiation Focusing and Steering in FELs

A. Radiation Beam Envelope Equation

We first consider the dynamics of an axially symmetric radiation field in the FEL. For a linearly polarized wiggler field and axially symmetric electron beam having a Gaussian density profile, the appropriate index of refraction for the FEL mechanism[4,5,9,12] is

$$n(r,z,a) = 1 + \frac{1}{2} \frac{\omega_b^2(r,z)}{\omega^2} \left\langle \frac{e^{-i\psi}}{\gamma} \right\rangle \frac{a_w}{|a(r,z)|} \quad , \qquad (18)$$

where $\omega_b^2(r,z) = \omega_{bo}^2 (r_{b0}/r_b(z))^2 \exp(-r^2/r_b^2(z))$, $r_b(z)$ is the electron beam radius, $r_{b0} = r_b(0)$, $\omega_{b0} = (4\pi|e|^2 n_{b0}/m_0)^{1/2}$ is the initial beam plasma frequency on axis, n_{b0} is the initial beam density on axis, $a_w = |e|B_w/k_w m_0 c^2$ is the normalized wiggler amplitude, B_w is the wiggler magnetic field strength, k_w is the wiggler wave number, γ is the electron's Lorentz factor, ψ is the electron's phase in the ponderomotive wave potential and $\langle \ \rangle$ denotes the ensemble average over all electrons. Substituting (18) into (4) and noting that $|1-n|\ll1$, gives the FEL source function

$$S(r,z) = \frac{-\omega_b^2(r,z)}{c^2} a_w \left\langle \frac{e^{-i\psi}}{\gamma} \right\rangle \frac{a(r,z)}{|a(r,z)|} \quad . \qquad (19)$$

Since the electron beam radius, r_b, may not be matched with respect to the focusing fields (wiggler gradients) and defocusing effects (beam emittance) we allow r_b to be a function of z (this case is considered in Sec. IIIC). To proceed with the analysis we assume that in the source function the complex radiation field amplitude in (5) can be approximated by the lowest order mode, $a_{0,0}(z)\exp(-(1-i\alpha)r^2/r_s^2)$. With this assumption the source function can be written as

$$S(\xi,z) = -4\nu(a_w/r_b^2)\ \frac{a_{0,0}}{|a_{0,0}|}\ \left\langle\frac{e^{-i\psi}}{\gamma}\right\rangle e^{-\left(r_s^2/r_b^2-i\alpha\right)\xi/2}, \qquad (20)$$

where $\nu = (\omega_{bo}\ r_{bo}/2c)^2 = I_b/17\times10^3$ is Budker's constant and I_b is the electron beam current in amperes. The moments of the source function, $F_{m,p}(z)$, are given by (12a)

$$F_{m,0} = -4\ \frac{c}{\omega}\ \nu(a_w/r_b^2)\ \frac{a_{0,0}}{|a_{0,0}|}\ \left\langle\frac{e^{-i\psi}}{\gamma}\right\rangle \frac{(r_s^2/r_b^2-1)^m}{(r_s^2/r_b^2+1)^{m+1}}, \qquad (21)$$

where we have assumed ψ to be constant across the electron beam. Since we are considering an axially symmetric electron beam and radiation field we note that $a_{m,p} = F_{m,p} = G_{m,p} = 0$ for $p > 0$. Substituting (21) into (14a,b) and (15) yields

$$r_s r_s' - 2c\alpha/\omega = -2\frac{c}{\omega}\ C(z)\ \langle\sin\ \psi\rangle, \qquad (22a)$$

$$r_s^2\alpha' - 2(1 + \alpha^2)c/\omega = -4\frac{c}{\omega}\ C(z)\ \left(\langle\cos\ \psi\rangle + \alpha\ \langle\sin\ \psi\rangle\right), \qquad (22b)$$

$$A_{m,0}(z)= \frac{2c}{r_s^2\omega}\left[\alpha + i(2m+1) - C(z)\ \left(\langle\sin\ \psi\rangle+i(2m+1)\langle\cos\psi\rangle\right)\right], \qquad (22c)$$

where $C(z) =(2\nu/\gamma)H(z)a_w/|a_{0,0}(z)|$, $H(z) =(1-F)/(1+F)^2$ and $F(z) = r_b^2/r_s^2$ is the filling factor. The function $C(z)$ measures the coupling between the radiation and electron beam and decreases as the radiation grows.

Equations (22a) and (22b) can be combined to give the following envelope equation for the radiation beam

$$r_s'' + K^2(z,r_b,r_s,|a_{0,0}|)r_s = 0, \qquad (23a)$$

where the initial condition on r_s' is found from (22a) and

11

$$K^2 = (2c/\omega)^2 \left[-1 + C^2 \langle \sin\psi \rangle^2 + 2C \langle \cos\psi \rangle + (\omega/2c) r_s^2 \, C' \langle \sin\psi \rangle \right] r_s^{-4}.$$

(23b)

The first term on the right-hand side of (23b) is defocusing and corresponds to the usual diffraction expansion, the second and third terms are always focusing while the last term is a defocusing contribution.

B. Radiation Focusing

Focusing occurs when $K^2 \geq 0$. In the high gain trapped particle regime, the condition for a perfectly guided beam ($K = 0$) cannot be maintained since K^2 decreases as the radiation grows. In the small signal, exponential gain regime the quantities $\langle \sin\psi \rangle$ and $\langle \cos\psi \rangle$ may be calculated from the linearized orbit equations. The envelope equation may then be solved to determine r_s as a function of distance along the wiggler. One finds that in this regime, conditions for a perfectly guided radiation beam can be achieved.[13]

Using (11a) or (13a) we find that the magnitude of $a_{0,0}(z)$ evolves according to

$$(\partial/\partial z + (A_{0,0} + A_{0,0}^\star)) |a_{0,0}|^2 = -i(F_{0,0} \, a_{0,0}^\star - F_{0,0}^\star a_{0,0}).$$

(24)

Substituting (21) and (22c) with $m = 0$ into (24) and using (22a) yields

$$\frac{\partial}{\partial z} (r_s |a_{0,0}|) = \frac{4c}{\omega} \frac{\nu}{\gamma} a_w \frac{r_s \langle \sin\psi \rangle}{(r_s^2 + r_b^2)},$$

(25)

where $(r_s |a_{0,0}|)^2$ is proportional to the radiation power, $P(z) = 2.15 \times 10^{10} (|a_{0,0}(z)| r_s/\lambda)^2$ [Watts]. Equation (25) should be solved together with (23a) and show that the maximum rate of increase in power occurs when $r_s = r_b$.

C. Radiation Steering in the FEL

In the FEL the centroid of the electron beam may be displaced off-axis by a misalignment, a redirection of the beam or because of the oscillations in the wiggler field. To determine the degree to which the radiation beam will follow or be steered by the electron beam, we consider the case where the electron beam centroid is displaced transversely in the x direction. The index of refraction in this case is given by (18) with $\omega_b^2(r,z)$ replaced by

$$\omega_b^2(r,\theta,z) = \omega_{b0}^2(r_{b0}/r_b)^2 \, e^{-r^2/r_b^2} \left(1 + (2rx_b(z)/r_b^2)\cos\theta\right), \qquad (26)$$

where $x_b(z)$ is the displacement of the electron beam's centroid and $|x_b| \ll r_b$. In the source term, given by (19), we consider only the lowest order symmetric and anti-symmetric mode with respect to the x axis, $a(r,\theta,z) \sim (a_{0,0} + a_{0,1} \, \xi^{1/2} \cos\theta)\exp(-(1-i\alpha)\xi/2)$. With this assumption the moments of the source function, $F_{m,p}(z)$, for $p = 0,1$ are,

$$F_{m,p} = -8 \, \frac{c}{\omega} \, \nu(a_w/r_b^2)\left\langle\frac{e^{-i\psi}}{\gamma}\right\rangle \frac{a_{0,0}}{|a_{0,0}|}\left(\varepsilon(z) + i\left(\frac{a_{0,1}}{a_{0,0}}\right)_I\right)^p \frac{(r_s^2/r_b^2 - 1)^m}{(r_s^2/r_b^2 + 1)^{m+p+1}} ,$$

$$(27)$$

where $\varepsilon(z) = 2^{1/2} \, x_b(z)r_s(z)/r_b^2$ and $G_{m,p} = 0$. For small displacements of the electron beam centroid it is easy to show that the centroid of the radiation beam is given by

$$x_L(z) = \frac{r_s(z)}{\sqrt{2}} \left(\frac{a_{0,1}}{a_{0,0}}\right)_R , \qquad (28)$$

where x_L is defined so that $|a|$ is proportional to $\exp(-((x - x_L)^2 + y^2)/r_s^2)$.

13

D. Effect of a Modulated Electron Beam

The electron beam envelope in the FEL can undergo modulations. The modulation is symmetric about the z-axis and can be caused by improper values for the beam emittance, radius and/or current injected into the wiggler region. For small perturbations about the matched beam radius, r_{b0}, we find from the electron beam envelope equation that $r_b(z) = r_{b0}$ $(1 + \Delta \sin(K_B z))$ where $r_{b0} = (2\varepsilon_n/a_w k_w)^{1/2}$, $K_B = a_w k_w/\sqrt{2}\gamma$ is the betatron wave number, due to the weak focusing effect of wiggler gradients, ε_n is the normalized emittance, $a_w = |e|B_w/(k_w m_0 c^2)$ and $\Delta \ll 1$. The modulation of the electron beam envelope may be included in the source term, Eq. (19), through the electron beam plasma frequency, $\omega_b(r,z)$. The effect of a modulated electron beam on the radiation beam is illustrated in the next section.

In cases where the electron beam centroid or envelope is displaced or modulated with a spatial period close to the wiggler period, it becomes necessary to include in the source function, Eq. (19), the rapidly varying part of the phase ψ. This rapidly oscillating contribution to the phase, $(a_w^2/(4 + 2a_w^2))\sin 2k_w z$, arises from the linearly polarized wiggler field.

IV. Numerical Results

In this section we apply the SDE formulation, given by (11) together with (12) to the FEL. Using the source term given in (4) and (18) we first present a comparison between; a) the exact numerical solution of the wave equation in (4), (using 64x64 Fourier modes), b) the solution obtained using a vacuum Laguerre modal expansion (B=0, using 10 modes) and c) the solution obtained from the Laguerre SDE approach (B = $F_{1,0}/a_{0,0}$, using 10 modes). The FEL parameters used in these illustrations are similar to those used in Ref. 14 and are given in Table I where the resonant phase approximation, $\langle \exp(-i\psi) \rangle = \exp(-i\psi_R)$, is used for demonstration purposes. Propagation distances are measured in terms of the Rayleigh length, $z_R = \pi r_s^2(0)/\lambda$ where λ is the wavelength and $r_s(0)$ is the minimum spot size.

For an axially symmetric configuration, Fig. 2 shows the radiation magnitude, $|a(r,z)|$ as a function of r at four Rayleigh lengths ($z = 4z_R = 42.8m$) for the (a), (b) and (c) methods of solution. The SDE solution (c) shows excellent agreement with solution (a), while solution (b) is in poor agreement. To continue this comparison we show in Fig. 3 the evolution of the radiation beam amplitude on-axis obtained from methods (a), (b) and (c) as a function of propagation distance. The SDE solution (c) is again in good agreement with solution (a) where as solution (b), beyond a Rayleigh length, grossly deviates from (a) and (c). The results in Figs. 2 and 3 clearly show the improved accuracy of the SDE approach over the conventional vacuum expansion method. As an example of radiation focusing, for an FEL in the small signal, exponential gain regime, the radiation beam radius is found to asymptotically approach a matched perfectly guided value as shown in Fig. 4. For this example, the parameters of Table I were used and five modes employed.

15

We now use the SDE method to illustrate the steering of the radiation beam when the electron beam is displaced off-axis. In these numerical illustrations, 10 radial modes ($m = 0,\ldots,9$) and 2 angular modes ($p = 0,1$) were used. In the first example, the electron beam centroid is displaced off-axis according to $x_b = x_c (1-\text{sech}(k_c z))$. Figure 5 shows the electron and radiation beam centroids x_b and x_L for $x_c = r_b/4 = 0.075$cm and $\lambda_c = 2\pi/K_c = 4z_R = 42.8$m. The radiation centroid follows and oscillates about the electron beam's centroid. Figure 6 shows the radiation profile at twelve Rayleigh lengths ($z = 12\ z_R$). The asymmetry of the radiation profile is apparent. Figure 7 shows another illustration of steering where the electron beam is displaced more abruptly, with $\lambda_c = z_R/4 = 2.7$m. After an initial transient, the radiation centroid is again steered by and oscillates about the electron beam's centroid. In the next example we take the electron beam centroid to be oscillating about the z-axis, $x_b = x_c \sin k_c z$, with amplitude $x_c = r_b/4$ and period $\lambda_c = z_R = 10.7$m. Figure 8 shows the electron and radiation centroids x_b and x_L, as a function of z/z_R. Because of the high gain in the radiation field, the radiation centroid eventually follows the average position of the electron beam's centroid. Figure 9 shows the distortion of the radiation profile due to the oscillating electron beam at twelve Rayleigh lengths ($z = 12z_R$). In the case where the electron beam centroid oscillation is due to the wiggler field, $x_c = a_w/\gamma k_w$ and $k_c = 2\pi/\lambda_w$, no noticeable change in the evolution of the radiation field (compared to the case for $x_c = 0$) is observed.

The last illustration is for the case where the electron beam envelope is spatially modulated. Using the parameters in Table I we find that $\varepsilon_n = 0.06$ cm-rad and $\lambda_B = 2\pi/K_B = 4.66$m. Figure 10 shows the amplitude of the radiation field on-axis as a function of propagation distance when the electron beam envelope is not matched, $r_b = r_{b0} (1 + \Delta \sin(K_B z))$, where $r_{b0} = 0.3$cm and $\Delta = 0.1$.

16

V. Conclusion

In this paper a technique for solving the three-dimensional wave equation with a driving current density has been developed. Using this source dependent expansion technique, a number of effects associated with radiation focusing and steering in the FEL have been illustrated. The formalism is used to derive a general envelope equation for the radiation beam. Using the envelope equation, we find that it is possible to have a stable guided optical beam in the exponential gain (small signal) regime but not in the high gain trapped particle regime. We also considered the effects on the radiation beam when the electron beam centroid is transversely displaced and when the electron beam envelope is modulated. The source dependent expansion approach lends itself to fast and accurate numerical solutions as well as to a better analytical description of focusing and steering in the FEL. We conclude by noting that this approach can be readily generalized to include both spatial and temporal variations in the radiation field in order to study sideband generation and focusing effects simultaneously in the FEL.

References

1. P. Sprangle and R. Smith, Phys. Rev. A $\underline{21}$(1), 293 (1980).

2. N. M. Kroll, P. L. Morton and M. N. Rosenbluth, IEEE J. Quantum Electron. $\underline{QE-17}$, 1436 (1981).

3. P. Sprangle, C. M. Tang and W. Manheimer, Phys. Rev. A $\underline{21}$(1),302 (1980).

4. P. Sprangle and C. M. Tang, Appl. Phys. Lett. $\underline{39}$(9), 677 (1981), also AIAA Journal, $\underline{19}$(9), 1164 (1981), also C. M. Tang and P. Sprangle, Free Electron Generator of Coherent Radiation, Phys. of Quantum Electron. $\underline{19}$, Addison-Wesley (1982).

5. E. T. Scharlemann, A. M. Sessler and J. S. Wurtele, Phys. Rev. Lett. $\underline{54}$ (17), 1925 (1985).

6. M. Xie, D. A. G. Deacon, Nucl. Instr. Meth. Phys. Res. $\underline{A250}$, 426 (1986).

7. G. T. Moore, Opt. Comm. $\underline{52}$, 46 (1984), $\underline{54}$, 121 (1985).

8. G. T. Moore, Nucl. Inst. Meth. Phys. Res. $\underline{A239}$, 19 (1985).

9. Free Electron Lasers, Proceedings of the 7th Intl. Conf. on FELs, Tahoe City, Sep 8-13, 1985, edited by E. T. Scharlemann and D. Prosnitz (North-Holland-Amsterdam).

10. G. I. Bourianoff, B. N. Moore, M. N. Rosenbluth, F. Waelbroeck, H. Waelbroeck, H. V. Wong, Bull. Am. Phys. Soc. $\underline{31}$, 1539 (1986).

11. C. M. Tang and P. Sprangle, IEEE J. of Quantum Electron. $\underline{QE-21}$, 970 (1985).

12. D. Prosnitz, A. Szoke and V. K. Neil, Phys. Rev. A $\underline{24}$, 1436 (1981).

13. B. Hafizi, P. Sprangle and A. Ting (to be published).

14. E. T. Scharlemann, J. Appl. Phys. $\underline{58}$(6), 2154 (1985).

Table I

Electron Beam

Current	I_b = 2kA, (ν = 0.118)
Energy	ε_b = 50 MeV, (γ = 100)
Radius	r_{b0} = 0.3 cm

Radiation Beam

Wavelength	λ = 10.6μm
Input Power	$P(z=0)$ = 230MW, ($|a(0,0)|$ = 1.84×10^{-4})
Spot Size	$r_s(0)$ = 0.6 cm, (z_R = 10.7 m)

Wiggler Field

Wavelength	λ_w = 8 cm
Wiggler Strength	B_w = 2.3 kG, (a_w = 1.716)
Resonant Phase	ψ_R = 0.358 rad

Figure Captions

Fig. 1 Schematic of radiation focusing and guiding in an FEL.

Fig. 2 Radiation amplitude profile, $|a(r,z)|$ for; a) exact numerical solution (64x64 Fourier modes), b) vacuum modal expansion solution (10 modes), and c) SDE solution (10 modes) at a distance of $z = 4z_R$ = 42.8 m.

Fig. 3 Radiation amplitude on axis, $|a(0,z)|$ for; a) exact numerical solution (64x64 Fourier modes), b) vacuum modal expansion solution (10 modes), and c) SDE solution (10 modes).

Fig. 4 Spatial evolution of the radiation spot size in the exponential gain regime for initial spot sizes; a) 0.35 cm, b) 0.24cm, and c) 0.15 cm.

Fig. 5 Electron and radiation beam centroids, x_b and x_L for a displaced electron beam, $x_b = x_c(1-\text{sech}(k_c z))$ with $x_c = r_b/4$ and $\lambda_c = 2\pi/k_c = 4z_R$.

Fig. 6 Radiation amplitude profile at $z = 12z_R$ for a displaced electron beam, $x_b = x_c(1-\text{sech}(k_c z))$ with $x_c = r_b/4$ and $\lambda_c = 2\pi/k_c = 4z_R$.

Fig. 7 Electron and radiation beam centroids, x_b and x_L for a displaced electron beam, $x_b = x_c(1-\text{sech}(k_c z))$ with $x_c = r_b/4$ and $\lambda_c = 2\pi/k_c = z_R/4$.

Fig. 8 Electron and radiation beam centroids, x_b and x_L for an oscillating electron beam, $x_b = x_c \sin k_c z$ with $x_c = r_b/4$ and $\lambda_c = 2\pi/k_c = z_R$.

Fig. 9 Radiation amplitude profile at $z = 12 z_R$ for an oscillating electron beam, $x_b = x_c \sin k_c z$ with $x_c = r_b/4$ and $\lambda_c = 2\pi/k_c = z_R$.

Fig. 10 Radiation amplitude on axis, $|a(0,z)|$ for a modulated electron beam, $r_b = r_{b0}(1 + \Delta \sin(K_B z))$ with $r_{b0} = 0.3$cm, $\Delta = 0.1$, $\lambda_B = 2\pi/K_B = 4.66$ m.
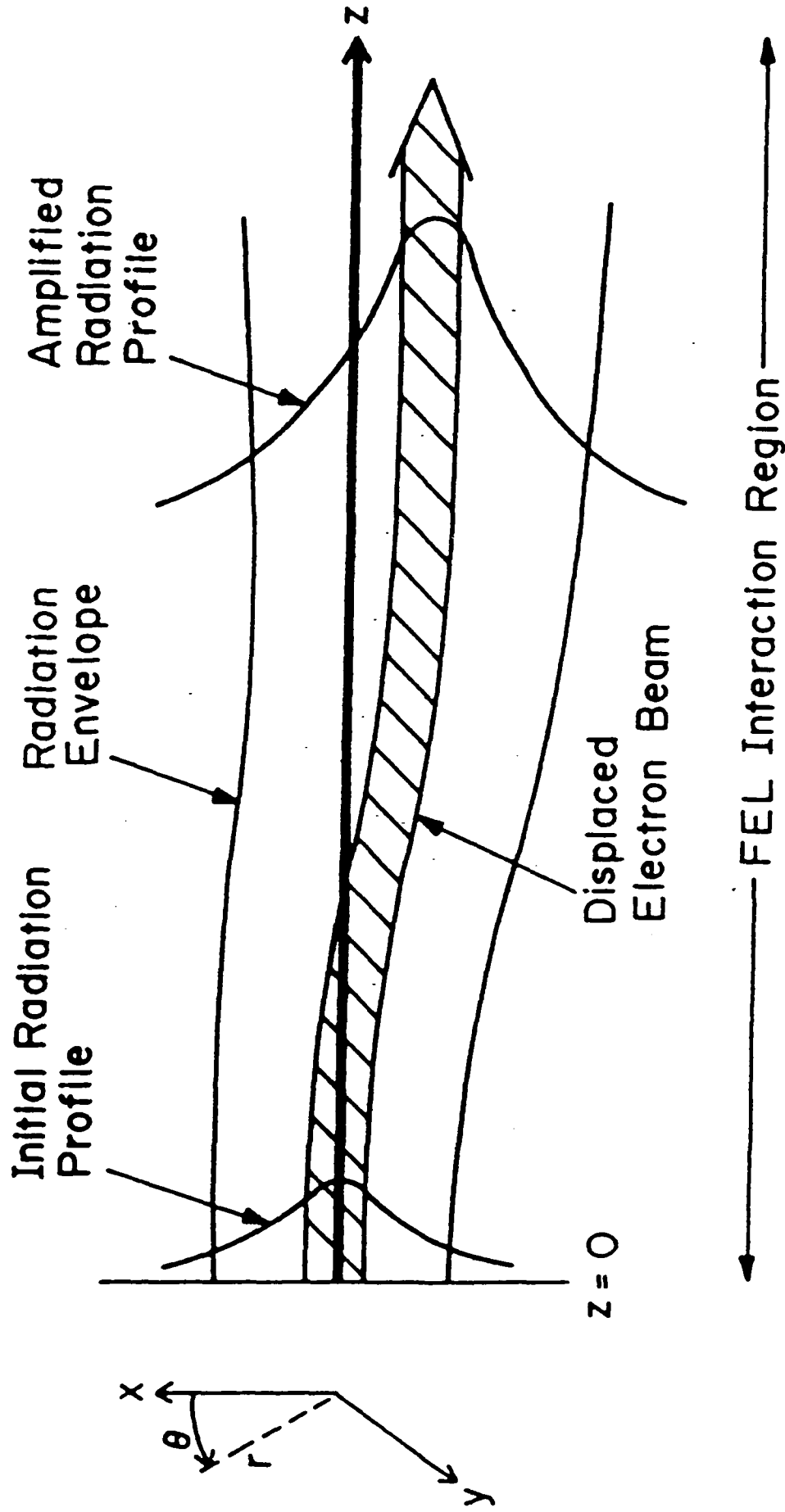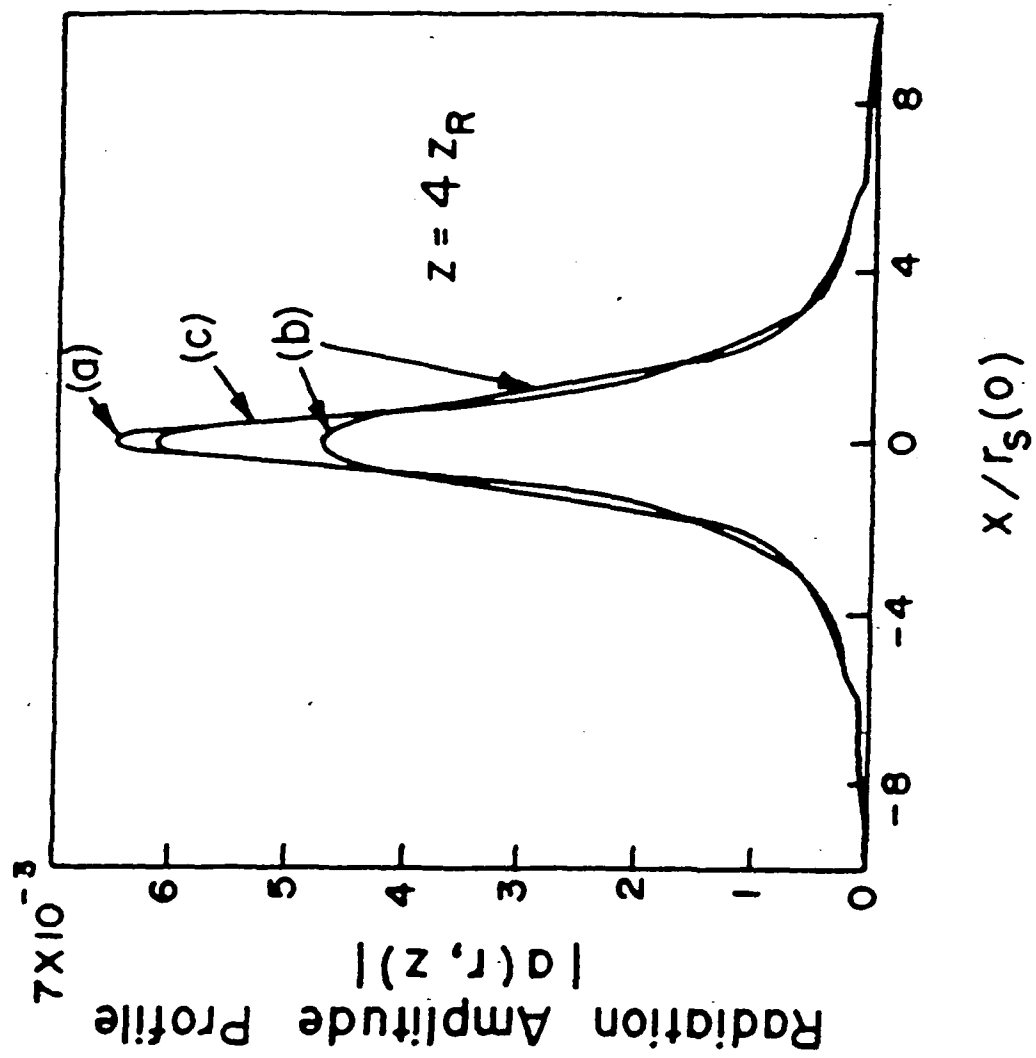
Schematic of Radiation Focusing and Guiding

Fig. 1

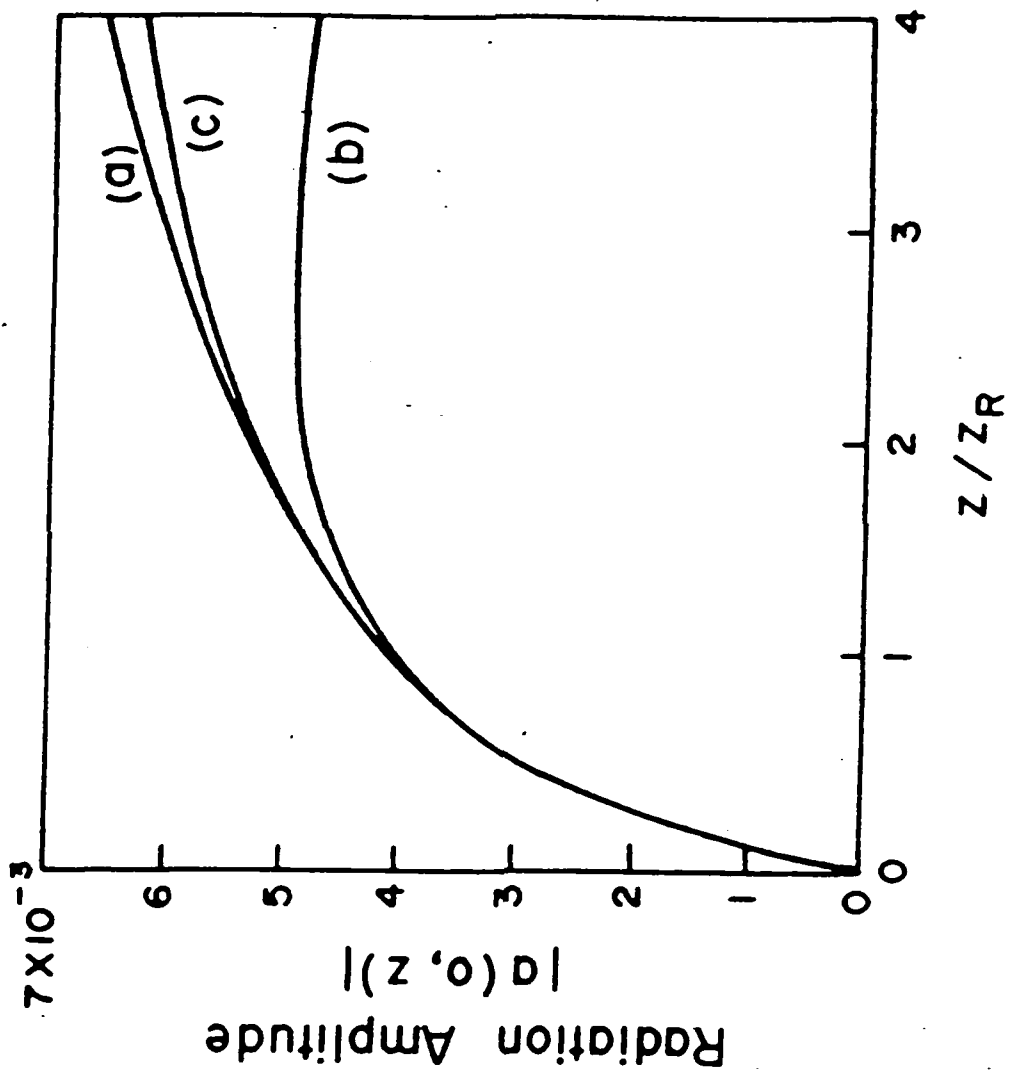Radiation Amplitude Profile $|a(r,z)|$

7×10^{-3}

6

5

4

3

2

1

0

-8 -4 0 4 8

$x/r_S(0)$

$z = 4\,z_R$

(a) (c) (b)

Fig. 2

Fig. 3

Radiation Amplitude $|a(0, z)|$

z/z_R

Fig. 4

Radiation 1/e Radius, (cm)

z(m)

Fig. 5

Fig. 6

Radiation Amplitude Profile
$|a(r,z)|$

$z = 12\, z_R$

$x/r_S(0)$

Fig. 7

Fig. 8

Fig. 9

Radiation Amplitude Profile $|a(r,z)|$

$z = 12\, z_R$

$X/r_S(0)$

Fig. 10

The plot shows Radiation Amplitude $|a(0,z)|$ (vertical axis, in units of 7×10^{-3}, marked 0, 1, 2, 3, 4, 5, 6) versus z/z_R (horizontal axis, marked 0 through 6).
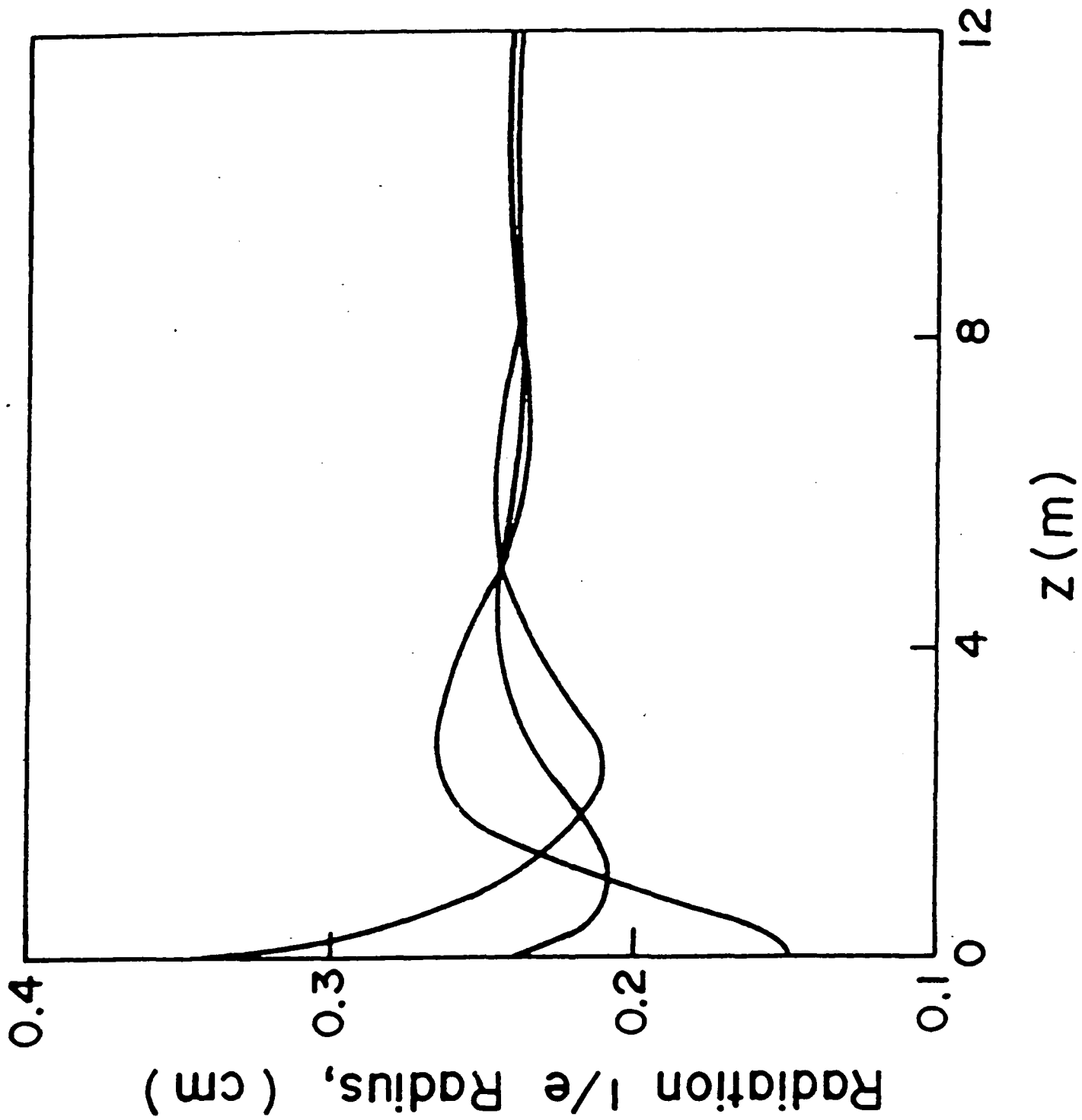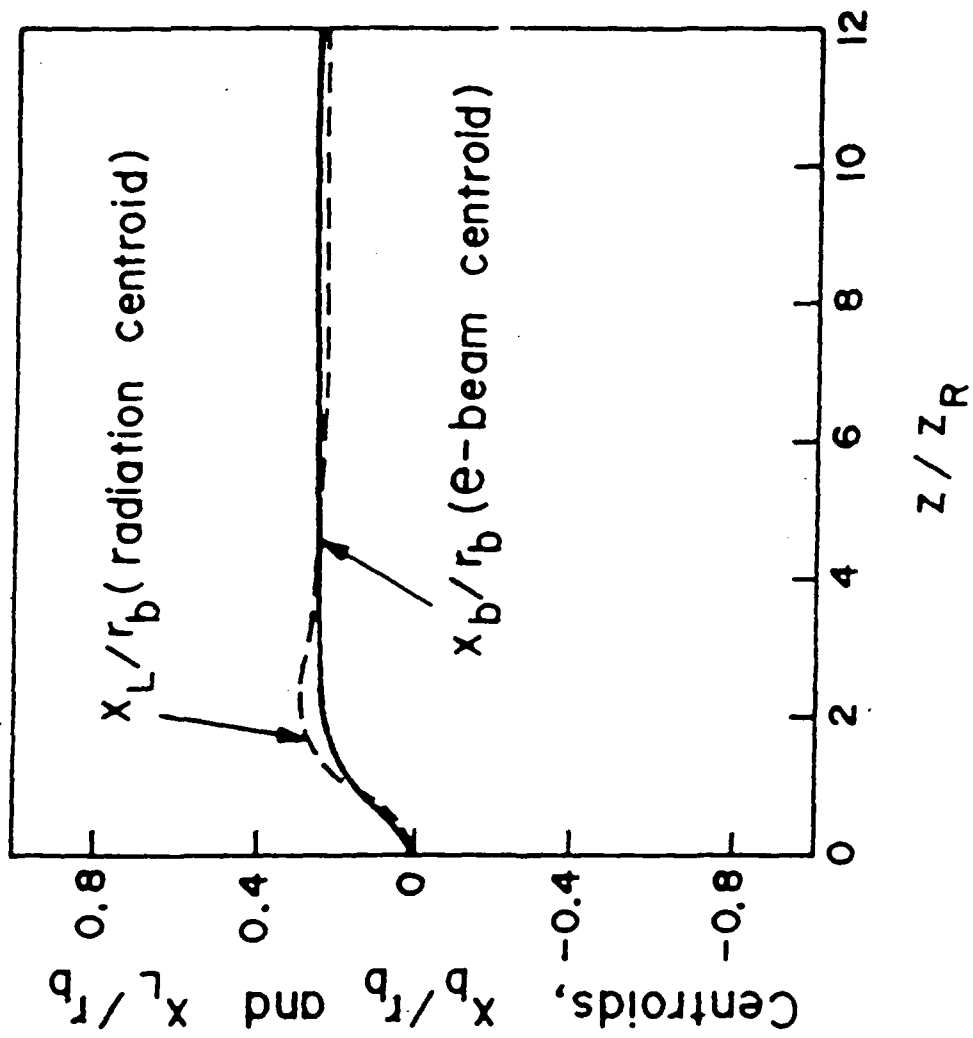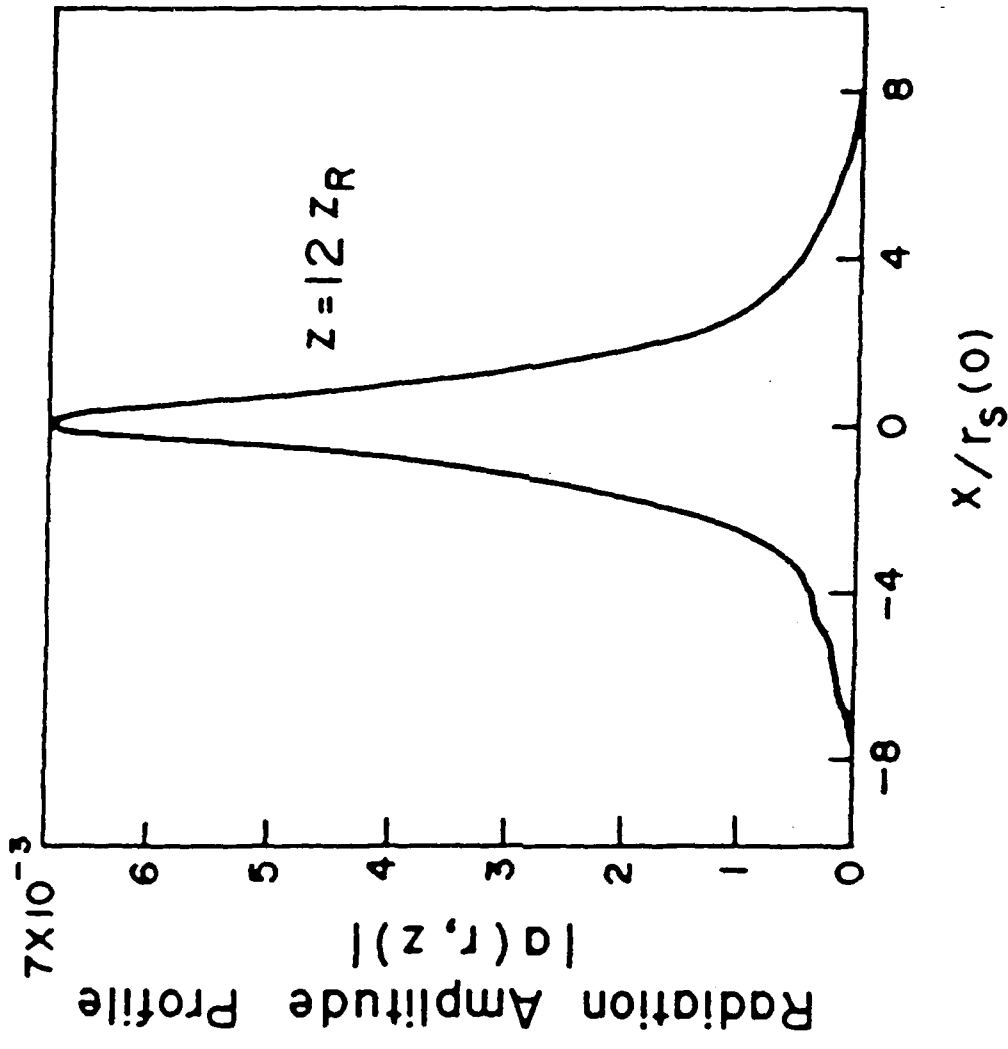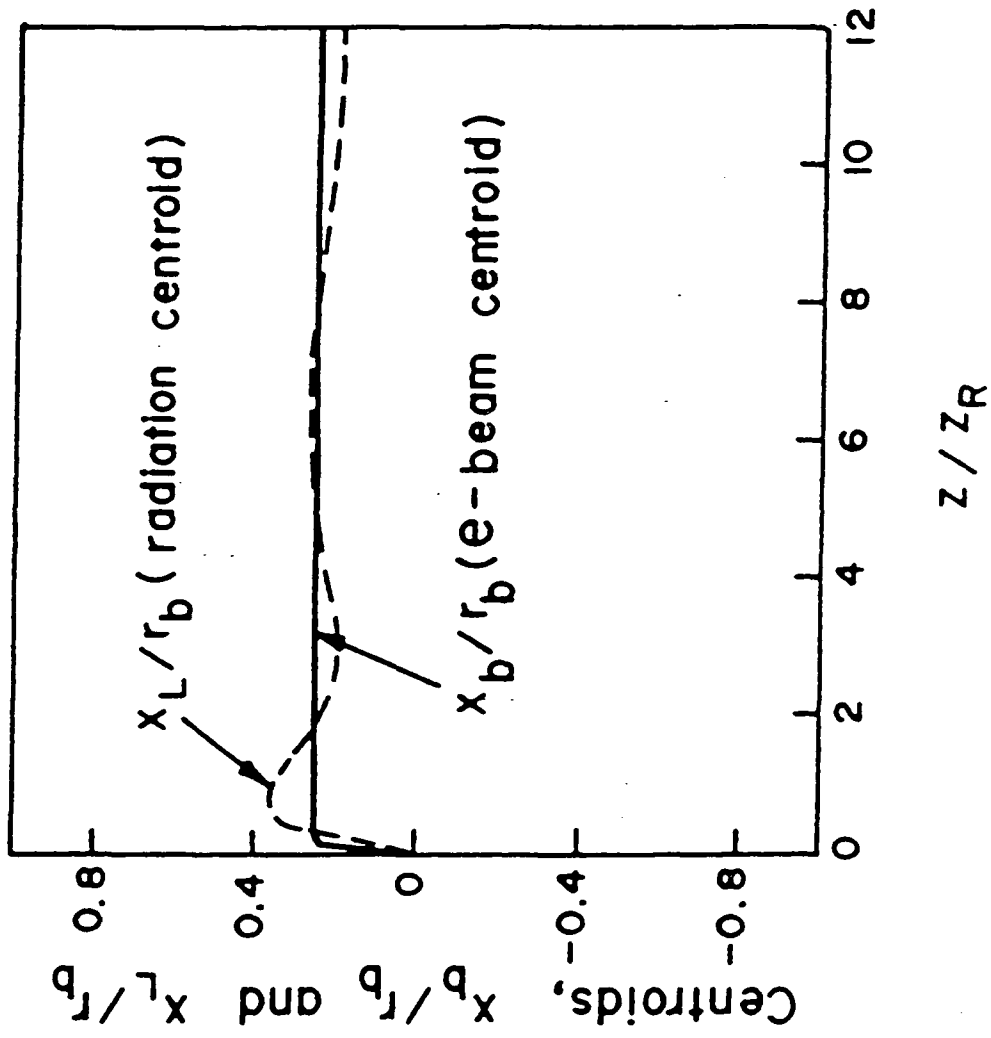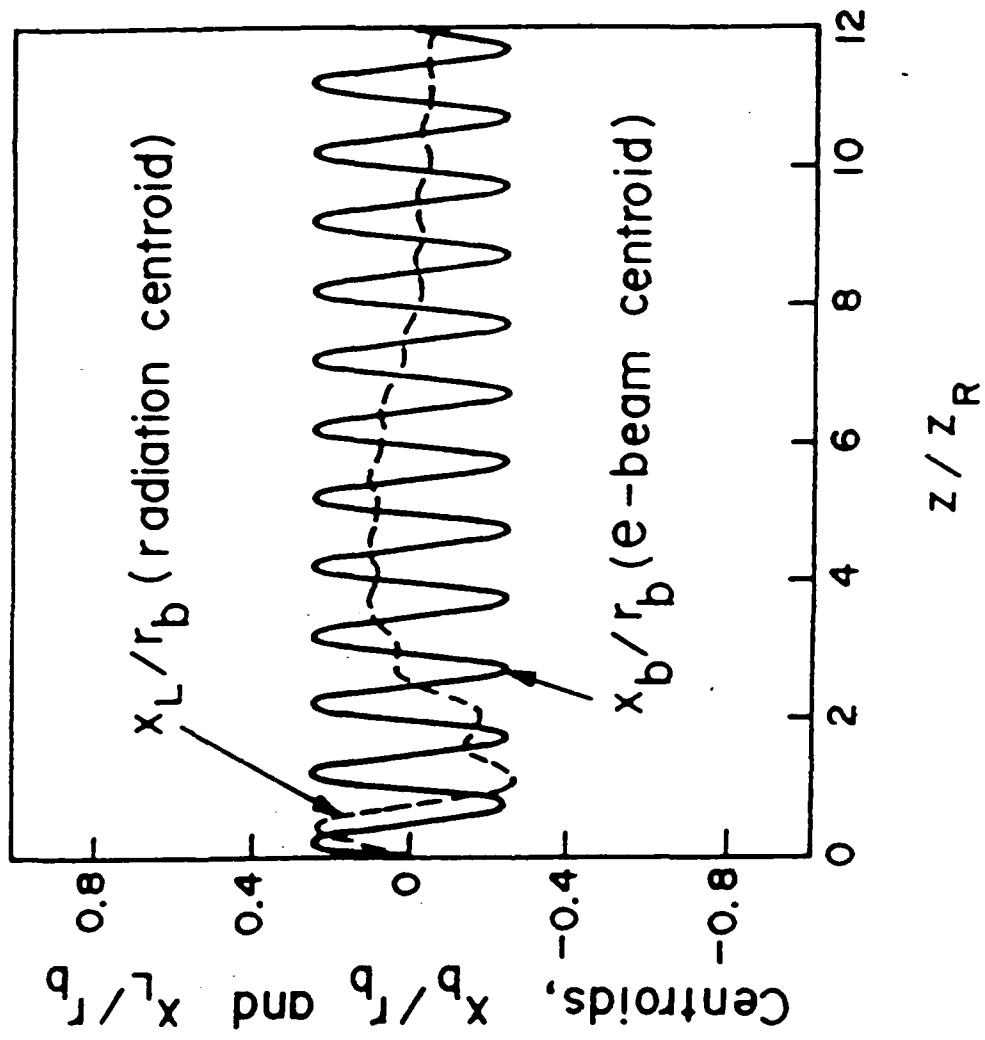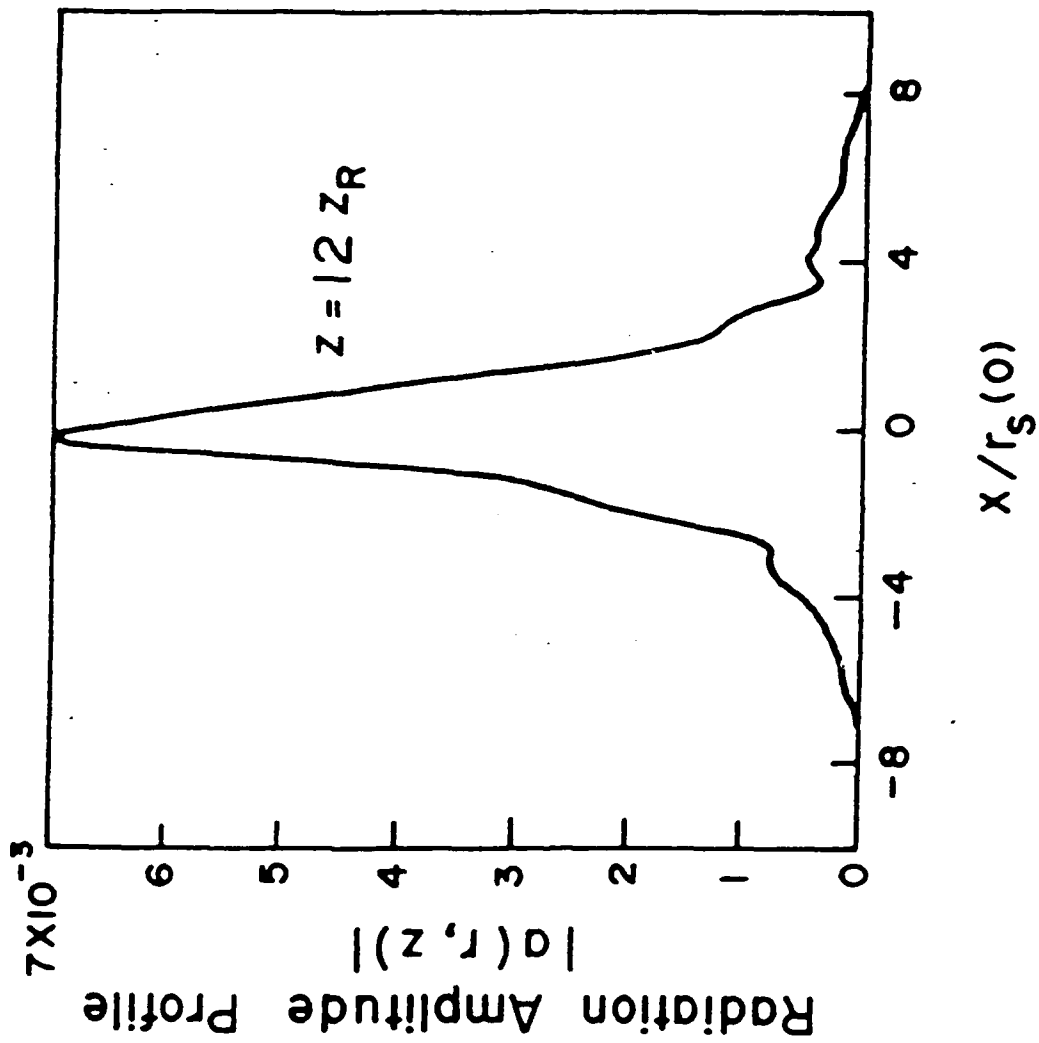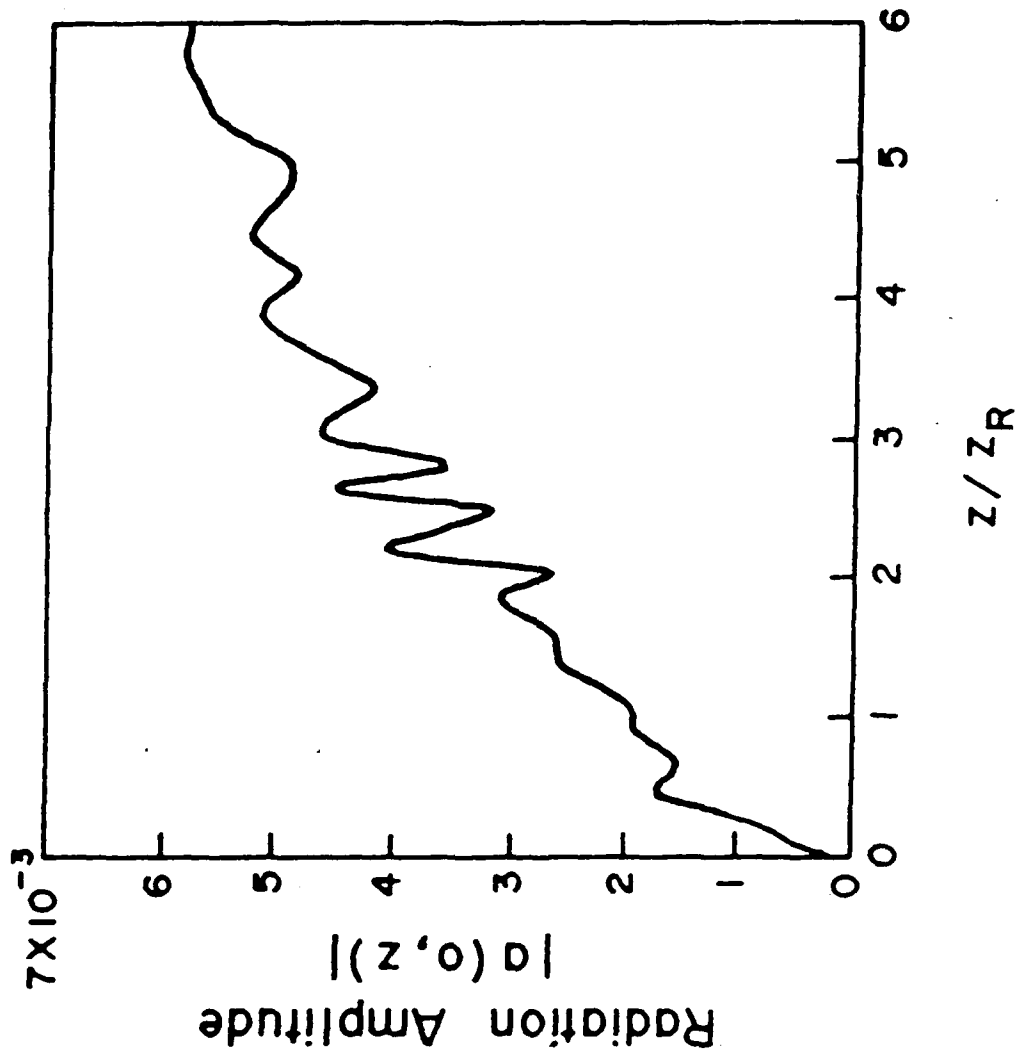
Appendix IV:

Radiation focusing and guiding in the Free
Electron Laser

II. Formulation of the Source Dependent Expansion (SDE)

The radiation focusing and guiding configuration for the FEL is shown in Fig. 2. In our model the vector potential of the linearly polarized radiation field is $A_R(r,\theta,z,t) = (1/2)A(r,\theta,z)\exp(i(\omega z/c-\omega t))\vec{e}_x + c.c.$, where $A(r,\theta,z)$ is the complex radiation amplitude, ω is the frequency and c.c. denotes the complex conjugate.

The radiation field satisfies the wave equation $(\nabla^2-c^{-2}\partial^2/\partial t^2)A_R = -4\pi c^{-1}J_x\vec{e}_x$, where $J_x(r,\theta,z,t)$ is the driving current density associated with the medium. Substituting A_R into the wave equation leads to the following reduced wave equation,

$$\left(\frac{1}{r}\frac{\partial}{\partial r}\left(r\frac{\partial}{\partial r}\right) + \frac{1}{r^2}\frac{\partial^2}{\partial\theta^2} + 2i\frac{\omega}{c}\frac{\partial}{\partial z}\right)a(r,\theta,z) = S(r,\theta,z), \qquad (1)$$

where $a(r,\theta,z) = |e|A/m_o c^2 = |a|\exp(i\phi)$ is the normalized complex radiation field amplitude and we have assumed that $a(r,\theta,z)$ is a slowly varying function of z, i.e., $a^{-1}\partial a/\partial z \ll \omega/c$. The source function, S, has the general form

$$S(r,\theta,z) = \frac{\omega^2}{c^2}(1-n^2(r,\theta,z,a))a(r,\theta,z), \qquad (2)$$

where $n(r,\theta,z,a)$ is the index of refraction associated with the medium and is in general complex.

We choose the following representation for $a(r,\theta,z)$ in terms of associated Laguerre polynomials,

$$a(r,\theta,z) = \sum_m \sum_p C_{m,p}(\theta,z)D_m^p(r), \qquad (3)$$

3

where $m = 0,1,2,\cdots,$ $p = 0,1,2,\cdots,$

$$C_{m,p}(\theta,z) = a_{m,p}(z)\cos p\theta + b_{m,p}(z)\sin r\theta, \qquad (4a)$$

$$D_m^p(r) = \left(\frac{\sqrt{2}r}{r_s(z)}\right)^p L_m^p\left(\frac{2r^2}{r_s^2(z)}\right)e^{-(1 - i\alpha(z))r^2/r_s^2(z)}. \qquad (4b)$$

In Eqs. (4a,b), $a_{m,p}(z)$ and $b_{m,p}(z)$ are complex, $r_s(z)$ is the radiation spot size, $\alpha(z)$ is related to the curvature of the wavefront and L_m^p is the associated Laguerre polynomial.

Substituting (3) into (1) and using the orthogonality properties of L_m^p, $\cos p\theta$, and $\sin p\theta$, we obtain,

$$\left(\frac{\partial}{\partial z} + A_{m,p}(z)\right)\begin{pmatrix}a_{m,p}\\b_{m,p}\end{pmatrix} - imB(z)\begin{pmatrix}a_{m-1,p}(z)\\b_{m-1,p}(z)\end{pmatrix} - i(m+p+1)B^*(z)\begin{pmatrix}a_{m+1,p}(z)\\b_{m+1,p}(z)\end{pmatrix}$$

$$= - i\begin{pmatrix}F_{m,p}(z)\\G_{m,p}(z)\end{pmatrix}, \qquad (5a,b)$$

where

$$A_{m,p}(z) = r_s'/r_s + i(2m+p+1)\left((1 + \alpha^2)c/\omega r_s^2 - \alpha r_s'/r_s + \alpha'/2\right), \qquad (6a)$$

$$B(z) = - \left(\alpha r_s'/r_s + (1 - \alpha^2)c/\omega r_s^2 - \alpha'/2\right) - i\left(r_s'/r_s - 2\alpha c/\omega r_s^2\right), \qquad (6b)$$

$*$ denotes the complex conjugate and the prime denotes a derivative with respect to z, i.e., $' = \partial/\partial z$ and

$$\begin{pmatrix}F_{m,p}(z)\\G_{m,p}(z)\end{pmatrix} = \frac{c}{2\pi\omega}\frac{m!}{(m+p)!}\int_0^{2\pi}d\theta\int_0^\infty d\xi\, S(\xi,\theta,z)\left(D_m^p(\xi)\right)^*\begin{pmatrix}(1+\delta_{p,0})^{-1}\cos p\theta\\\sin p\theta\end{pmatrix},$$

$$(6c,d)$$

4

where $\xi = 2r^2/r_s^2$.

The function $B(z)$ is arbitrary and if not specified, the equations for $a_{m,p}$ and $b_{m,p}$ in (5) are underdetermined. If we choose $B(z) = 0$, for example, we would in affect be expanding the radiation field in the conventional vacuum Laguerre modes.[7] We will show later that, in general, expansion in terms of the vacuum modes, $B = 0$, would require far too many modes to accurately describe the radiation beam over distances of many Rayleigh lengths. To find a more appropriate choice for $B(z)$, we consider the case where the radiation beam at $z = 0$ has a Gaussian radial profile symmetric about the z-axis. In this case the complex radiation amplitude, at $z = 0$, is given by $a(r,\theta,0) = a_{0,0} \exp (-(1 - i\alpha(0))r^2/r_s^2(0))$ and is independent of θ. Let us further assume that for $z > 0$ the radiation beam profile remains approximately Gaussian with a nearly circular cross section. In this case we expect the magnitude of the coefficients, $a_{m,p}(z)$ and $b_{m,p}(z)$ to become progressively smaller as m and p take on larger values. The lowest order approximation to the radiation beam is then given by the $a_{0,0}(z)$ mode. From (5a) we find that only the $m = 0,1$ and $p = 0$ equations are relevant and are $(\partial/\partial z + A_{0,0})a_{0,0} = - iF_{0,0}$ and $0 = - i(F_{1,0} - Ba_{0,0})$. We now have a specific expression for $B(z)$ in terms of one of the moments, $F_{1,0}$, of the source term. Substituting $B(z) = F_{1,0}(z)/a_{0,0}(z)$ into (6b) yields first order coupled differential equations for r_s and α. Also using $B(z) = F_{1,0}(z)/a_{0,0}(z)$ allows us to solve for $A_{m,p}$ in (6a) and hence for $a_{m,p}$ and $b_{m,p}$ in (5a,b).

5

III. Radiation Focusing and Guiding in FELs

A. Radiation Beam Envelope Equation

We first consider the dynamics of an axially symmetric radiation field in the FEL. For a linearly polarized wiggler field and axially symmetric electron beam having a Gaussian density profile, the appropriate index of refraction for the FEL mechanism[4,5,6,8] is

$$n(r,z,a) = 1 + \frac{1}{2} \frac{\omega_b^2(r,z)}{\omega^2} \left\langle \frac{e^{-i\psi}}{\gamma} \right\rangle \frac{a_w}{|a(r,z)|} , \qquad (7)$$

where $\omega_b^2(r,z) = \omega_{bo}^2 (r_{b0}/r_b(z))^2 \exp(-r^2/r_b^2(z))$, $r_b(z)$ is the electron beam radius, $r_{b0} = r_b(0)$, $\omega_{b0} = (4\pi|e|^2 n_{b0}/m_0)^{1/2}$ is the initial beam plasma frequency on axis, n_{b0} is the initial beam density on axis, $a_w = |e|B_w/k_w m_0 c^2$ is the normalized wiggler amplitude, B_w is the wiggler magnetic field strength, k_w is the wiggler wave number, γ is the electron's Lorentz factor, ψ is the electron's phase in the ponderomotive wave potential and $\langle \ \rangle$ denotes the ensemble average over all electrons. With the assumption that in the source function the complex radiation amplitude can be approximated by the lowest order mode, we find that (2) can be written as

$$S(\xi,z) = -4\nu(a_w/r_b^2) \frac{a_{0,0}}{|a_{0,0}|} \left\langle \frac{e^{-i\psi}}{\gamma} \right\rangle e^{-\left(r_s^2/r_b^2 - i\alpha\right)\xi/2} , \qquad (8)$$

where $\nu = (\omega_{bo} r_{bo}/2c)^2 = I_b/17\times10^3$ is Budker's constant and I_b is the electron beam current in amperes. Since we are considering an axially symmetric electron beam and radiation field we note that $a_{m,p} = F_{m,p} = 0$ for $p > 0$.

Using (8), equation (6b) can be used to obtain the following envelope equation for the radiation beam,

6

$$r_s'' + K^2(z,r_b,r_s,|a_{0,0}|)r_s = 0, \tag{9}$$

where

$$K^2 = (2c/\omega)^2 \left[-1 + C^2\langle\sin\psi\rangle^2 + 2C\langle\cos\psi\rangle + (\omega/2c)r_s^2 \, C'\langle\sin\psi\rangle \right] r_s^{-4}, \tag{10}$$

and $C(z) = (2\nu/\gamma)H(z)a_w/|a_{0,0}(z)|$, $H(z) = (1-F)/(1+F)^2$ and $F(z) = r_b^2/r_s^2$ is the filling factor. The function $C(z)$ measures the coupling between the radiation and electron beam and decreases as the radiation grows. The first term on the right hand side of (10) is defocusing and corresponds to the usual diffraction expansion, the second and third terms are always focusing while the last term is a defocusing contribution. The envelope equation in (9) indicates that in the high gain trapped particle regime, conditions for a matched beam can not be maintained. However, in the low gain trapped particle regime or in the exponential gain regime, conditions for a nearly matched beam can be achieved. Using (5a) we find that the magnitude of $a_{0,0}(z)$ evolves according to

$\partial(r_s|a_{0,0}|)/\partial z = (4c/\omega)(\nu/\gamma)a_w r_s\langle\sin\psi\rangle/(r_s^2+r_b^2)$, where $(r_s|a_{0,0}|)^2$ is proportional to the radiation power, $P(z) = 2.15\times10^{10}(|a_{0,0}(z)|r_s/\lambda)^2$ [Watts].

B. Radiation Guiding in the FEL

In the FEL the centroid of the electron beam may be displaced off-axis by a misalignment, a redirection of the beam or because of the oscillations in the wiggler field. To determine the degree to which the radiation beam will follow or be guided by the electron beam, we consider the case where the electron beam centroid is displaced transversely in the

x direction. The index of refraction in this case is given by (7) with $\omega_b^2(r,z)$ multiplied by $(1 + 2(r_s x_b/r_b^2)\cos\theta)$ where $x_b(z)$ is the displacement of the electron beam's centroid and $|x_b| \ll r_b$. In the FEL source term we consider only the lowest order symmetric and anti-symmetric mode with respect to the x axis, $a(r,\theta,z) \sim (a_{0,0} + a_{0,1}\xi^{1/2}\cos\theta)\exp(-(1-i\alpha)\xi/2)$. With this assumption the moments of the source function, $F_{m,p}(z)$, for $p=0,1$, can be evaluated. For small displacements of the electron beam centroid it is easy to show that the centroid of the radiation beam is given approximately by

$$x_L(z) = \frac{r_s(z)}{\sqrt{2}} \left(\frac{a_{0,1}}{a_{0,0}}\right)_R, \tag{11}$$

where x_L is defined so that $|a|$ is proportional to $\exp(-((x - x_L)^2 + y^2)/r_s^2)$ and $(\;)_R$ denotes the real part.

C. Effect of a Modulated Electron Beam

The electron beam envelope in the FEL can undergo modulations. The modulation is symmetric about the z-axis and can be caused by improper values for the beam emittance, radius and/or current injected into the wiggler region.

For small perturbations about the matched beam radius, r_{b0}, we find from the electron beam envelope equation that $r_b(z) = r_{b0} (1 + \Delta\sin(K_B z))$ where $r_{b0} = (2\varepsilon_n/a_w k_w)^{1/2}$, $K_B = a_w k_w/\sqrt{2}\gamma$ is the betatron wave number, due to the weak focusing effect of wiggler gradients, ε_n is the normalized emittance, and $\Delta \ll 1$.

8

IV. Numerical Results

In this section we apply the SDE formulation, given by (5) together with (6), to the FEL. Using the source term given in (2) together with (7) we first present a comparison between; a) the exact numerical solution of the wave equation in (1), (using 64x64 Fourier modes), b) the solution using a vacuum Laguerre modal expansion (B=0, using 10 modes) and c) the solution from the Laguerre SDE approach (B = $F_{1,0}/a_{0,0}$, using 10 modes). The FEL parameters used in these illustrations are similar to those used in Ref. 9 and are given in Table I where the resonant phase approximation, $\langle\exp(-i\psi)\rangle = \exp(-i\bar{\psi}_R)$, is used for demonstration purposes and $z_R = \pi r_s^2(0)/\lambda$ is the Rayleigh length, λ is the wavelength and $r_s(0)$ is the minimum spot size.

For an axially symmetric configuration, we show in Fig. 2 the evolution of the radiation beam amplitude on-axis obtained from methods (a), (b) and (c), as a function of propagation distance. The SDE solution (c) is in excellent agreement with solution (a) while solution (b), beyond a Rayleigh length, grossly deviates from (a) and (c). This indicates that more modes are required for the vacuum expansion solution. The excellent results obtained with the SDE approach are also reflected in the radiation amplitude profile.

We now use the SDE method to illustrate guiding of the radiation beam when the electron beam is displaced off-axis. In these numerical illustrations, 10 radial modes (m = 0,...,9) and 2 angular modes (p = 0,1) were used. In the first example, the electron beam centroid is displaced off axis according to $x_b = x_c (1-\text{sech}(k_c z))$. Figure 3 shows the electron and radiation beam centroids, x_b and x_L for $x_c = r_b/4 = .075$cm and $\lambda_c = 2\pi/k_c = z_R/4 = 2.7$m. After an initial transient, the radiation centroid is

guided by and oscillates about the electron beam's centroid. In the next example we take the electron beam centroid to be oscillating about the z axis, $x_b = x_c \sin k_c z$, with amplitude $x_c = r_b/4$ and period $\lambda_c = z_R = 10.7m$. Figure 4 shows the electron and radiation beam centroids. Because of the high gain in the radiation field the radiation centroid eventually follows the average position of the electron beam's centroid. In the case where the electron beam centroid oscillation is due to the wiggler field, $x_c = a_w/\gamma k_w$ and $k_c = 2\pi/\lambda_w$, no noticeable change in the evolution of the radiation field (compared to the case for $x_c = 0$) is observed.

The last illustration is for the case where the electron beam envelope is spatially modulated. Using the parameters in Table I we find that $\varepsilon_n = 0.06$ cm-rad and $\lambda_B = 2\pi/K_B = 4.66m$. Figure 5 shows the amplitude of the radiation field on-axis as a function of propagation distance when the electron beam envelope is not matched, $r_b = r_{b0} (1 + \Delta\sin(K_B z))$, where $r_{b0} = 0.3cm$ and $\Delta = 0.1$

Table I

Electron Beam

    Current $\qquad\qquad\qquad I_b = 2kA,\ (\nu = 0.118)$

    Energy $\qquad\qquad\qquad \varepsilon_b = 50\ MeV,\ (\gamma = 100)$

    Radius $\qquad\qquad\qquad r_{b0} = 0.3\ cm$

Radiation Beam

    Wavelength $\qquad\qquad \lambda = 10.6\mu m$

    Input Power $\qquad\qquad P(z=0) = 233\ MW,\ (|a(0,0)| = 1.84 \times 10^{-4})$

    Spot Size $\qquad\qquad r_s(0) = 0.6\ cm,\ (z_R = 10.7\ m)$

Wiggler Field

    Wavelength $\qquad\qquad \lambda_w = 8\ cm$

    Wiggler Strength $\qquad B_w = 2.3\ kG,\ (a_w = 1.716)$

    Resonant Phase $\qquad \psi_R = 0.358\ rad$

References

1. P. Sprangle and R. Smith, Phys. Rev. A, $\underline{21}$(1), 293 (1980).

2. P. Sprangle, C. M. Tang and W. Manheimer, Phys. Rev. A, $\underline{21}$(1), 302 (1980).

3. N. M. Kroll, P. L. Morton and M. N. Rosenbluth, IEEE J. Quantum Electron, QE-17, 1436 (1981).

4. P. Sprangle and C. M. Tang, Appl. Phys. Lett. $\underline{39}$(9), 677 (1981), also AIAA Journal, $\underline{19}$(9), 1164 (1981).

5. E. T. Scharlemann, A. M. Sessler and J. S. Wurtele, Phys. Rev. Lett. $\underline{54}$ (17), 1925 (1985).

6. Free Electron Lasers, Proceedings of the 7th Intl. Conf. on FELs, Tahoe City, Sept. 8-13, 1985, edited by E. T. Scharlemann and D. Prosnitz (North-Holland-Amsterdam).

7. C. M. Tang and P. Sprangle, IEEE J. of Quantum Electronics, QE-21, 970 (1985).

8. D. Prosnitz, A. Szoke and V. K. Neil, Phys. Rev. A $\underline{24}$, 1436 (1981).

9. E. T. Scharlemann, J. Appl. Phys. $\underline{58}$(6), 2154 (1985).

Figure Captions

Fig. 1   Schematic of radiation focusing and guiding in an FEL.

Fig. 2   Radiation amplitude on axis, $|a(0,z)|$ for a) exact numerical
          solution (64x64 Fourier modes), b) vacuum modal expansion solution
          (10 modes), and c) SDE solution (10 modes) at distance of
          $z = 4z_R = 42.8$ m.

Fig. 3   Electron and radiation beam centroids, x_b and x_L for a displaced
          electron beam, $x_b = x_c(1-\text{sech}(k_c z))$ with $x_c = r_b/4$ and
          $\lambda_c = 2\pi/k_c = z_R/4$.

Fig. 4   Electron and radiation beam centroids, x_b and x_L for an
          oscillating electron beam, $x_b = x_c \sin k_c z$ with $x_c = r_b/4$ and
          $\lambda_c = 2\pi/k_c = z_R$.

Fig. 5   Radiation amplitude on axis, $|a(0,z)|$ for a modulated electron
          beam, $r_b = r_{b0}(1 + \Delta \sin(K_B z))$ with $r_{b0} = 0.3$cm, $\Delta = 0.1$ and
          $\lambda_B = 2\pi/K_B = 4.66$ m.

Appendix V:

Radiation focusing, guiding and steering in the Free Electron Laser

RADIATION FOCUSING, GUIDING AND STEERING IN FREE ELECTRON LASERS

P. Sprangle, A. Ting[*], B. Hafizi[**] and C. M. Tang

Naval Research Laboratory
Washington, DC 20375-5000

Abstract

In a free electron laser (FEL), the radiation field, wiggler field and electron beam resonantly couple and modify the refractive index in the vicinity of the electron beam. The refractive index is modified such that the radiation beam will tend to focus upon the electron beam. A method for solving the 3-D wave equation for the FEL process is outlined. This approach, called the source dependent expansion method, provides an excellent analytical and numerical technique for studying optical focusing, guiding and steering in FELs. A radiation envelope equation is derived. Conditions and parameters necessary to achieve guided radiation beams (constant radius) in the exponential gain regime are obtained for FELs driven by either induction linacs or rf linacs. Immediately prior to saturation in the exponential gain region, the ponderomotive potential is large enough to trap the beam electrons. The wiggler field, at this point, could be tapered to further increase the operating efficiency. The possibility of bending or steering radiation beams in FELs is discussed and a condition necessary for radiation guiding along a curved electron beam orbit is obtained.

Introduction

In many short wavelength free electron laser devices the radiation beam will not be confined or guided by a structure such as a waveguide. Furthermore, in order to provide high gain and efficiency, it is usually necessary for the interaction length (length of wiggler field) to be long compared to the diffraction length (Rayleigh length) associated with the radiation beam. In the FEL the tendency of the radiation beam to diffract away over a distance of a few Rayleigh lengths can be overcome by a focusing phenomenon arising from the resonant coupling of the radiation and wiggler fields with the electron beam [1,2]. This radiation focusing effect plays a central role in the practical utilization of the FEL. This phenomenon was first analyzed for the low gain FEL with transverse effects where it was shown that the diffractive spreading of the radiation beam could be overcome by a focusing effect arising from the modified index of refraction [1]. Optical guiding in FELs operating in the small signal exponential gain regime has been studied for the asymptotic behavior of the radiation beam [3-6]. Recently, a general formalism for optical focusing, guiding and steering has been developed and applied to FELs [7].

In the following, we employ a modal expansion technique to examine the optical beam as it propagates through the wiggler. The formalism has the merit that with only a few modes it permits an accurate solution of the wave equation throughout the interaction region.

Model

In our model, the vector potential of an axially symmetric, linearly polarized, radiation field is

$$A_R(r,z,t) = A(r,z) e^{i(\omega z/c - \omega t)} e_x/2 + c.c., \qquad (1)$$

where $A(r,z)$ is the complex radiation field amplitude, ω is the frequency and c.c. denotes the complex conjugate.

The wave equation governing A_R is

$$\left(\frac{1}{r}\frac{\partial}{\partial r}\left(r\frac{\partial}{\partial r}\right) + \partial^2/\partial z^2 - c^{-2}\partial^2/\partial t^2\right)A_R = -\frac{4\pi}{c} J_x e_x, \qquad (2)$$

where $J_x(r,z,t)$ is the driving current density. Substituting (1) into (2) leads to the following reduced wave equation,

$$\left(\frac{1}{r}\frac{\partial}{\partial r}\left(r\frac{\partial}{\partial r}\right) + 2i\frac{\omega}{c}\frac{\partial}{\partial z}\right)a(r,z) = S(r,z,a), \qquad (3)$$

where $a(r,z) = |e|A/m_e c^2 = |a|\exp(i\phi)$ is the normalized complex radiation amplitude and we have assumed that $a(r,z)$ is a slowly varying function of z, i.e., $|(\partial a/\partial z)/a| \ll \omega/c$. The source function, S, is given by,

$$S = -\frac{4\omega}{c}\int_0^{2\pi/\omega} J_x(r,z,t)e^{-i(\omega z/c - \omega t)}dt. \qquad (4)$$

It is possible to relate the source function, S, to the index of refraction associated with the medium by noting that the wave equation for A_R in a nonmagnetic, time-independent, nonlinear medium is $(\nabla^2 - (n^2(r,z,a)/c^2)\partial^2/\partial t^2)A_R = 0$, where n is the index of refraction associated with the medium and is, in general, complex and a nonlinear function of $a(r,z)$. Comparing the reduced wave equation written in terms of $n(r,z,a)$ with (3) we find that the source function can be written in terms of n.

$$S(r,z,a) = (\omega/c)^2\left(1-n^2(r,z,a)\right)a(r,z). \qquad (5)$$

Source Dependent Expansion Method

In order to solve (3) we will use the source dependent expansion (SDE) method [7]. In this method, we choose the following representation for $a(r,z)$ in terms of Laguerre-Gaussian functions,

$$a(r,z) = \sum_m a_m(z)L_m\left(\frac{2r^2}{r_s^2(z)}\right)e^{-(1-i\alpha(z))r^2/r_s^2(z)}. \qquad (6)$$

where $m = 0,1,2,\cdots$. In Eq. (6), $a_m(z)$ are the complex amplitude coefficients, $r_s(z)$ is the radiation spot size, $\alpha(z)$ is related to the radius of curvature of the radiation beam wavefront, $R = -(\omega/2c)r_s/\alpha$ and L_m is the Laguerre polynomial. Solving for the unknown quantities a_m, r_s and α in terms of the source term S allows us to completely describe the radiation dynamics. The representation in (6) is underspecified, since, when (6) is substituted into (3) and moments of the source function taken, there remain more unknown quantities than available equations. The additional degrees of freedom in our representation allow us to specify a particular functional relationship for the unknown quantities r_s and α in such a way that, if the radiation beam profile remains approximately Gaussian, the number of modes needed to accurately describe the radiation beam is small. This yields the following first order coupled differential equations for r_s and α,

$$r_s' - 2c\alpha/\omega r_s = -r_s H_I, \qquad (7a)$$

$$\alpha' - 2(1+\alpha^2)c/\omega r_s^2 = 2(H_R + \alpha H_I). \qquad (7b)$$

and a set of first order ordinary differential equations for the complex amplitudes $a_m(z)$.

$$a_m = A_m a_m - i\left[F_m - mBa_{m-1} - (m+1)B^* a_{m+1}\right].\tag{7c}$$

where $B = F_m / a_m$, $' = \partial/\partial z$, and $( )_{R,I}$ denotes the real and imaginary part of the enclosed function. In Eqs. (7), the functions A_m, B, and F_m are given by

$$A_m(z) = r_s'/r_s + i(2m+1)\left[(1 + a^2)c + m_s^2 - \alpha r_s'/r_s + \alpha'/2\right],$$

$$B(z) = -\left(\alpha r_s'/r_s + (1-a^2)c + m_s^2 - \alpha'/2\right) - i\left(r_s'/r_s - 2\alpha c/m_s^2\right),$$

$$F_m(z) = \frac{c}{2\omega}\int_0^\infty d\zeta\, S(\zeta,z)L_m(\zeta)\exp(-(1+i\alpha)\zeta/2),$$

where $\zeta = 2r^2/r_s^2$.

The merits of the SDE method can be demonstrated in a comparison between: a) the exact numerical solution of the wave equation in (3), (using 64x64 Fourier modes), b) the solution using a vacuum Laguerre-Gaussian modal expansion (10 modes) and c) the solution from the Laguerre-Gaussian SDE approach (10 modes). Figure 1 shows the radiation beam amplitude on-axis obtained from methods (a), (b) and (c) after four Rayleigh lengths for the FEL parameter in Table I. The SDE solution (c) is in excellent agreement with solution (a) while solution (b), beyond a Rayleigh length, grossly deviates from (a) and (c).
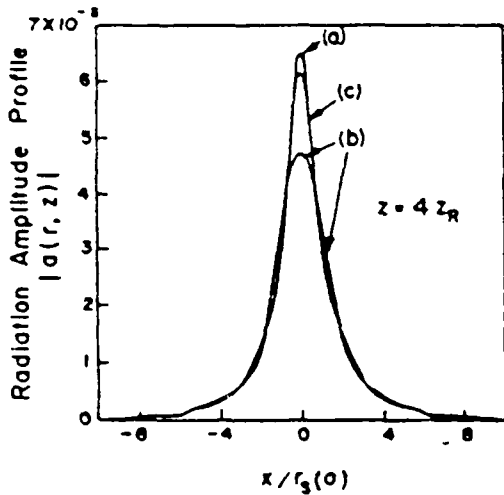

Fig. 1 Radiation amplitude profile, $|a(r,z)|$ for: a) exact numerical solution (64x64 Fourier modes), b) vacuum modal expansion solution (10 modes), and c) SDE solution (10 modes) at a distance of $z = 4Z_R$.

Refractive Index Associated with FELs

In the following derivation of the refractive index associated with the FEL, a number of simplifying assumptions are made. We assume, for example, that the beam electrons are monoenergetic without betatron oscillations and that the radiation is of a single frequency [8]. To obtain an expression for the refractive index we write the nonlinear driving current density, J_x, as

$$J_x = -|e|n_b(r)v_w(z)v_{oz}\int \delta(z-\bar{z}(t,t_o))dt_o,\tag{8}$$

where $n_b(r)$ is the ambient beam density, v_{oz} is the axial electron velocity at $z = 0$, t_o is the time a given electron crosses the $z = 0$ plane.

$$v_w(z) = |e|A_w/m_o c(\exp(ik_w z) + c.c.)e_x/2.$$

is the wiggle velocity, γ is the Lorentz factor, A_w is the vector potential amplitude of the planar wiggler field and $k_w = 2\pi/\lambda$ is the wiggler wave number. Substituting (8) into the expression for S, (4), gives

$$S = \left(\frac{\omega_b(r)}{c}\right)^2 a_w\int_0^\infty dt\,\omega/2\pi\int dt_o e^{-i\left(\left(\frac{\omega}{c}+k_w\right)z - \omega t\right)}\delta(t-\tau(z_o,t))/\gamma.$$
$$\tag{9}$$

where $a_w = |e|A_w/m_o c^2$, $\tau = t_o + \int_0^z dz''/v_z(z'',t_o)$ and the t_o integration is over all entry times. Equating (9) with (5) and carrying out the integration over t, we find the index of refraction associated with the FEL to be given by

$$n_{fel}(r,z,a) = 1 + (\omega_b^2(r)/2\omega^2)\frac{a_w}{|a|}\left\langle\frac{e^{-i\psi}}{\gamma}\right\rangle_{\psi_o}.\tag{10}$$

where

$$\psi = \int_0^z\left(\omega/c + k_w - i\ln(a/|a|) - \omega/v_z(z,\psi_o)\right)dz + \psi_o.$$

is the relative phase between the electron and the ponderomotive wave, $\psi_o = -\omega t_o$ is the initial phase of a given electron and $\left\langle\ \right\rangle_{\psi_o} = (2\pi)^{-1}\int_0^{2\pi}d\psi_o$ is an ensemble average over the initial phases. The radial profile of the index of refraction as given by Eq. (10) supports self-focusing of the radiation in an FEL. It should be noted, for completeness, that the relative phase satisfies the pendulum equation given by

$$\partial^2\psi/\partial z^2 = \partial k_w/\partial z - \gamma^{-2}(\omega/c)\left[4\partial a_w^2/\partial z - k_w a_w a\sin\psi\right].\tag{11}$$

Radiation Beam Envelope Equation

Equations (7a) and (7b) can be combined to give the following envelope equation for the radiation beam

$$r_s'' + K^2 r_s = 0,\tag{12}$$

where

$$K^2 = (2c/\omega)^2\left\{-1 + C^2\langle\sin\psi\rangle^2 + 2C\langle\cos\psi\rangle + (\omega/2c)r_s^2 C'\langle\sin\psi\rangle\right\}r_s^{-4}.$$
$$\tag{13}$$

and $C(z) = (2v/\gamma)G(z)a_w/|a_o(z)|$, measures the coupling between the radiation and electron beam. $v = (\omega_{bo}\,r_b/2c)^2 = I_b/17\times10^3$ is Budker's constant, I_b is the electron beam current in amperes. $G(z) = (1-f)/(1+f)^2$ and $f(z) = (r_b/r_s)^2$ is the filling factor associated with a Gaussian electron beam density profile. The first term on the right-hand side of (13) is the usual diffraction term, the second and third terms are focusing while the last term provides a focusing or defocusing contribution. In the high gain trapped particle regime, $\langle\sin\psi\rangle$ and $\langle\cos\psi\rangle$ are approximately constant, while $|a_o(z)|$ increases with z. Hence, K depends on z and a guided beam ($r_s' = 0$) cannot be exactly maintained in this regime, although, the radiation envelope is still reasonably well-confined. In the low gain trapped particle regime $|a_o(z)|$ increases slightly and, therefore, a guided beam can be approximately

achieved. In either the Compton or Raman exponential gain regime, conditions for a stable guided beam can be found.

Guided Radiation Beams in the Exponential Gain Regime

In this section, we obtain the necessary conditions to achieve guided radiation beams in both the Compton (noncollective) and Raman (collective) exponential gain regimes. By considering the lowest order mode (Gaussian profile) we find that the source term appropriate for the high gain Compton and Raman regime is, respectively,

$$S(r,z) = \frac{(\omega_b(r)/c)^2 (a_v k_v f_B)^2}{\gamma(1+a_v^2/2)} \, a(r,z) \left\{ \begin{array}{c} \dfrac{1}{(\Delta k - i\Gamma)^2} \\[8pt] \dfrac{\gamma^{1/2}\gamma_z c}{2\omega_b(r)(\Delta k - i\Gamma)} \end{array} \right.$$

(14a,b)

where Δk and Γ are the wave number shift and growth rate respectively and f_B is the usual difference of Bessel functions due to the linear wiggler. The lowest order mode is taken to have the form

$$a(r,z) = a_o(0)\exp(i\int_o^z (\Delta k - i\Gamma)dz' - (1-i\alpha)r^2/r_s^2).$$ (15)

For the purposes of illustration, we will consider the Compton FEL regime in which the electron beam has a Gaussian density profile, $n_b(r) = n_o \exp(-r^2/r_b^2)$.

The conditions for a guided radiation beam require that the waist and curvature of the radiation beam remain constant, ($r_s' = \alpha' = 0$). Setting $r_s' = \alpha' = 0$ in Eqs. (7a,b) and solving for Γ, Δk, r_s, and α, the following results for a guided beam are obtained.

$$\Gamma = (1+\alpha^2)^{-1}(1+2f)^{-1}\Gamma_o, \qquad \Delta k = \alpha\Gamma. \qquad (16a,b)$$

$$r_s = \left(\frac{\gamma}{\nu}\right)^{1/4} \frac{\lambda_v}{2^{7/4}\pi\gamma f_B^{1/2}} \frac{(1+a_v^2/2)^{3/4}}{a_v^{1/2}} \frac{f^{1/4}(1+2f)^{3/2}}{(1+3f/2)^{3/4}}. \quad (16c)$$

$$r_s(f=1) = 0.25 \, \lambda_v \left(\frac{\gamma}{\nu}\right)^{1/4} \frac{(1+a_v^2/2)^{3/2}}{\gamma f_B^{1/2} a_v^{1/2}}, \qquad (16d)$$

$$\alpha = (f/(2+3f))^{1/2}, \qquad (16e)$$

where $\Gamma_o = 2f_B(\nu/\gamma)^{1/2}a_v k_v(1+a_v^2/2)^{-1/2}$ and $f = r_b^2/r_s^2$ is

the filling factor.

Figure 2 shows the spatial evolution of the radiation waist for the induction linac driven FEL parameters in Table I. The parameters in Table I are consistent with Eqs. (16) and have been chosen to produce a guided radiation beam in the Compton exponential gain regime. The guided beam conditions can be shown to be stable [9], this is shown numerically by changing the spot size of the injected radiation beam. Figure 3 shows that irrespective of the initial value, the spot size asymptotes to the matched (guided) beam value. Figure 4 shows the evolution of the spot size for the rf linac-driven FEL parameters in Table II. As in Table I, the parameters in Table II have been chosen to produce a guided radiation beam in the Compton exponential gain regime and are consistent with Eqs. (16).

Fig. 2 Spatial evolution of the radiation spot size in the exponential gain regime for induction linac driven FEL parameters given in Table I.

Fig. 3 Spatial evolution of the radiation spot size in the exponential gain regime for initial spot sizes: a) 0.35 cm, b) 0.24 cm, and c) 0.15 cm.
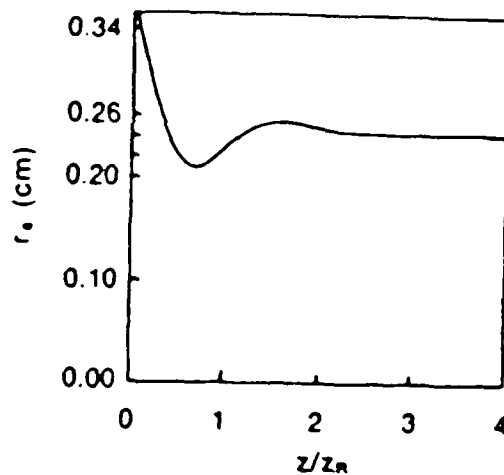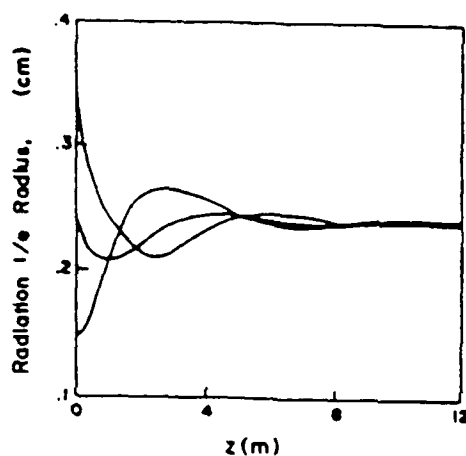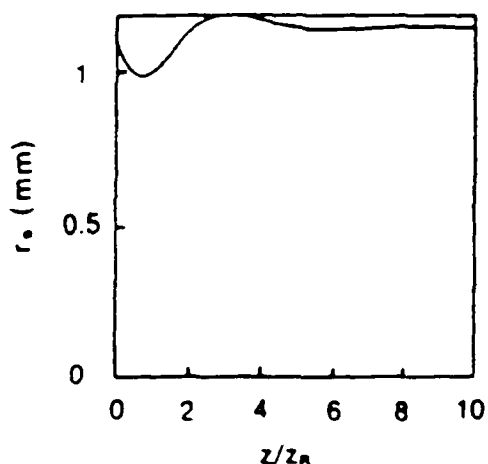

Fig. 4 Spatial evolution of the radiation spot size in the exponential gain regime for rf linac driven FEL parameters given in Table II

Free Electron Lasers driven by either induction or rf linacs could initially operate in the guided, exponential gain regime until saturation occurs. Immediately prior to saturation, the ponderomotive potential can be large enough, as in the above illustrations, to trap a significant fraction of the beam electrons. At this point, the wiggler field can be spatially tapered to achieve a significant increase in the operating efficiency and a somewhat smaller input signal into the FEL amplifier.

To determine the viability of tapering the wiggler, prior to saturation, the trapping potential associated with the ponderomotive wave is needed. For linearly polarized waves, the fractional trapping potential is

$$\frac{|e|\phi_{trap}}{vm_oc^2} = 2\sqrt{2}\left(\frac{aa_w}{(1+a_w^2/2)}\right)^{1/2}. \tag{17}$$

The radiation amplitude at saturation can be obtained from the intrinsic efficiency of the FEL. Using arguments based on electron trapping in the ponderomotive wave, we find that the intrinsic efficiency in the exponential (maximum) gain regime is

$$\eta = \Delta k/k_w. \tag{18}$$

Using the induction linac parameters in Table I as an illustration, we find that the intrinsic efficiency is $\eta = \Delta k/k_w = 0.66\%$. From this, the fractional trapping potential at the end of the exponential gain regime is $|e|\phi_{trap}/vm_o c^2 = 6\%$, making it possible to trap the electron beam while tapering the wiggler field. In addition, the initial fractional energy spread of the electron beam must be somewhat less than η. This places a limitation on the fractional energy spread of the electron beam, $\delta E/E_b < 0.66\%$. One contribution to the beam energy spread is the transverse emittance, $\delta E/E_b = (1/2)(\epsilon_n/r_b)^2$. Therefore, the normalized beam emittance must satisfy, $\epsilon_n < (2\Delta k/k_w)^{1/2}r_b = 0.034$ cm-rad.

Bending and Guiding of Radiation Beams

Using the SDE formalism, it is possible to discuss the bending of a radiation beam by a curved electron beam in an FEL. For small displacements of the electron beam centroid, a nonaxisymmetric modal expansion similar to (6) can be performed and the spatial evolution of the centroid of the radiation beam found. Figure 5 shows the centroids of the electron and radiation beams for an FEL in the trapped particle regime with parameters given in Table I. Steering of the radiation beam by the electron beam is clearly demonstrated in this figure.

It is interesting to consider the conditions under which the radiation beam could be guided by a curved electron beam, as shown in Fig. 6. Such a situation could make possible a cyclic FEL driven by, for example, a betatron generated electron beam. In a cyclic FEL, the radiation beam would be guided by a circular electron beam. The wiggler field, which is along the circular orbit of the electron beam, cannot be spatially contoured. Therefore, in the trapped particle regime, enhancement of the FEL efficiency must be achieved by inducing an accelerating electric field along the beam orbit. For cyclic electron beams, the induced electric field can be generated by increasing the magnetic flux within the orbit of the electron beam.
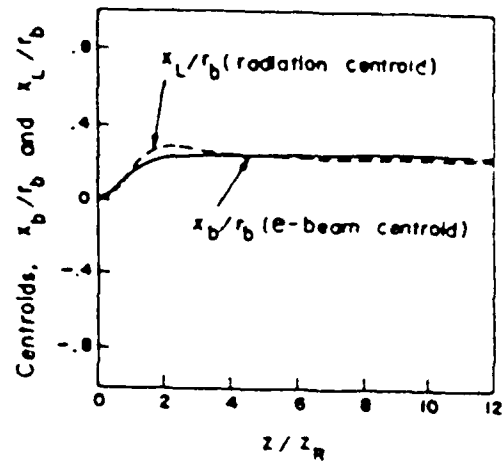

Fig. 5 Electron and radiation beam centroids, x_b and x_L for a displaced electron beam. $x_b = x_c(1-\text{sech}(k_c z))$ with $x_c = r_b/4$ and $\lambda_c = 2\pi/k_c = 4Z_R$.
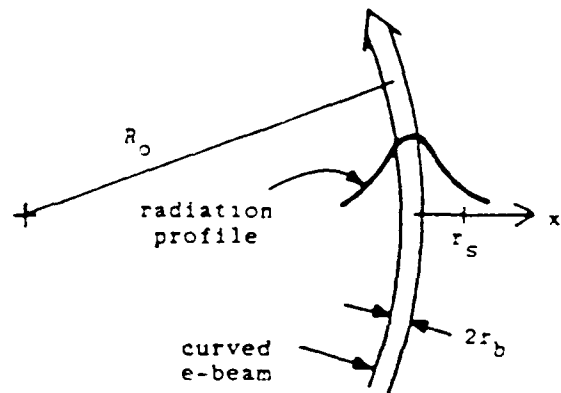
Fig. 6 Configuration showing guiding of radiation beam by a curved electron beam with radius of curvature, R_o.

To examine the conditions under which guiding can be achieved in the exponential gain regime, we denote the radial position by $r = R_o + x$, where R_o is the radius of curvature of the electron beam and x is the radial displacement from the center of the curved electron beam (see Fig. 6). The FEL refractive index (correct to order x/R_o) is

$$n = n_{fel} + x/R_o, \tag{19}$$

where n_{fel} is given by (10). In the exponential gain regime, a guided radiation beam in a curved FEL is possible if $R_o \geq R_{min}$ where

$$R_{min} = r_s/|\text{Re}(1-n_{fel})|. \tag{20}$$

Substituting the expressions for Γ, Δk and r_s from Eqs. (16), into (20) yields

$$R_{min} = \frac{4(1+f)f\gamma^2 r_b}{(1+2f)(3f+2)^{1/2}f_B a_w(1+a_w^2/2)^{1/2}(v/\gamma)^{1/2}}. \tag{21a}$$

$$R_{min}(f=1) = \frac{12\gamma^2 r_b}{f_B a_w(1+a_w^2/2)^{1/2}(v/\gamma)^{1/2}} \tag{21b}$$

For a numerical example of R_{min}, consider the following parameters. $\gamma = 100$. $I = 2$ kA. $r_b = 0.3$ cm. $a_w = 1.72$. $f = 1$ and $f_B = 0.85$ (Table I). For these parameters, the minimum turning radius required for a guided radiation beam is $R_{min} = 455$ m.

Table I

Parameters Associated with an Induction Linac Driven FEL in the Exponential Gain Regime

Electron Beam

Current	$I_b = 2$kA. ($\nu = 0.118$)
Energy	$E_b = 50$ MeV. ($\gamma = 100$)
Radius	$r_b = 0.3$ cm
Emittance	$\epsilon_n < 34\times10^{-3}$ cm-rad

Wiggler Field

Wavelength	$\lambda_w = 8$ cm
Wiggler Strength	$B_w = 2.3$ kG ($a_w = 1.72$)

Radiation Beam

Wavelength	$\lambda = 10.6$ um
Spot Size (guided beam)	$r_s = 0.25$ cm. ($Z_R = 2$ m)
e-folding length	$L_e = 1/\Gamma = 94$ cm

Intrinsic Efficiency	$\eta = \Delta k/k_w = 0.66\%$
Saturated Power	$P_{sat} = 660$ MW ($a = 7\times10^{-4}$)
Trapping Potential	$|e|\phi_{trap}/\gamma m_0 c^2 = 6.0\%$

Table II

Parameters Associated with an RF Linac Driven FEL in the Exponential Gain Regime

Electron Beam

Peak Current	$I_b = 500$ A
Energy	$E_b = 150$ MeV
Radius	$r_b = 1$ mm
Emittance	$\epsilon_n \leq 7\times10^{-3}$ cm-rad

Wiggler Field (planar)

Wavelength	$\lambda_w = 12$ cm
Wiggler Strength	$B_w = 900$ G ($a_w = 1$)

Radiation Beam

Wavelength	$\lambda = 1$ um
Spot Size (guided beam)	$r_s(0) = 1.1$ mm ($Z_R = 3.8$ m)
e-folding length	$L_e = 1/\Gamma = 196$ cm

Intrinsic Efficiency	$\eta = \Delta k/k_w = 0.25\%$
Saturated Power	$P_{sat} = 180$ MW ($a = 7.25\times10^{-5}$)
Trapping Potential	$|e|\phi_{trap}/\gamma m_0 c^2 = 2\%$

Conclusion

The source dependent expansion (SDE) method provides an excellent analytical and numerical technique for studying optical focusing, guiding and steering in FELs. We find that guided radiation beams in the FEL can be achieved both in the Compton and Raman exponential gain regimes but cannot be maintained in the high gain trapped particle (tapered wiggler) regime.

Free electron lasers driven by either induction linacs, such as the ATA, or high current rf linacs can operate in the guided, exponential gain regime until saturation occurs. At this point, the wiggler field could be spatially tapered so as to operate the FEL in the trapped particle regime in order to further increase the operating efficiency.

We also examined the possibility of bending or steering radiation beams in FELs. We find a condition which places a lower limit on the radius of curvature of the electron beam necessary for the radiation to be guided along a curved path.

References

[1] P. Sprangle and C.M. Tang. Appl. Phys. Lett. 39. 677 (1981).

[2] N.M. Kroll, P.L. Morton and M.N. Rosenbluth. IEEE J. Quantum Electron. QE-17. 1436 (1981).

[3] G.T. Moore, Nucl. Instrum. Methods in Phys. Res. A239. 19 (1985).

[4] E.T. Scharlemann, A.M. Sessler and J.S. Wurtele. Phys. Rev. Lett. 54. 1925 (1985).

[5] J.E. LaSala, D.A.G. Deacon and E.T. Scharlemann. Nucl. Instrum. Methods in Phys. Res. A250. 389 (1986).

[6] M. Xie and D.A.G. Deacon, Nucl. Instrum. Methods in Phys. Res. A250. 426 (1986).

[7] P. Sprangle, A. Ting and C.M. Tang. accepted for publication in Phys. Rev. A (1987) and Phys. Rev. Lett. (1987); also in Proceedings of 8th Intl. FEL Conf. held 1-5 Sep 1986 in Glasgow. Scotland.

[8] P. Sprangle. C.M. Tang and W. Manheimer. Phys. Rev. A, 21, 302 (1980).

[9] B. Hafizi, P. Sprangle and A. Ting, submitted to Phys. Rev. A (1987).

Appendix VI:

Optical gain, phase shift, and profile in the
Free Electron Laser

I. Introduction

A well-known feature of the free-electron laser (FEL) is that the refractive index of the medium is a complex function and hence the radiation is amplified and to some extent focused in the vicinity of the electron beam.[1,2] It may then be possible for the electron and radiation beams to interact over an extended length along the wiggler, with the diffractive tendency being compensated by the FEL interaction, thereby enhancing the efficiency of the process.

Considerable progress has been made in studying this process by several authors.[3-8] The purpose of this paper is to apply the formalism of the Gaussian-Laguerre modal source dependent expansion (SDE) of Ref. 8 to examine the propagation and guiding of the optical wave in an amplifier operating in the exponential gain regime, for a variety of operating conditions.

The plan of this paper is as follows. In Section II the formalism of the SDE is employed to obtain the evolution equations for the radius and the curvature for the lowest order mode of the optical beam, along with the relevant dispersion relation for a Gaussian electron beam driving an FEL amplifier in the small signal regime. In Section III numerical solutions of the single-mode equation for the radius of the optical beam are presented and compared to the result from a multi-mode truncation of the radiation field. In this case, and for cases not presented herein, the single-mode and multi-mode results indicate that the radiation beam profile entering the wiggler asymptotes to a <u>unique</u> form after an initial transient. Additionally, the numerical values of the radius of the radiation envelope and of the wavefront curvature are in fair agreement, irrespective of the degree of mode truncation, indicating the usefulness of the single-mode equations. Limiting ourselves to these equations, the

1

electron beam is then allowed to oscillate at the betatron wavelength and
the resulting radiation profile examined. It is found that the optical
beam envelope follows that of the electrons with almost identical
wavelength, but retarded in phase. Section IV discusses the results,
deriving formulae for the matched radiation beam profile (i.e., radius and
curvature) in terms of the electron beam and wiggler parameters. It is
shown analytically that perturbations of the profile are spatially damped
out, consistent with the numerical observations indicating a unique,
asymptotic matched radius and curvature. Appendix A presents the necessary
details required to derive the source term, for the wave equation, for a
planar wiggler and an electron beam with uniform density along the
direction of propagation. Appendix B considers the effect of the
modulation of the electron beam on the optical wave. Specifically, a
simple analysis, taking into account sideband generation, indicates that
the dispersion characteristics of the primary wave are only slightly
modified for typical experimental parameters. Appendix C presents the
details of the stability calculation.

II. Mathematical Formulation

The purpose of the present section is to present the salient features
of the source dependent expansion method[8] so as to fix the notation and for
reference in the subsequent sections.

For a planar wiggler, it is appropriate to assume a linearly polarized
radiation vector potential

$$\underline{A} = (1/2) A(r,\theta,z)\exp\left[i\left(\frac{\omega z}{c} - \omega t\right)\right]\underline{e}_x + c.c.,$$

with angular frequency ω and complex amplitude A. In the slowly varying
envelope approximation, the wave equation reduces to

$$\left(\frac{1}{r}\frac{\partial}{\partial r} r \frac{\partial}{\partial r} + \frac{1}{r^2}\frac{\partial^2}{\partial \theta^2} + \frac{2i\omega}{c}\frac{\partial}{\partial z}\right)a = S(r,\theta,z), \tag{1}$$

where $a = |e|A/m_0 c^2$, and the source function is given by

$$S(r,\theta,z) = -\frac{8\pi|e|}{m_0 c^3}\left\{J_x(r,\theta,z)\exp\left[-i\left(\frac{\omega z}{c} - \omega t\right)\right]\right\}_{slow} . \tag{2}$$

Here e is the charge on an electron of (rest) mass m_0, $J_x(r,\theta,z)$ is the
current density and $\{\ \}_{slow}$ indicates that only the spatially and
temporally slow part of the quantity in braces is to be retained.

The basic premise of the work presented herein is that the radiation
field is azimuthally symmetric and the vector potential is expressible as:

$$a(r,\theta,z) = \sum_{m=0}^{\infty} a_m(z)D_m(\xi,z), \tag{3}$$

with $D_m = L_m(\xi) \exp\{-[1-i\alpha(z)]\xi/2\}$, where $\xi = 2r^2/r_s^2(z)$, $r_s(z)$ is related
to the radiation spot size, $\alpha(z)$ is proportional to the curvature of the
wavefront, and $L_m(\xi)$ is the Laguerre polynomial of order m.

Now, if the transverse profile of the radiation beam is close to a
Gaussian, the lowest order mode is expected to dominate[3,5,7,8], and,
following Ref. 8, it is simple to show that the associated vector potential
evolves according to

$$\left(\frac{\partial}{\partial z} + A_0\right)a_0 = -i F_0, \tag{4}$$

and the spot size and wavefront curvature evolve via

3

$$\frac{d}{dz} r_s - \frac{2c\alpha}{\omega r_s} = -r_s \left(\frac{F_1}{a_0}\right)_I , \tag{5a}$$

$$\frac{d}{dz} \alpha - 2(1+\alpha^2)\frac{c}{\omega r_s^2} = 2\left[\left(\frac{F_1}{a_0}\right)_R - \alpha\left(\frac{F_1}{a_0}\right)_I\right], \tag{5b}$$

where

$$A_0 = \frac{1}{r_s} \frac{d}{dz} r_s + i\left[(1+\alpha^2) \frac{c}{\omega r_s^2} - \frac{\alpha}{r_s} \frac{d}{dz} r_s + \frac{1}{2} \frac{d}{dz} \alpha\right],$$

the F's are given by the following overlap integral:

$$F_m(z) = \frac{c}{2\omega} \int_0^\infty d\xi \, S(\xi,z)D_m^*(\xi,z), \tag{6}$$

and the label R (I) indicates the real (imaginary) part.

Noting that $L_0(\xi) = 1$, the normalized vector potential is seen to be given by [Eq. (3)]

$$a(r,\theta,z) = a_0(z) \exp\left\{-[1-i\alpha(z)]\frac{r^2}{r_s^2(z)}\right\}, \tag{7}$$

where, in the exponential gain, small-signal regime,

$$a_0(z) = a(o) \exp\left\{i \int_0^z dz_1\left[\Delta k(z_1) - i\Gamma(z_1)\right]\right\}. \tag{8}$$

Here a(o) is the input signal at z = o, and the two components of the refractive index are given by

$$n_z = [1 + \frac{c\Delta k}{\omega}] - i \frac{c}{\omega} \left(\Gamma - r^2 \frac{\partial}{\partial z} \frac{1-i\alpha}{r_s^2}\right) \tag{9a}$$

$$n_r = \frac{2cr}{\omega r_s^2} (\alpha + i). \tag{9b}$$

4

Assuming the electron beam profile to be given by

$$n_b(z) = n_{bo} \left[\frac{r_{bo}}{r_b(z)}\right]^2 \exp\left[-\frac{r^2}{r_b^2(z)}\right], \tag{10}$$

where $r_b(z)$ is the electron beam radius at z and n_{bo} is the beam density at $r_b(z) = r_{bo}$, the source term in Eq. (1) may be readily evaluated (Appendix A), to obtain

$$S(r,z) = f_B \frac{\omega_{bo}^2}{2\gamma^3 c^2} \left[\frac{r_{bo}}{r_b(z)}\right]^2 \exp\left(-\frac{r^2}{r_b^2}\right) \frac{\omega \, k_v a_v^2 a}{c(\Delta k - i\Gamma)^2}, \tag{11}$$

where the vector potential of the planar wiggler of periodicity $2\pi/k_v$ is given by

$$\underline{A}_v = A_v \cos(k_v z)\underline{e}_x, \tag{12}$$

$$a_v = |e|A_v/m_o c^2, \tag{13}$$

γ is the relativistic mass factor, f_B is the usual difference of Bessel functions, $f_B = J_0(\zeta) - J_1(\zeta)$, $\zeta = (1/4)a_v^2/[1 + (1/2)a_v^2]$, and

$$\omega_{bo} = \left(4\pi|e|^2 n_{bo}/m_o\right)^{1/2}$$

is the plasma frequency of the electron beam with density n_{bo}.

Substituting Eqs. (8) and (11) into Eq. (6) and making use of Eqs. (4) and (5), it is simple to show that the equations reduce to

$$\frac{d\alpha}{d(k_v z)} = 2(1+\alpha^2)\left(\frac{ck_v}{\omega}\right)\frac{1}{(k_v r_s)^2} + 2\left[\left(\frac{F_1}{k_v a_o}\right)_R - \alpha\left(\frac{F_1}{k_v a_o}\right)_I\right], \tag{14a}$$

$$\frac{d\left(k_v r_s\right)^2}{d\left(k_v z\right)} = 4\alpha\left(\frac{ck_v}{\omega}\right) - 2\left(\frac{F_1}{k_v a_o}\right)_I \left(k_v r_s\right)^2, \tag{14b}$$

5

$$\frac{\Delta k}{k_v} - i\frac{\Gamma}{k_v} + 2\left(\frac{ck_v}{\omega}\right)\frac{1-i\alpha}{\left(k_v r_s\right)^2} + 2\left(\frac{F_1}{k_v a_0}\right)\left[1 + \left(\frac{r_b}{r_s}\right)^2\right] = 0, \tag{14c}$$

where

$$\frac{F_1}{k_v a_0} = f_B\left(\frac{\omega_{bo}}{ck_v}\right)^2\left[\frac{r_{bo}}{r_b(z)}\right]^2\frac{a_v^2}{2\gamma^3}\frac{\left(r_b/r_s\right)^2}{\left[1+2(r_b/r_s)^2\right]^2}\left(\frac{\Delta k}{k_v} - i\frac{\Gamma}{k_v}\right)^{-2}. \tag{14d}$$

The spatial evolution of the system is governed by the differential system (14a) and (14b) along with the dispersion relation (14c), the solution of which yields $\alpha(z)$, $r_s(z)$, $\Delta k(z)$ and $\Gamma(z)$.

III. Numerical Results

Having obtained the single mode system of Eqs. (14), it is of interest to determine the extent to which it approximates the general solution in (3). Once it is established that Eqs. (14) provide an adequate representation of the general solution, it is then possible to study a variety of problems of interest by solving a simple set of equations.

Briefly, the numerical procedure for solving an initial-value problem is the following. Substituting Eq. (14d) into Eq. (14c) yields a cubic (algebraic) equation for $\Delta k - i\Gamma$ which may be solved, at each z, in terms of $r_s(z)$, $\alpha(z)$ and $r_b(z)$, thus enabling Eqs. (14a) and (14b) to be stepped forward in z. Since in the absence of source terms an input radiation signal diffracts away on the scale length defined by the Rayleigh range z_R,

$$z_R = \frac{\omega\, r_s^2(z)}{2c}\bigg|_{z=0}, \tag{15}$$

6

It is informative to present the numerical results with the distance along the wiggler measured in units of the Rayleigh range. In all the numerical results to be presented, the radiation field is assumed to be in the form of plane waves at the entrance to the wiggler, i.e., $\alpha(z=0) = 0$.

Case I

To begin with, Fig. 1 shows the results for the following parameters: beam current, $I_b = 270$ A, $r_{bo} = 0.01$ cm, $\gamma = 2000$, $2\pi/k_v = 10$ cm, $a_v = 6.15$ and $r_s(z=0) = 0.02$ cm. Noting the factor of $2^{1/2}$ difference between the definition of a_v in Eq. (13) and that in Ref. 4, it is clear from Fig. 1(a) that after a transient oscillation over a distance of about 20 Rayleigh ranges, the radiation spot size approaches a value quite close to that obtained with the two-dimensional FEL code FRED at the Lawrence Livermore National Laboratory (LLNL).[4] We also find that for all the numerical cases examined, a unique, asymptotic spot size is obtained irrespective of the initial optical waist. Figure 1(b) shows the spatial evolution of α, indicating that it, too, approaches a constant value after an initial transient behavior.

The solid curve in Fig. 2 shows the evolution of $1/e$ width of the radiation amplitude with a five mode ($m=0,1,2,3,4$) source dependent expansion calculation using the same set of FEL parameters. The radiation field is represented by Eq. (3) and the source term is given by Eq. (11). With the assumption that the fundamental mode dominates, only the Δk and Γ of a_o (r,z) are involved in the source function and they are obtained from Eqs. (14c) and (14d). It is found that the fundamental mode remains dominant over many Rayleigh lengths. For comparison the dashed curve in Fig. 2 shows the fundamental mode spot size of Fig. 1(a), and the asymptotic results are seen to differ by about 10%. This suggests that the

7

single-mode system of Eqs. (14) may be regarded as a reasonable and accurate simplification of Eq. (3). Henceforth the results presented pertain to Eqs. (14).

Case II

Figure 3 presents the results for a case where the electron beam is not matched; i.e., the envelope of the electron beam is modulated:

$$r_b(z) = r_{bo} + \delta r_b \sin(k_\beta z), \tag{16}$$

where δr_b is the amplitude of the modulation and for simplicity k_β is chosen to be equal to the betatron wave number[10] $k_v a_v/(\sqrt{2}\gamma\beta_z)$, neglecting self-fields.[11] β_z is the beam speed along the wiggler axis normalized to c. The parameters, typical of the Advanced Test Accelerator experiment at LLNL, are $I_b = 2$ kA, $r_{bo} = 0.3$ cm, $\gamma = 100$, $2\pi/k_v = 8$ cm, $a_v = 1.72$, $r_s(z=0) = 0.35$ cm. In Fig. 3, where $\delta r_b/r_{bo} = 0.1$, it is observed that the optical spot size follows the modulations in the electron envelope apparently identically. Specifically, a number of cases were examined with $\delta r_b/r_{bo}$ up to 0.4. In all cases the electron and optical beams oscillate with almost identical wavelength, although the radiation beam appears to lag behind in phase. However, defining the modulation depth $\Delta = [(r)_{max} - (r)_{min}]/[(r)_{max} + (r)_{min}]$, it is found from Fig. 3(a) that $\Delta_s = 0.087$ whereas, from Eq. (16), $\Delta_b = \delta r_b/r_{bo} = 0.1$. Although the modulation depth of the electron beam differs from that of the radiation beam, it is found that Δ_s increases in proportion to δr_b.

More generally, allowing for the defocusing effect of self-fields, there is always the possibility of a small amplitude ripple on the electron beam envelope and hence on the radiation beam envelope. In Appendix B, generation of sidebands is considered in a simplified model and found to

8

have, for typical cases, an insignificant effect on the linear dispersion characteristics of the primary optical wave, as implicitly assumed by employing the source term in Eq. (11) in the present case.

IV. Analysis of Results

One interesting feature of the numerical results is that in all cases the radiation spot size has a unique, asymptotic limit irrespective of the initial value. The asymptotic value of r_s and of α is determined by the fixed points of Eqs. (14a) and (14b); i.e., at the fixed point

$$2(1+\alpha^2) \, \frac{ck_v}{\omega} \, \frac{1}{(k_v r_s)^2} \; + \; 2 \left[\left(\frac{F_1}{k_v a_o} \right)_R - \alpha \left(\frac{F_1}{k_v a_o} \right)_I \right] = 0, \qquad (17a)$$

$$4\alpha \, \frac{ck_v}{\omega} - 2 \left(\frac{F_1}{k_v a_o} \right)_I \left(k_v r_s \right)^2 = 0. \qquad (17b)$$

Combining Eqs. (17a) and (17b) one obtains

$$(1 - i\alpha)^2 \, \frac{ck_v}{\omega} + (k_v r_s)^2 \left(\frac{F_1}{k_v a_o} \right) = 0,$$

which, upon making use of Eq. (14d), yields

$$\Delta k = \frac{k_v^2 r_b \eta^{1/2}}{1+2f} \, \frac{\alpha}{1+\alpha^2}, \quad \Gamma = \Delta k/\alpha,$$

where

$$\eta = f_B \left(\frac{\omega}{ck_v} \right) \left(\frac{\omega_{bo}}{ck_v} \right)^2 \left(\frac{r_{bo}}{r_b} \right)^2 \frac{a_v^2}{2\gamma^3},$$

and $f = (r_b/r_s)^2$ is the filling factor. Substituting the expressions for Δk and Γ into the dispersion relation (14c), one obtains

$$\alpha = [f/(3f + 2)]^{1/2},$$

$$r_s = \frac{(\gamma/\nu)^{1/4}}{2^{3/4} k_\nu \gamma f_B^{1/4}} \frac{(1+a_\nu^2/2)^{3/4}}{a_\nu^{1/2}} \frac{f^{1/4}(1+2f)^{3/2}}{(1+3f/2)^{3/4}},$$

where $\nu = (\omega_{bo} r_{bo}/2c)^2$ is Budker's parameter. These expressions may be used to obtain the asymptotic spot size for a given filling factor, and then one obtains the corresponding electron beam radius via $r_b = r_s f^{1/2}$. To avoid complications arising at the outer edges of the op cal beam, where the field amplitude is small, typically a filling factor $f \leq 1/2$ is appropriate. It is also possible to rearrange the expression for r_s to obtain

$$f^3 + f^2 + \left(\frac{1}{4} - \frac{3}{2} q\right) f - q = 0,$$

where

$$q = \left[a_\nu^2 \left(\frac{2f_B}{\gamma/\nu}\right)\left(\frac{\gamma r_b k_\nu}{2}\right)^4\right]^{1/3} \frac{1}{1+a_\nu^2/2}.$$

The cubic equation for f may be solved to obtain an explicit expression for r_s. Noting that the sum and the product of the three roots of the cubic equal -1 and q, respectively, it follows that there is a unique, real value for the asymptotic spot size r_s.

To examine stability, it is convenient to define

$$Y = \frac{\Delta k}{k_\nu} - i \frac{\Gamma}{k_\nu},$$

and substitute Eq. (14d) into Eq. (14c) to obtain the local dispersion relation:

10

$$\gamma^3 + 2\left(\frac{ck_v}{\omega}\right)\frac{1-i\alpha}{(k_v r_s)^2}\gamma^2 = -2\frac{ck_v}{\omega}\eta\left(\frac{r_b}{r_s}\right)^2\frac{1+(r_b/r_s)^2}{\left[1+2(r_b/r_s)^2\right]^2}, \qquad (18)$$

which may be solved iteratively. It turns out that for the parameters of Case I, at the lowest order, the right-hand side balances the quadratic term on the left. The relevant root, with Δk, $\Gamma > 0$, may be substituted into Eq. (14d) to obtain, for $\alpha > 0$,

$$\frac{F_1}{k_v a_0} = \frac{-ck_v}{\omega}\frac{1-i\alpha}{(k_v r_s)^2+(k_v r_b)^2} - \frac{1}{2}\left[\frac{\eta}{2(1+\alpha^2)}\right]^{1/2}\frac{\alpha-i\left[1+(1+\alpha^2)^{1/2}\right]}{\left[1+(1+\alpha^2)^{1/2}\right]^{1/2}}$$

$$\cdot\frac{(k_v r_s)^2}{(k_v r_s)^2+2(k_v r_b)^2}\frac{(k_v r_s)(k_v r_b)}{\left[(k_v r_s)^2+(k_v r_b)^2\right]^{1/2}}. \qquad (19)$$

Perturbing Eqs. (14a) and (14b) about the fixed point and making use of Eq. (19), it is simple to show that the perturbation is spatially damped, thus indicating the stability of the fixed point. The algebraic details are relegated to Appendix C.

Another aspect of the results which is of interest pertains to the nature of the phase fronts and the flux of optical power in the asymptotic region. From Eqs. (7) and (8) it is simple to check that, in differential form, the surfaces of constant phase are given by $(\omega/c + \Delta k)\delta z + (2r\alpha/r_s^2)\delta r = 0$, and hence, noting that Δk, $\alpha > 0$, the wavefronts are divergent in the direction of propagation. Consistent with this, there is a nonvanishing transverse component of the Poynting flux. Specifically, for $r/r_s \lesssim 1$ the ratio of flux of optical energy in the transverse direction to that along the z axis is $\sim \alpha r/k r_s^2 \ll 1$.

V. Conclusion

Based on the results presented herein, the simplicity and accuracy of the single-mode Gaussian-Laguerre approximation to the solution of Maxwell's equations has been demonstrated. It is shown that, in the exponential gain regime of operation of an FEL amplifier, there is a unique, asymptotic spot size for the radiation beam irrespective of that at the entrance of the wiggler. There is, however, a transverse flux of optical power. It is shown analytically that the asymptotic profile (i.e., the radius and the curvature at large z) is stable to small amplitude perturbations. With a spatially modulated electron beam envelope, that of the optical beam is found to oscillate on the same spatial scale.

References

1. N. M. Kroll, P. L. Morton, and M. N. Rosenbluth, IEEE J. Quantum Electron. QE-17, 1436 (1981).

2. P. Sprangle and C. M. Tang, Appl. Phys. Lett. 39, 677 (1981).

3. G. T. Moore, Nucl. Instrum. Methods in Phys. Res. A239, 19 (1985).

4. E. T. Scharlemann, A. M. Sessler, and J. S. Wurtele, Phys. Rev. Lett. 54, 1925 (1985).

5. G. T. Moore, Nucl. Instrum. Methods in Phys. Res. A250, 381 (1986).

6. J. E. LaSala, D.A.G. Deacon and E. T. Scharlemann, Nucl. Instrum. Methods in Phys. Res. A250, 389 (1986).

7. M. Xie and D.A.G. Deacon, Nucl. Instrum. Methods in Phys. Res. A250, 426 (1986).

8. P. Sprangle, A. Ting and C. M. Tang (submitted to Physical Review Letters and Physical Review A).

9. E. T. Scharlemann, A. M. Sessler and J. S. Wurtele, Nucl. Instrum. Methods in Phys. Res. A239, 29 (1985).

10. E. T. Scharlemann, J. Appl. Phys. 58, 2154 (1985).

11. E. P. Lee and R. K. Cooper, Particle Acc. 7, 83 (1976).

12. P. Sprangle, C. M. Tang and C. W. Roberson, Nucl. Instrum. Methods in Phys. Res. A239, 1 (1985).

Appendix A: Source Term

In this appendix, the details of the evaluation of the source term S in Eq. (11) are presented.

The FEL source current, $J_x(r,\theta,z)$, in a linear wiggler is given by

$$J_x(r,\theta,z) = -|e|\delta n_b(r,\theta,z)v_x$$

$$= -\frac{|e|^2 \delta n_b e^{-ik_v z}}{2\gamma m_o c} A_v + c.c.$$

where δn_b is the perturbed beam density and the relation $v_x = v_v = |e|A_v \cdot \cos(k_v z)/\gamma m_o c$ has been used. Equation (2) can then be written as

$$S(r,\theta,z) = \left\{ \frac{4\pi|e|^2 \delta n_b a_v}{\gamma m_o c^2} e^{-i\left[(k + k_v)z - \omega t\right]} \right\}_{slow} \tag{A1}$$

where $k = \omega/c$.

The perturbed beam density can be evaluated from the continuity equation,

$$\frac{d\delta n_b}{dt} = -n_b \frac{\partial \delta v_z}{\partial z}, \tag{A2}$$

and the equation of motion in the z-direction,

$$\frac{dv_z}{dt} = -\frac{|e|}{\gamma m_o} \left[\frac{v_x B_y}{c} - \frac{v_z\left(v_x E_x\right)}{c^2} \right] \tag{A3}$$

where electron self-field effects are neglected. Taking the convective time derivative of Eq. (A2), and incorporating the linearized version of Eq. (A3), one can arrive at the following equation for the perturbed beam density,

$$\frac{d^2 \delta n_b}{dt^2} = -\frac{|e|n_b}{\gamma m_o} \frac{\partial}{\partial z}\left(\frac{\partial}{\partial z} + \frac{v_z}{c^2}\frac{\partial}{\partial t}\right)\phi_{pond} \qquad (A4)$$

where

$$\phi_{pond} = -\frac{|e|A_v A}{4\gamma m_o c^2} e^{i\left[(k + k_v)z - \omega t\right]} + c.c.$$

With the assumption that $A(r,\theta,z)$ is a slowly varying function of z, i.e., $|\partial \ln A/\partial z| \ll k_v \ll k$, Eq. (A4) becomes

$$\frac{d^2 \delta n_b}{dt^2} = \frac{|e|^2 n_b A_v A}{2\gamma^2 m_o^2 c^2} k_v k e^{i\left[\left(k + k_v\right)z - \omega t\right]} + c.c. \qquad (A5)$$

where the resonance condition, $\omega = v_z(k + k_v)$ is used.

For a near Gaussian radiation field in the exponential gain regime,

$$A(r,\theta,z) = A_o(r,\theta,z) = A_o(o)\exp\left\{i\int_o^z [\Delta k(z_1) - i\Gamma(z_1)]dz_1 - [1 - i\alpha(z)]\frac{r^2}{r_s^2(z)}\right\}$$

and assuming Δk, Γ, α and r_s are slowly varying functions of z, Eq. (A5) can be integrated immediately to give

$$\delta n_b = \frac{|e|^2 n_b A_v A \, k \, k_v}{2\gamma^2 m_o^2 c^4 (\Delta k - i\Gamma)^2} e^{i\left[(k + k_v)z - \omega t\right]} + c.c. \qquad (A6)$$

When Eq. (A6) is substituted into Eq. (A1), taking into account the usual difference of Bessel functions for a planar wiggler, and Eq. (10) for the beam profile, the source function in Eq. (1) is then given by Eq. (11).

15

Appendix B: Sideband Generation

In this appendix generation of sidebands to the primary optical wave, due to the spatial modulation of the electron beam, is analyzed. It is to be emphasized that the following analysis is intended merely to show that the dispersion characteristics of the primary optical wave are only slightly modified [$\sim (\delta N_o/N_o)^2$] for typical experimental parameters, as implicitly assumed in applying the results of Appendix A to the case of a modulated electron beam in Section III.

The development of the linear theory herein generalizes that of Sprangle et al.,[12] to which reference should be made for further details.

The form of the vector potential of a planar wiggler employed in this appendix is slightly different to that given by Eq. (12):

$$\underline{A}_w = A_w \Big[\exp(ik_w z) - c.c.\Big]\underline{e}_x,$$

where A_w is purely imaginary, and that of the linearly polarized radiation field is taken to be of the form

$$\underline{A} = \Big\{A_+ \exp\Big[ik_+ z - i\omega t\Big] + \underline{A} \exp\Big[ik_- z - i\omega t\Big]$$

$$+ A_o \exp\Big(ik\,z - i\omega t\Big) + c.c.\Big\}\ \underline{e}_x,$$

where it is assumed that the electron density, modulated at the betatron wavelength $2\pi/k_\beta$, has the simple form

$$n_o = N_o + \frac{\delta N_o}{2}\Big[\exp(ik_\beta z) + c.c.\Big],$$

with $k_\beta \ll k_w \ll k$, and $k_+ = k + k_\beta$, $k_- = k - k_\beta$.

16

Following Ref. 12, the wave equation is found to be

$$\left(\frac{\partial^2}{\partial z^2} - \frac{1}{c^2}\frac{\partial^2}{\partial t^2} - \frac{\omega_b^2}{\gamma_o c^2}\right)\underline{A} = \frac{4\pi|e|^2}{\gamma_o m_o c^2}\delta n \underline{A}_v,$$

where γ_o is the relativistic factor in the absence of the radiation field, $\omega_b = (4\pi n_o|e|^2/m_o)^{1/2}$, and δn is the density perturbation caused by the radiation. Note that the velocity v_{zo} along the wiggler axis is not affected by the betatron oscillation and hence γ_o, to lowest order in $|eA_v/\gamma_o m_o c^2|^2$, is not a function of z. Defining the ponderomotive potential

$$\phi_{pond} = \frac{-|e|}{\gamma_o m_o c^2}\underline{A}_v \cdot \underline{A},$$

the momentum, continuity and Poisson's equations may be combined to obtain

$$\frac{d^2}{dt^2}\delta n - \frac{v_{zo}}{n_o}\left(\frac{\partial n_o}{\partial z}\right)\frac{d}{dt}\delta n + \frac{4\pi n_o|e|^2}{m_o\gamma_o\gamma_z^2}\delta n + \frac{|e|}{m_o\gamma_o\gamma_z^2}\left(\frac{\partial n_o}{\partial z}\right)\frac{\partial\phi}{\partial z}$$

$$= \frac{-|e|}{m_o\gamma_o}\frac{\partial}{\partial z}n_o\left(\frac{\partial}{\partial z} + \frac{v_{zo}}{c^2}\frac{\partial}{\partial t}\right)\phi_{pond}, \qquad (B1)$$

where $\gamma_z = (1-v_{zo}^2/c^2)^{-1/2}$, ϕ is the scalar potential, and terms such as $\partial^2 n_o/\partial z^2$, which are on the order of k_β^2, have been neglected.

Writing $k_+ = k + k_\beta$, $k_- = k - k_\beta$,

$$\delta n = \left\{\delta n_+ \exp\left[i\left(k_+ + k_v\right)z - i\omega t\right] + \delta n_- \exp\left[i\left(k_- + k_v\right)z - i\omega t\right]\right.$$

$$\left. + \delta n_o \exp\left[i\left(k + k_v\right)z - i\omega t\right] + c.c.\right\},$$

noting that, on the left-hand side of Eq. (B1), the ratio of the fourth to the third term is on the order of $k_\beta/k \ll 1$, one finds that

17

$$
\begin{bmatrix}
m_{11} + \varepsilon^2 a_- & \varepsilon m_{12} & m_{13} \\
\varepsilon m_{21} & m_{22} + \varepsilon^2 a_{22} & \varepsilon m_{23} \\
m_{31} & \varepsilon m_{32} & m_{33} + \varepsilon^2 a_+
\end{bmatrix}
\begin{bmatrix}
A_+ \\
A_o \\
A_-
\end{bmatrix}
= 0,
$$

where $\varepsilon = (\delta N_o / 2 N_o)$, and m_{13}, $m_{31} = O(\varepsilon^2)$. It is then simple to show that, correct to $O(\varepsilon^2)$, the dispersion relation is given by

$$
m_{22} - \left(\frac{\delta N_o}{2 N_o}\right)^2 \left(\frac{m_{32} m_{23}}{m_{33}} + \frac{m_{12} m_{21}}{m_{11}}\right) + \left(\frac{\delta N_o}{2 N_o}\right)^2 \left[a_{22} + m_{22}\left(\frac{a_+}{m_{33}} + \frac{a_-}{m_{11}}\right)\right] = 0,
$$

where

$$
m_{22} = m_{22}(k) = \left\{\left[\omega - (k + k_w)v_{zo}\right]^2 - \frac{\omega_{bo}^2}{\gamma_o \gamma_z^2}\right\}\left(k^2 - \frac{\omega^2}{c^2} + \frac{\omega_{bo}^2}{\gamma_o c^2}\right)
$$

$$
- \frac{2\omega_{bo}^2}{\gamma_o^3} k\, k_w\, a_w^2,
$$

is the usual matrix element for the primary wave, $m_{11} = m_{22}(k_+)$,
$m_{33} = m_{22}(k_-)$,

$$
m_{12} = m_{12}(k_+, k, k_\beta)
$$

$$
= \frac{\omega_{bo}^2}{\gamma_o c^2} \left\{\left[\omega - (k_+ + k_w)v_{zo}\right]^2 - \frac{\omega_{bo}^2}{\gamma_o \gamma_z^2}\right\}
$$

$$
+ \left\{k_\beta v_{zo}\left[\omega - (k + k_w)v_{zo}\right] - \frac{\omega_{bo}^2}{\gamma_o \gamma_z^2}\right\}
$$

$$
\cdot \left(k^2 - \frac{\omega^2}{c^2} + \frac{\omega_{bo}^2}{\gamma_o c^2}\right) - \frac{2\omega_{bo}^2}{\gamma_o^3} k_+ k_w a_w^2,
$$

$$m_{21} = m_{12}\left(k, k_+, -k_\beta\right), \quad m_{23} = m_{12}\left(k, k_-, k_\beta\right), \quad m_{32} = m_{12}\left(k_-, k, -k_\beta\right),$$

$$a_{22} = -\frac{2\omega_{bo}^4}{\gamma_o^2 \gamma_z^2 c^2} + \frac{2\omega_{bo}^2 k_\beta^2 v_{zo}^2}{\gamma_o^2 c^2},$$

$$a_{\substack{-\\+}} = \frac{\omega_{bo}^2}{\gamma_o c^2} \left\{ k_\beta v_{zo}\left[\omega - \left(k + k_v\right)v_{zo}\right] \mp \frac{\omega_{bo}^2}{\gamma_o \gamma_z^2} \right\},$$

and $\omega_{bo} = (4\pi e^2 N_o/m_o)^{1/2}$. Note that with the definition chosen for A_v in this appendix, $a_v^2 = (eA_v/m_o c^2)^2 < 0$.

To proceed along the lines of Ref. 12, it is convenient to write

$$m_{22} = M_{22} + C_{22},$$

where

$$M_{22} = \left\{\left[\omega - \left(k + k_v\right)v_{zo}\right]^2 - \frac{\omega_{bo}^2}{\gamma_o \gamma_z^2}\right\} \left(k^2 - \frac{\omega^2}{c^2} + \frac{\omega_{bo}^2}{\gamma_o c^2}\right),$$

and

$$C_{22} = \frac{-2\omega_{bo}^2}{\gamma_o^3} k\, k_v a_v^2$$

is the "coupling" term. The dispersion relation then becomes

$$\left[1 + \left(\frac{\delta N_o}{2N_o}\right)^2 \left(\frac{a_+}{m_{33}} + \frac{a_-}{m_{11}}\right)\right] M_{22} = -\left[1 + \left(\frac{\delta N_o}{2N_o}\right)^2 \left(\frac{a_+}{m_{33}} + \frac{a_-}{m_{11}}\right)\right] C_{22}$$

$$+ \left(\frac{\delta N_o}{2N_o}\right)^2 \left(\frac{m_{12} m_{21}}{m_{11}} + \frac{m_{32} m_{23}}{m_{33}} - a_{22}\right). \tag{B2}$$

M_{22} yields the dispersion relation for uncoupled electromagnetic and space charge waves. The right-hand side of Eq. (B2) introduces the FEL interaction and coupling to sidebands, and its effect is included iteratively. At the lowest order, $M_{22} = 0$ for some (ω, k). Substituting in the right-hand side, the second set of terms vanishes; the term proportional to C_{22} survives.

Substantial modification of this dispersion relation is expected if

$$1 + \left(\frac{\delta N_o}{2N_o}\right)^2 \left(\frac{a_+}{m_{33}} + \frac{a_-}{m_{11}}\right) \ll 1$$

i.e., if

$$\frac{\delta N_o}{N_o} \sim 2\, k_\beta c \omega_{bo}^{-3/2} \left(2k\, v_{zo}\right)^{1/2} \gamma_z^{1/2} \gamma_o^{3/4}.$$

For typical experimental parameters, the right-hand side of this equation exceeds unity, whereas $\delta N_o/N_o \ll 1$, implying the insignificance of the effect of modulation on the dispersion relation.

Appendix C: Stability Analysis

The purpose of this appendix is to establish the stability of the fixed point (r_s, α) of Eqs. (14).

Perturbing Eqs. (14a) and (14b) about the fixed point and making use of Eq. (19), it is seen that the perturbation evolves according to:

$$\frac{d}{d(k_v z)} \begin{pmatrix} \delta\alpha \\ \delta x \end{pmatrix}$$

$$= 2 \begin{pmatrix} a_{11} & a_{12} \\ a_{21} & a_{22} \end{pmatrix} \begin{pmatrix} \delta\sigma \\ \delta x \end{pmatrix},$$

where $x = (k_v r_s)^2$, $y = (k_v r_b)^2$,

$$a_{11} = \frac{-\alpha(ck_v/\omega)}{x+y} + X_I + \frac{\partial}{\partial\alpha}\left(X_R - \alpha X_I\right),$$

$$a_{12} = \frac{-(1+\alpha^2)(ck_v/\omega)y(2x+y)}{x^2(x+y)^2} + \frac{\partial}{\partial x}\left(X_R - \alpha X_I\right),$$

$$a_{21} = \frac{x X_I}{\alpha} - x\frac{\partial}{\partial\alpha}X_I,$$

$$a_{22} = -\frac{\alpha(ck_v/\omega)}{(x+y)^2} - \frac{\partial}{\partial x}\left(x X_I\right),$$

and

$$X = -\frac{1}{2}\left[\frac{\eta}{2(1+\alpha^2)}\right]^{1/2} \frac{\alpha - i\left[1 + \left(1+\alpha^2\right)^{1/2}\right]}{\left[1 + \left(1+\alpha^2\right)^{1/2}\right]^{1/2}} \frac{x}{x+2y}\left(\frac{xy}{x+y}\right)^{1/2}. \quad (C1)$$

Assuming that $\delta\alpha$, $\delta x \sim \exp(\lambda k_v z)$, one finds that

$$\lambda = -\left[\frac{\alpha(ck_v/\omega)(x+2y)}{(x+y)^2} + S_2 + S_1\right] \pm \left\{\left[\frac{-\alpha(ck_v/\omega)x}{(x+y)^2} + S_2 - S_1\right]^2 - S_3\right\}^{1/2},$$

21

where

$$S_1 = -\frac{\partial X_R}{\partial \alpha} + \alpha \frac{\partial X_I}{\partial \alpha},$$

$$S_2 = \frac{\partial}{\partial x}\left(x X_I\right),$$

$$S_3 = -4x\left(\frac{X_I}{\alpha} - \frac{\partial X_I}{\partial \alpha}\right)\left[\frac{-\left(1+\alpha^2\right)\left(ck_v/\omega\right)y(y+2x)}{x^2(x+y)^2} + \frac{\partial}{\partial x}\left(X_R - \alpha X_I\right)\right].$$

(Note that all the variables in this appendix are evaluated at the fixed point.) Making use of Eq. (C1) it is simple to show that $X_I/\alpha - \partial X_I/\partial \alpha > 0$, $\partial(X_R - \alpha X_I)/\partial x < 0$, whence $S_3 > 0$ and hence, noting that $S_2 + S_1 > 0$, and that the perturbation solution for Eq. (18) implies $S_1 < \alpha(ck_v/\omega)/(x+y)$, one finds that Re $\lambda < 0$, thus indicating the stability of the fixed point to small amplitude perturbations.

Fig. 1.   Spot size (r_s), α, phase shift (Δk), and gain (Γ) vs. distance along the viggler.   z is normalized to the Rayleigh range z_R.   In (c) and (d) the number on the ordinate must be multiplied by 10^{-4} and 10^{-3} to obtain the actual value for $\Delta k/k_v$ and Γ/k_v, respectively.

Fig. 2.   (1/e)-width of the optical field vs. distance along the viggler. Solid curve: 5 mode system; dashed curve: 1 mode system.

Fig. 3.   Spot size (r_s), α, phase shift (Δk), gain (Γ), and radius of electron beam (r_b) vs. distance along viggler.

Figure (a)–(d): Plots of r_s (cm), a, $\Delta k / k_w \times 10^{-4}$, and $\Gamma / k_w \times 10^{-3}$ versus z/z_R.

(a) r_s (cm) vs z/z_R

(b) a vs z/z_R

(c) $\Delta k / k_w \times 10^{-4}$ vs z/z_R

(d) $\Gamma / k_w \times 10^{-3}$ vs z/z_R